2008

Location awareness in cognitive radio networks

Hasari Celebi
University of South Florida

Location Awareness in Cognitive Radio Networks

by

Hasari Celebi

A dissertation submitted in partial fulfillment
of the requirements for the degree of
Doctor of Philosophy
Department of Electrical Engineering
College of Engineering
University of South Florida

Major Professor: Hüseyin Arslan, Ph.D.
Frederick Martin , Ph.D.
Miguel A. Labrador, Ph.D.
Thomas Weller, Ph.D.
Leslaw Skrzypek, Ph.D.
Paris H. Wiley, Ph.D.

Date of Approval:
June 24, 2008

Keywords: cognitive positioning systems, dynamic spectrum access, dispersed spectrum utilization, environment awareness, location sensing, Cramer-Rao lower bound, range accuracy adaptation, time delay estimation, whole spectrum utilization

DEDICATION

To my family and parents.

ACKNOWLEDGEMENTS

I wish to express my gratitude to my advisor, Dr. Huseyin Arslan, for his guidance and continuous encouragement throughout the development of this dissertation. It has been very enjoyable and fruitful to work under his supervision and learn from him. His helpful discussions and comments initiates many new ideas and research directions with successful results presented in this dissertation.

I wish to thank each committee member: Dr. Frederick Martin, Dr. Miguel A. Labrador, Dr. Thomas Weller, Dr. Leslaw Skrzypek, and Dr. Paris H. Wiley for serving in my committee, their valuable times, feedbacks, and recommendations that improve the quality of this dissertation. In addition, I appreciate Dr. Carlos Smith for chairing my dissertation defense session. Furthermore, many thanks to the administration and staff of the Electrical Engineering department, especially Gayla Montgomery, Irene Wiley, Maria Du, Becky Brenner, and Norma Paz for their kind helps throughout my doctoral study.

Special thanks go to Dr. Sinan Gezici for his help and comments on the development of some parts in Chapter 5 of this dissertation. In addition, Mohammad Juma deserves acknowledgement for providing some measurement results in Chapter 7 of this dissertation. The administration of Logus Broadband Wireless Solutions Inc. and Honeywell definitely deserves many thanks for supporting myself financially during my doctoral study.

I wish to thank my friends in wireless communications and signal processing group: Dr. Kemal Ozdemir, Dr. Ismail Guvenc, Dr. Tevfik Yucek, Serhan Yarkan, Mustafa E. Sahin, Hisham A. Mahmoud, Sadia Ahmed, Ali Gorcin, Sabih Guzelgoz, Ahmed Hesham, Evren Terzi, and Omar H. Zakaria. I enjoyed working and sharing many things with them. I wish the best for all of them in their future careers and lives.

I would like to express my deepest gratitude to my wife for her encouragement and patience throughout my doctoral study. You always were there to share my concerns and happiness and whenever I need hope and motivation. Especially, you took care of our lovely two sons, Yusuf and Enes, in my absence at home and allowing me study long hours at the school. I will never forget your support, patience, understanding, and sacrifice. Finally, I would like to thank to my dear parents, brothers, and sister for their continuous supports, sacrifices, and encouragements over the years.

TABLE OF CONTENTS

LIST OF TABLES

LIST OF FIGURES

LOCATION AWARENESS IN COGNITIVE RADIO NETWORKS

Hasari Celebi

ABSTRACT

Cognitive radio is a recent novel approach for the realization of intelligent and sophisticated wireless systems. Although the research and development on cognitive radio is still in the stage of infancy, there are significant interests and efforts towards realization of cognitive radio. Cognitive radio systems are envisioned to support context awareness and related systems. The context can be spectrum, environment, location, waveform, power and other radio resources. Significant amount of the studies related to cognitive radio in the literature focuses on the spectrum awareness since it is one of the most crucial features of cognitive radio systems. However, the rest of the features of cognitive radio such as location and environment awareness have not been investigated thoroughly. For instance, location aware systems are widespread and the demand for more advanced ones are growing. Therefore, the main objective of this dissertation is to develop an underlying location awareness architecture for cognitive radio systems, which is described as *location awareness engine*, in order to support goal driven and autonomous location aware systems.

A cognitive radio conceptual model with location awareness engine and cycle is developed by inspiring from the location awareness features of human being and bat echolocation systems. Additionally, the functionalities of the engine are identified and presented. Upon providing the functionalities of location awareness engine, the focus is given to the development of cognitive positioning systems. Furthermore, range accuracy adaptation, which is a cognitive behavior of bats, is developed for cognitive positioning systems.

In what follows, two main approaches are investigated in order to improve the performance of range accuracy adaptation method. The first approach is based on idea of improving the spectrum availability through hybrid underlay and overlay dynamic spectrum access method. On the other hand, the second approach emphasizes on spectrum utilization, where we study performance

of range accuracy adaptation from both theoretical and practical perspectives considering whole spectrum utilization approach. Furthermore, we introduced a new spectrum utilization technique that is referred as dispersed spectrum utilization. The performance analysis of dispersed spectrum utilization approach is studied considering time delay estimation problem in cognitive positioning systems. Afterward, the performance of whole and dispersed spectrum utilization approaches are compared in the context of cognitive positioning systems.

Finally, some representative advanced location aware systems for cognitive radio networks are presented in order to demonstrate some potential applications of the proposed location awareness engine in cognitive radio systems.

CHAPTER 1

INTRODUCTION

Cognitive radio is a promising concept for the realization of smart and advanced wireless systems. One of the main features of cognitive radio is to support context awareness such as spectrum, location, environment, waveform, power, and infrastructure awareness. The majority of cognitive radio studies in the literature are focused on spectrum awareness capability of cognitive radio systems. The remainder features of cognitive radio systems such as location awareness has not been studied thoroughly.

Location awareness term in this dissertation is defined to embody sensing, learning, decision making, and adaptation of location information. Location information has been traditionally used for positioning systems and consequently location-based services (LBS). Nevertheless, the demands on higher quality of services (QoS) such as goal driven and autonomous location aware applications from mobile users as well as wireless network operators motivate system designers to exploit utilization of location information in wireless networks. Recently, it has been realized that LBS are not the only applications where location information can be used. It can be utilized for different applications and solving some issues in wireless networks. The applications based on utilization of location information (i.e., location aware applications) can be folded under four categories: LBS, network optimization, transceiver optimization, and environment identification.

Extensive utilization of location information for different applications and support of goal driven and autonomous location aware systems require incorporation of a location information hierarchy into network structure. Although some of the existing wireless network structures have miniature location information management systems, they do not have cognition capabilities such as goal driven and autonomous operation to support goal driven and autonomous location aware systems. However, cognitive radio networks [2]- [5] are promising systems for supporting goal driven and autonomous location aware applications due to their inherent cognitive features. Hence, location information management system with cognition capabilities, which is referred as location awareness engine, can

be realized in cognitive radio networks. As a result, goal driven and autonomous location aware applications can be supported by embodying location awareness engine to cognitive radio networks. Therefore, there is a need to develop location awareness engine for cognitive radio networks, which is the focus of this dissertation.

In the present dissertation, a cognitive radio architecture with location and environment awareness cycles and engines is introduced. Consequently, a conceptual model for location awareness engine is developed for cognitive radio systems by inspiring from the location awareness features of human beings and bats. Similarly, a conceptual architecture for environment awareness engine is proposed as well due to the tight relationship between location and environment awareness concepts. The functionalities of each engine are identified and presented in this dissertation. However, the focus of the dissertation is the development of some functionalities and algorithms of the location awareness engine in cognitive radio systems. Specific contributions in the present dissertation are outlined in a later section in this chapter.

1.1 Location and Environment Awareness in the Nature

Location and environment awareness concept can be defined as being cognizant of location and associated environment. The creatures in the nature have been considered as models for the most of innovations in the science history. Similarly, most of the creatures in the nature have already location and environment awareness capabilities to some extent and they have considered as models for incorporating such capabilities to electronic devices [6]. For instance, bat has location and environment awareness capabilities for navigation and capture of preys [7], known as echolocation. The bats emit high frequency ultrasonic signals ($20 - 200$KHz) from their mouths (i.e. transmitters) and listen to the echoes reflected back from environment using their ears (i.e. receivers) as illustrated in Fig. 1.1. The received echoes are processed by these animals for different purposes such as navigation and ranging. In addition, the following are some cognitive behaviors of bats:

- Object recognition,
- Object tracking,
- Range adaptation,
- Velocity adaptation.

A more intricate example is the human being that is equipped with sophisticated location and environment awareness capabilities. Human beings have multiple sensors such as ears, eyes, and skin that can be utilized for being aware of their location and corresponding environments as illustrated in Fig. 1.2. Moreover, the collected signals through these sensors (e.g. optic and acoustic signals) are converted into electrical signals that the brain can interpret. Hence, the human being can be aware of its location and surrounding environment by processing the sensed signals in the brain. Consequently, the human being can adapt himself/herself to the surrounding environment accordingly. As a result, location and environment awareness mechanisms in the human being mainly consist of sensing, awareness, and adaptation processes, which is illustrated in Fig. 1.3.

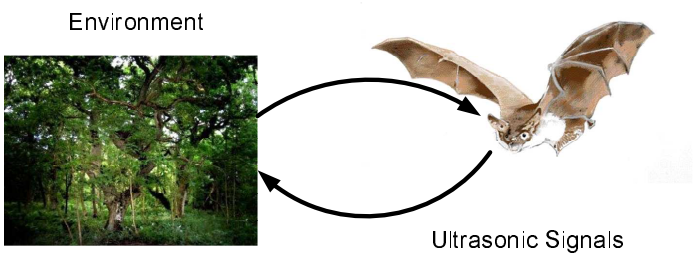

Figure 1.1 Illustration of location and environment awareness in bat echolocation system.

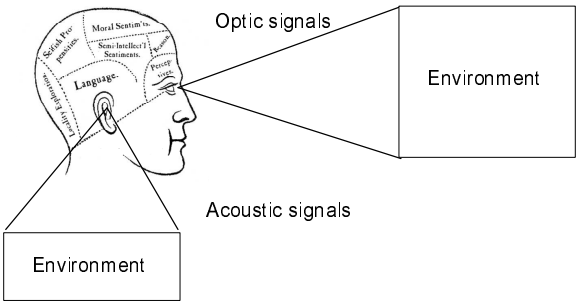

Figure 1.2 Illustration of location and environment awareness in human being using eyes and ears (Human head image by courtesy of [1]).

1.2 Location and Environment Awareness in Wireless Systems

Location and environment awareness features can be introduced to electronic systems, and such approaches have been investigated extensively for biologically inspired robotics [8]. However, it is difficult to say this for wireless systems. Utilization of location information in wireless systems

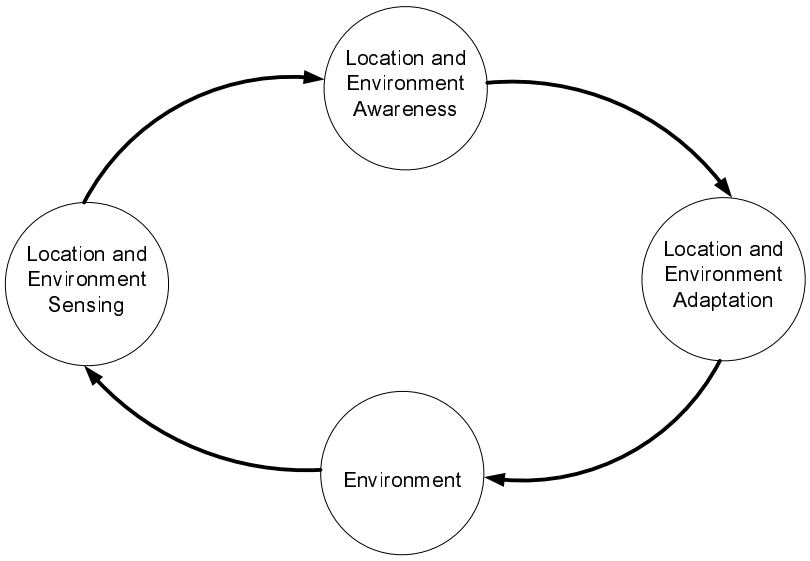

Figure 1.3 Simplified conceptual model of location and environment awareness cycles for the creatures (e.g. human, bat).

has been limited to positioning systems and LBS [9]. Nevertheless, the aforementioned advanced location and environment awareness capabilities of the human being or bat can be introduced to wireless systems as well [2], [9]. This can be accomplished by using cognitive radio technology invented by Mitola [10]. Although there are some significant efforts such as formation of IEEE SCC41 standard [11] to technically define cognitive radio and related terminologies such as SDR, a globally recognized definition of cognitive radio does not exist yet [12]. In this dissertation, we adopt the following definition that includes all the features of cognitive radio transceiver reported in the literature [13]:

- Sensing,
- Awareness,
- Learning,
- Decision,
- Adaptation,
- Reconfigurability,
- Goal driven and autonomous operation.

According to the definition, cognitive radio has sensing, awareness, and adaptation features, which are the main ingredients of location and environment awareness conceptual model for the creatures shown in Fig. 1.3. Hence, the consequent conclusion is that cognitive radio is one of the most promising technologies towards realization of these two capabilities in wireless systems [2, 9, 12, 14]. The following natural question that arise is: How to realize such advanced capabilities in cognitive radios?, especially location awareness, which is the main focus of this dissertation. Therefore, a cognitive radio architecture with location and environment awareness capabilities is introduced in the following section in order to respond to the above question.

1.3 Cognitive Radio with Location and Environment Awareness Capabilities

Cognitive radio is one of the most promising technologies to realize advanced and autonomous location and environment awareness capabilities in wireless systems [2], [9], [12]. The cognitive radio architecture with location, environment, and spectrum awareness capabilities shown in Fig. 1.4 is considered as the main system model in this dissertation [15]. The proposed model consists of four engines:

- Cognitive engine,
- Spectrum awareness engine,
- Location awareness engine,
- Environment awareness engine.

In this architecture, cognitive engine is the main engine that supervises the other engines in order to accomplish goal driven and autonomous tasks. The main responsibility of spectrum awareness engine is to handle all the tasks related to dynamic spectrum (e.g., acquiring available bands, corresponding carrier frequencies, and bandwidths). Similarly, environment awareness engine is responsible for managing environment information (e.g., number of paths, corresponding path delays and coefficients). In addition, the main responsibility of location awareness engine is to handle all the tasks related to location information. Cognitive engine determines the optimal system parameters for achieving autonomous task using the information collected from the engines that are participated. Cognitive engine generates signal with the specified parameters using the adaptive waveform generator as well as the sensing interface in order to interact with surrounding environment [15]. Note that

adaptive waveform generator/processor ideally is an interface that can generate and process any type of waveform at the transmitter and receiver sides, respectively. Antennas are the only sensing interface in conventional wireless systems to interact with the surrounding environment. The information acquired from the surrounding environment using only antennas can be inadequate. On the other hand, cognitive radio has an advanced sensing interface that consists of different sensing systems such as radiosensing, radiovision, and radiohearing. These sensing systems are utilized collectively or individually to acquire and learn comprehensive knowledge from the surrounding environment [15].

The development of location awareness engine in the proposed cognitive radio architecture is the focus of this dissertation, which is only emphasized further. The remainder functionalities of the proposed cognitive radio architecture are active research areas. As a result, the contributions on location awareness engine presented in this dissertation are summarized in the following section.

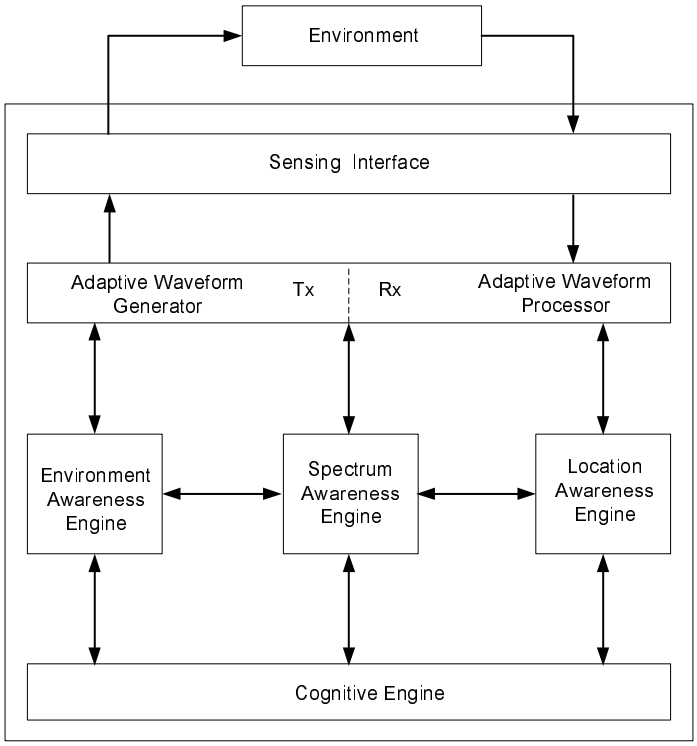

Figure 1.4 Simplified block diagram for a cognitive radio system.

1.4 Overview of the Dissertation

In this section, the major contributions of this dissertation are itemized first, and then details of the contributions are summarized chapter by chapter.

- Conceptual model for location and environment awareness engines and some representative location aware systems in cognitive radio systems (Chapters 2, 7),
- Cognitive positioning systems and range accuracy adaptation (Chapter 3),
- Time delay estimation using whole spectrum utilization approach (Chapter 4),
- Time delay estimation using dispersed spectrum utilization approach (Chapter 5),
- Comparison of whole and dispersed spectrum utilization approaches for time delay estimation (Chapter 6).

1.4.1 Chapter 2: Location and Environment Awareness in Cognitive Radios

In this chapter, a cognitive radio architecture with location and environment awareness engines is introduced. A location awareness engine architecture is proposed for the realization of location awareness in cognitive radios and networks. The main functionalities of the proposed location awareness engine are location sensing, seamless positioning and interoperability, statistical learning and tracking, security and privacy, mobility management, adaptation of location aware systems, and location aware applications. Similarly, an environment awareness engine that has functionalities of environment sensing, topographical information acquisition, object recognition and tracking, meteorological information acquisition, adaptation of environment aware systems, and environment aware applications is proposed. The details of the functionalities of both engines are presented in this chapter. Furthermore, the details of the sensing interface are presented. The proposed cognitive radio architecture is a promising model to support advanced and autonomous location and environment aware applications (e.g. advanced LBS). Finally, main conclusions are presented[1].

1.4.2 Chapter 3: Cognitive Positioning Systems

In this chapter, a positioning system for the location awareness engine, which is referred as cognitive positioning systems (CPSs) is proposed. The proposed CPSs can have multiple cognition capabilities such as range accuracy adaptation. The CPSs with range accuracy adaptation feature

[1]Majority of the content presented in this chapter are published in [2] and [15].

can support numerous goal driven and autonomous location aware systems. Therefore, maximum likelihood (ML) range accuracy adaptation algorithm is proposed for the CPSs by inspiring from the range adaptation skill of the bats. In addition, main error sources that can affect the performance of range accuracy adaptation method including dynamic spectrum, transmission, channel, and reception effects are discussed. In what follows, the performance of the proposed ML range accuracy adaptation is studied in the dynamic spectrum access environments. Then, three potential approaches for improving the performance of the range accuracy adaptation method are presented. These approaches are hybrid overlay and underlay dynamic spectrum access systems (HDSASs), dispersed spectrum utilization, and utilization of suboptimal lower bounds such as Ziv-Zakai lower bounds (ZZLB) for parameter optimization. The details of the first approach are provided. Finally, the concluding remarks are presented[2].

1.4.3 Chapter 4: Time Delay Estimation Using Whole Spectrum Utilization Approach

In this chapter, theoretical analysis of time of arrival (TOA) high accuracy ranging algorithm for cognitive radio systems that has dynamic spectrum access capability is performed. An impulse radio UWB signal occupying a whole band is considered. The asymptotic frequency domain Cramer-Rao bound (CRB) of the ranging algorithm that takes the frequency dependent feature (FDF) and phase of multipath components (MPCs) into account is derived through Whittle formula. The effects of FDF-MPCs and related parameters such as absolute bandwidth and operating center frequency on the ranging accuracy are investigated.

Certain channel parameters may have significant impact on the TOA estimation accuracy. Therefore, a generic list of such parameters is also presented and their statistics are obtained through computer simulations using IEEE 802.15.4a channel models. The effects of different channel environments and transceiver parameters on the statistics are investigated. Consequently, numerical and simulations results are presented. This is followed by presenting the main conclusions[3].

1.4.4 Chapter 5: Time Delay Estimation Using Dispersed Spectrum Utilization Approach

In this chapter, a new spectrum utilization technique is introduced, which is referred dispersed spectrum utilization systems. This new technique is developed considering time delay estimation

[2]Majority of the content presented in this chapter are published in [12, 16] and filed as a patent.
[3]Majority of the content presented in this chapter are published in [17, 18].

problem in cognitive positioning systems. More specifically, fundamental limits on time delay estimation are studied for dispersed spectrum utilization systems in cognitive radios, which facilitate opportunistic use of spectral resources. First, a generic Cramer-Rao lower bound (CRLB) expression is obtained for unknown channel coefficients and carrier-frequency offsets (CFOs). Then, various modulation schemes are considered and the effects of unknown channel coefficients and CFOs on the accuracy of time delay estimation are quantified. Finally, numerical studies are performed in order to verify the theoretical analysis[4].

1.4.5 Chapter 6: Comparison of Whole and Dispersed Spectrum Utilization for Time Delay Estimation

Performance of whole and dispersed spectrum utilization methods are compared in the context of time delay estimation in cognitive positioning systems. A cognitive radio (CR) transceiver architecture for both whole and dispersed spectrum utilization approaches is proposed. A combining technique based on maximizing signal to noise ratio (SNR) criterion is introduced for the dispersed spectrum utilization approach. Furthermore, the corresponding Cramer-Rao lower bound (CRLB) in additive white Gaussian noise channel (AWGN) for both approaches are presented. Consequently, performance of both approaches are compared for theoretical and practical cases. The results show that the dispersed spectrum utilization method has a great potential to exploit the efficiency of spectrum utilization and support goal driven and autonomous cognitive radio systems[5].

1.4.6 Chapter 7: Location Aware Systems in Cognitive Wireless Networks

The focus of this chapter is to provide some potential location aware applications with preliminary results. We demonstrate utilization of location information in cognitive wireless networks (CWNs) by presenting some representative location-based services (LBS), location-assisted network optimization applications (e.g. location-assisted spectrum management, network plan and expansion, and handover), location-assisted transceiver optimization, and location-assisted channel environment identification. Possible solutions to the implementation issues are proposed and the remaining open issues are also addressed[6].

[4]Majority of the content presented in this chapter is submitted to a journal [19] and filed as a patent.
[5]Majority of the content presented in this chapter are filed as a patent.
[6]Majority of the content presented in this chapter are published in [2, 9].

CHAPTER 2

LOCATION AND ENVIRONMENT AWARENESS IN COGNITIVE RADIOS

2.1 Introduction

Advances in mobile computing and enabling technologies along with user demands for new and improved applications are the main driving forces for the evolution of concepts of wireless systems. For instance, the location awareness concept for wireless systems has been traditionally used to imply positioning, tracking and location-based services (LBS). Relative to location awareness, environment awareness is a new concept and it has not been investigated as much as location awareness. Relying on the recent advances in mobile computing and enabling technologies such as introduction of sophisticated processors (e.g. microprocessors and FPGAs) and software defined radio (SDR) technology [9], it is time for paradigm shift in location and environment awareness systems. In this dissertation, we consider the location and environment awareness capabilities of human beings and bats as models for the realization of advanced and autonomous location and environment awareness features in cognitive radio systems.

The cognition cycle composed of fundamental cognitive tasks such as observe, orient, learn, plan, decide, and act introduced by Mitola [10]. Then, Haykin introduced a simpler cognitive cycle that focuses on three fundamental cognitive tasks, which are Radio-scene analysis, channel identification, and transmit-power control and dynamic spectrum management [20]. In order to develop practical and solid cognitive radio systems, these cognition cycles need to be converted into cognitive radio transceiver form. Therefore, in this chapter, we propose a conceptual model for cognitive radio transceiver systems that consists of location, environment, and spectrum awareness cycles and engines. The proposed cognitive radio architecture is shown in Fig. 2.1. The details of the proposed architecture are presented in the following section. In the remaining of this section, previous studies related to each cycle and engine are provided.

Haykin introduced the idea of cognitive radar along with cognition cycle for environment awareness, which is a physical realization of bat echolocation system [21]. Although cognitive radar is considered as a standalone device in [21], it can be considered as a subset of cognitive radio and one of the most promising methods for the realization of environment awareness in cognitive radios. Afterward, radio map environment method for cognitive radio networks is introduced [22]. As an alternative architecture to the aforementioned two studies, we propose an environment awareness cycle along with a comprehensive environment awareness engine by inspiring from environment awareness features of bats in this chapter. Unlike to environment awareness in cognitive radios, there is not any solid study in the literature on the location awareness of cognitive radios to the author' best knowledge. Therefore, we also propose a conceptual model for location awareness cycle and engine by inspiring from location awareness features of bats in this chapter [2], [9]. In addition, the functionalities of each engine are identified and presented.

2.2 Proposed Cognitive Radio Architecture

Before proceeding to discuss the proposed cognitive radio architecture with location and environment awareness engines, it is worth providing some clarifications in the terminology. Note that sensing, learning, memory, judgement, decision mechanisms, and adaptation are folded into awareness term in this study. Moreover, although location and associated environment are tightly coupled concepts, we treat them separately throughout this chapter unless otherwise stated. In addition, environment is briefly defined as the volume oriented at a specific location. Detailed definition of environment is provided in a later section.

A conceptual model for cognitive radios including location and environment awareness engines and cycles shown in Fig. 2.1 is proposed in order to support advanced and autonomous location and environment aware systems. Due to the relevancy, spectrum awareness engine is included to the model without details. We refer to [23] for details on spectrum awareness. However, cognitive radio is not limited to these three engines. According to the model in Fig. 2.1, location and environment awareness engines consist of sensing, awareness core, and adaptation systems, respectively similar to the location and environment awareness cycles of creatures in the nature. In this model, location and environment awareness engines receive tasks from cognitive engine and they report back the results to the cognitive engine for achieving goal driven and autonomous location and environment aware application at hand. Furthermore, both engines can utilize various sensors

and adaptive waveform generator and processor capabilities of cognitive radio to interact with and learn the surrounding environments. Additionally, there are direct or indirect (through cognitive engine) collaborations between both engines. For instance, environment awareness engine senses the environmental parameters [24] and provides these parameters (e.g. frequency dependency constant of channel environment [17]) to the location awareness engine. Similarly, the spectrum awareness engine senses the spectrum [25] and provides the spectrum information (e.g. available bandwidth) to the location awareness engine. The details of the functionalities of the proposed model are presented in the following sections.

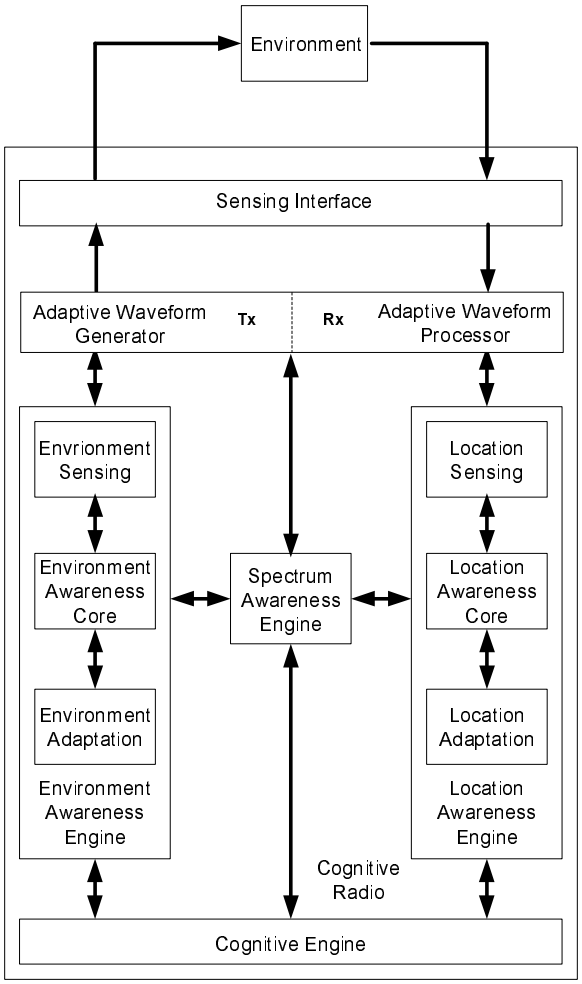

Figure 2.1 A conceptual model for cognitive radio systems with location and environment awareness cycles and engines.

2.2.1 Sensing Interface

Sensing process is composed of mainly two components, which are sensors and associated data post processing methods. Similar to the creatures in the nature, different sensors have been used in wireless systems for sensing. Sensors are utilized to convert the signals acquired from environment to electrical signals so that cognitive radios can interpret. The acquired signals can be in different format such as electromagnetic, optic, and sound. Therefore, sensors can be categorized under three types: electromagnetic, image, and acoustic sensors. Note that the corresponding data post-processing algorithm for each sensing technique is different. Inspiring from the sensing features of the creatures, we classify the sensing mechanisms in cognitive radios under three main categories based on the type of sensors used:

- Radiosensing,
- Radiovision,
- Radiohearing.

Radiosensing is a sensing technique utilizing electromagnetic sensors and the associated post processing schemes. Similarly, radiovision is a sensing approach using image sensors and the corresponding post-processing schemes. Finally, radiohearing is a sensing method employing acoustic sensors and the associated post-processing schemes. Although sensing interface is a common functionality in cognitive radio systems to interact with environment and other users, we study the sensing methods from location and environment aware systems perspective. As a result, the details of sensing interface are discussed in the context of location and environment awareness in this section.

2.2.1.1 Radiosensing Sensors

Although light can be considered as an electromagnetic wave, we study the image sensors in a separate section due to widely usage of image sensors in the literature. The most widely used radiosensing (electromagnetic) sensor in wireless systems is the antenna, which is the focus of this section. The antenna is a transducer that converts electromagnetic signals into electrical signals and vice versa. For instance, in the antenna-based wireless positioning systems, location information is estimated from the received signal statistics such as time-of-arrival (TOA), receive signal strength indicator (RSSI), and angle-of-arrival (AOA) [12]. It is envisioned that cognitive radios will have advanced location awareness capabilities using antenna-based algorithms. Therefore, we propose a

radiosensing based positioning method in Chapter 3, which is CPS. Since weather-induced impairment can affect the performance of wireless systems, performance of cognitive radios and networks can be improved as well by having meteorological information of the operating environment. Such information can be acquired by cognitive radios either from a central server or embedded auxiliary sensors such as thermometer and barometer.

2.2.1.2 Radiovision Sensors

Radiovision sensors such as image sensors are devices that capture optic signals from the environment and convert them to electrical signals in order to construct the corresponding image. These sensors have been already used in different areas such as digital cameras and computer vision systems. Computer vision is a branch of artificial intelligence aiming to provide vision systems functioning like human vision in computers. The recent advances in vision systems such as cognitive vision systems [26] and scene analysis [9], [27] show the feasibility of designing cognitive radios with vision capabilities. Cognitive radio with cognitive vision systems can have a capability to convert the acquired scene state into text, image or voice formats depending on the applications. Consequently, numerous image based location and environment aware applications [28], [29] can be developed. However, it is a challenging task to embody cognitive radios with such advanced cognitive vision systems due to low power, cost and size limitations. Assuming that cognitive radio has cognitive vision system capabilities, another challenge is the placement of image sensors since it is required to point such sensors towards the target direction or object. However, this is not a problem in human being since the eyes are located in the most strategic position of human body. Different solutions can be developed to address this issue in cognitive radios, especially when the continuous scene acquisition is required. For instance, image sensors (e.g. video camera) along with an Ultrawideband (UWB) transceiver can be mounted to the user's hat, which is known as wearable computing devices in the literature [30]. In such a solution, a digital camera acquires the images and transmits them to the cognitive radio located in a part of the body (e.g. pocket) for the data post-processing using UWB transceiver.

2.2.1.3 Radiohearing Sensors

One of the radiohearing sensors is an acoustic sensor, which is a transducer that converts acoustic signals into electrical signals and vice versa. This type of sensor has already been used in different

wireless systems. The main idea behind acoustic technique is utilizing sound propagation to navigate, detect objects, and communicate. Nevertheless, our concern here is the utilization of acoustic signals for cognitive location and environment aware systems. For instance, acoustic location estimation techniques (e.g. sonar [31]) can be utilized for cognitive location aware applications. Furthermore, bat echolocation is a perfect example for the active sonar, which can be employed for developing numerous environment aware systems. Ideally, cognitive radio with passive sonar functioning like human ear or active sonar functioning like bat echolocation are envisioned. There are some efforts towards achieving these goals such as Cricket indoor location system [32]. Another potential utilization of acoustic sensor in cognitive radios is extracting environmental features from the sensed sound signal similar to human beings and bats. For instance, a blind or closed-eye person can infer to his/her location from the sounds that he/she hears. More specifically, a blind or closed-eye person can determine whether he/she is in a forest or zoo if he/she hears the sounds of various animals. Similarly, cognitive radio can utilize its microphone, which is an integral part of the most of wireless devices, for location aware applications. One potential approach is to capture sound signal as a fingerprint and then compare it to predefined fingerprints in database for the extraction of certain environmental features.

Image sensors are utilized mainly in passive manner (only receiver) whereas acoustic and electromagnetic sensors are used in active manner (both transmitter and receiver) in wireless systems. Furthermore, image sensors mainly require to point cognitive radios towards the target direction in order to receive the optical signals. On the other hand, antennas may not require pointing depend on the antenna type used such as omnidirectional antennas. For instance, a cognitive radio with omnidirectional antenna can continuously interact with RF environment even if it is located in a pocket or bag. Note that several antenna based location aware algorithms for cognitive radios and networks are proposed in [2], [12]. Furthermore, since cognitive radio has a common sensing interface including different sensors, it can utilize one or combination of the sensors depending on the autonomous task at hand. For instance, cognitive radio can use both image and acoustic sensors for supporting goal driven and autonomous location and environment aware applications similar to the utilization of both eyes and ears by human being.

2.2.2 Location Awareness Engine

A conceptual model for location awareness engine in cognitive radios is introduced in this section [2], [9]. The proposed model for the location awareness engine in cognitive radios is illustrated in Fig. 2.2. The model consists of the following main subsystems:

- Location sensing,
- Location awareness core,
- Adaptation of location aware systems.

In what follows, we describe the functionalities of each of these subsystems in details.

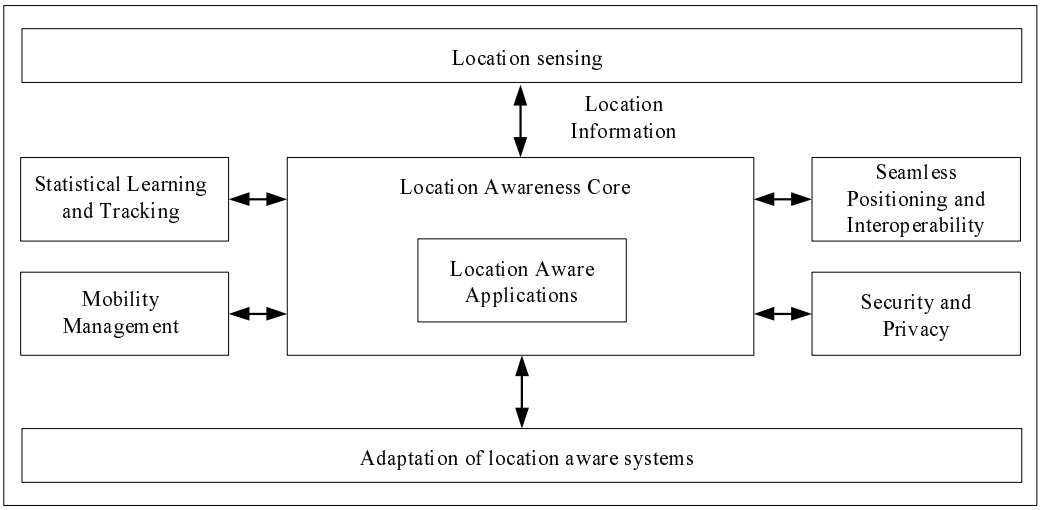

Figure 2.2 Block diagram of location awareness engine for cognitive radios and networks.

2.2.2.1 Location Sensing Methods

One of the fundamental features of the location awareness engine is to estimate the location information of target object in a given format. The format of location information (e.g. datum and dimension) that needs to be sensed can have significant effects on the complexity of location aware algorithms [9]. Therefore, a taxonomy of location information for location awareness in cognitive radios is presented in this section. The proposed taxonomy is illustrated in Fig. 2.3.

In this study, the place occupied by a designated user, device or mainly object is described as location. The object can be physical or virtual and consequently location information of the object

can be either physical or virtual position [33]. The position term is defined as the coordinates of a single point in space that represents the location of an object. The physical position of an object is obvious as the name implies. On the other hand, the virtual position is defined as the invisible position (e.g. internet protocol (IP) address), which is relative to some known entity whose physical location may or may not be precisely known [33]. This type of location information is commonly encountered in the wired networks such as world wide web (WWW) access networks. For instance, a cognitive radio can log into a remote computer (or device) through Internet on the other side of the earth, but the geographic position of that computer may not be known precisely. The position of such device is referred as virtual position. However, cognitive radio can retrieve the physical position of the remote computer from the virtual position along with some additional information. Therefore, virtual position is considered as a form of physical position in this chapter. Mapping virtual position to the corresponding physical position already exists in the Internet domain. Extracting physical position of a remote device from its virtual position information can be useful for cognitive radios. Such information can be used to develop efficient location-assisted routing protocol. Physical position of an object can be either absolute or relative. The absolute position is referred to the complete coordinate knowledge of an object. On the other hand, the relative position is defined as the position of an object (e.g. cognitive radio device) relative to another or neighbor objects that do or do not know their absolute positions [34]. Note that a cognitive radio device can estimate its absolute position using its relative position along with the absolute position of the reference device that is used during relative positioning. Absolute position estimation techniques are more mature and widely used compared to relative position estimation methods. As a result, cognitive radio device can switch between absolute and relative position estimation methods depending on the accuracy requirements. We refer to [34] for the details on relative positioning techniques, and absolute and relative position terms are discussed in the sequel.

The absolute and relative position of a cognitive radio can be quantified using coordinate systems. There are numerous global, continental and country-specific reference coordinate systems for absolute position of an object such as North American Datum (NAD), European Datum (ED50), Tokyo Datum (TD), and Earth Centered Fixed (ECF), World Geodetic Systems (WGS). Each of these reference coordinate systems have various revisions. Among these, WGS-84 is a well known standard reference coordinate system, which is also currently being used by the GPS. To achieve interoperability between these different reference coordinate systems, cognitive radios can have co-

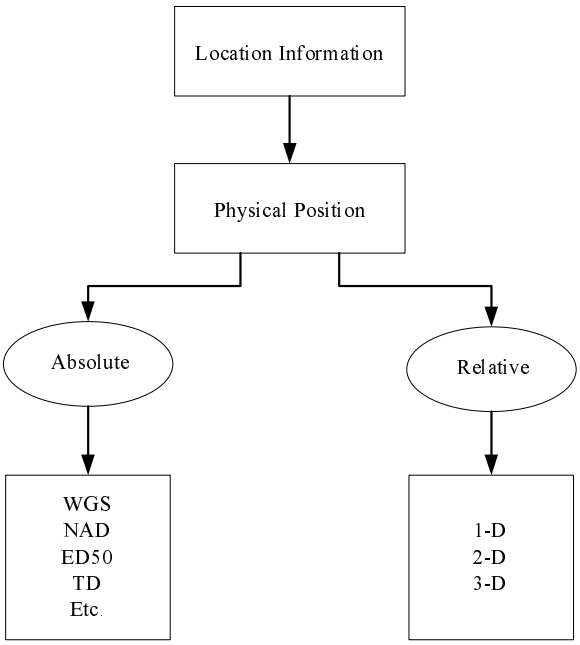

Figure 2.3 A taxonomy of location information.

ordinate systems converter. For instance, cognitive radios can employ standard Molodensky datum conversion algorithm [35].

Relative position information can be classified under three groups of reference coordinate systems [2]:

- 1-dimensional (1-D): It provides the location of a cognitive radio in a single axis (x or y or z). For instance, the distance between a transmitter and a receiver (or two cognitive radios) is a *1-D* location information. This information can be used for the ranging and network authorization purposes in cognitive wireless networks, which is also currently being used by many wireless networks. Time parameter can be added to this type of location information.

- 2-D: It provides the position of a cognitive radio in a plane (i.e. (x, y)). This type of location information is also estimated by some of the existing wireless communications systems. Time parameter can be added to this type of location information.

- 3-D: It provides the location of a cognitive radio in three dimensions (x, y, z). For instance, cognitive wireless networks can have a capability to estimate the *3-D* location of a cognitive radio node. Time parameter can be included to this type of location information.

Notice that the accuracy of reference coordinate system model along with the resolution of positioning technique that are employed can affect the performance of location aware systems. In what follows, we discuss the details of different location sensing methods:

- Radiosensing methods: Antenna-based location sensing algorithms have been studied extensively for wireless positioning systems and they can be categorized under three groups:
  - Range-based schemes,
  - Range-free schemes,
  - Pattern matching-based schemes.

  Evaluation of these methods in the context of cognitive radio can be found in [9]. The legacy antenna-based location estimation methods do not have cognition capabilities that cognitive radios require. Therefore, an antenna-based positioning method, which is referred as Cognitive Positioning Systems (CPS), is introduced along with range accuracy adaptation capability in Chapter 3. The details of the CPS can be found in Chapter 3.

- Radiovision methods: Image sensors are used for visual location sensing methods [30]. In this approach, the location of observer is estimated solely based on the images acquired from the image sensors. The relationship between video camera mounted to the user hat and cognitive engine in cognitive radios resembles to the relationship between eye and brain in the human body. By using wearable computing devices such as video camera, signals (e.g. video) from the scene are acquired and sent to cognitive radio. The acquired images can be processed using advanced digital image and signal processing techniques (e.g. pattern analysis and machine intelligence algorithms [27]) to construct the scene state in the desired formats: text, image, video, and voice. One of the well known visual location sensing techniques is *scene analysis* [27], [28], [29]. Scene analysis simply is a pattern matching based location sensing technique similar to RF pattern matching based methods (e.g. RF fingerprinting) [36]. Acquired images are used as patterns in the scene analysis, whereas channel statistics (e.g. TOA) are utilized as patterns in the RF pattern matching based methods. One of the well known consequent steps is comparison of the acquired pattern to the patterns in a pre-built database.

Note that the location accuracy of radiovision based location sensing methods is pretty rough compared to other location sensing methods such as radiosensing based schemes. Therefore, radiovision based sensing methods are preferable for object and environment recognition rather than location sensing. Two of the main drawbacks of radiovision based sensing techniques are the requirement of image database and extensive image processing power. Compared to robotics and computer systems, implementing radiovision techniques such as cognitive vision systems in cognitive radios is a challenging task due to low power, cost and size constraints.

- Radiohearing methods: Radiohearing based location sensing methods utilize acoustic sensors for interacting with environments. Similar to radiosensing based location sensing techniques, radiohearing based location sensing methods can be implemented using three group of schemes: range-based, range-free and pattern matching based techniques. The majority of the studies in the literature focuses on the first two methods and these studies are mostly for legacy location estimation techniques to the best of author's knowledge. Cognitive radio is a promising technology to realize advanced radiohearing based location sensing techniques functioning similar to bat echolocation systems. For instance, cognitive radio can acquire sound signal and use it as a pattern. In addition, it can look at the spectrum of the captured sound pattern and compare it with spectrum patterns stored in the database in order to infer to the location. Different radiohearing based location sensing methods using the aforementioned three approaches can be developed for the realization of location awareness in cognitive radios.

The main objective of this core is to perform critical tasks related to location information such as learning, reasoning, and making decisions. The core has the following functionalities:

- Seamless positioning and interoperability,
- Security and privacy,
- Statistical learning and tracking,
- Mobility management,
- Location aware applications.

The details of location aware applications are provided in Chapter 7. The remaining functionalities are discussed in this section.

2.2.2.2 Seamless Positioning and Interoperability

Seamless positioning is defined as a system that can keep the position accuracy at a predefined level regardless of the changes in channel environment. There are mainly two approaches for achieving seamless positioning: waveform-based methods and environment sensing-based methods. The first approach is based on utilization of appropriate waveform or technology depending on the user requirements and environment [37]. This requires supporting all or predefined waveforms of the existing and future positioning systems and waveform switching mechanism. An example for the first approach is the European SPACE project [37]. The main objective of this project is to build a prototype positioning system that can provide centimeter level positioning accuracy anywhere and at all times. The SPACE prototype consists of the existing positioning waveforms, algorithms and sensors such as GPS, Galileo, 3G, UWB, WLAN, and Bluetooth. Depending on the user requirements and environments, the most appropriate positioning system is selected to achieve seamless positioning. Moreover, the prototype has plug and play integrated positioning system capability for supporting the existing and future positioning techniques. We refer to [37] for further details on the SPACE project.

The second approach, which does not require multiple waveforms, is based on sensing channel environment parameters (e.g. path loss coefficient [38]) and adapt the positioning algorithm accordingly in real-time. The proposed RSSI based location estimation algorithm for unknown channel environment in [38] is a good example for this approach. In the proposed algorithm, the location of target wireless device and path loss coefficient of the channel environment are jointly estimated to keep the predefined accuracy at constant level. Note that the path loss coefficient is not the only parameter to detect the changes in channel environments. For instance, frequency dependent coefficient is a recently discovered channel parameter that can be used for monitoring the environments [17]. As a result, multiple distinguished parameters of channel environment can be monitored to achieve seamless positioning, which is handled by environment awareness engine in cognitive radios. Compared to waveform-based methods, environment-sensing methods have lower complexity. As a result, cognitive radio is envisioned to have capability of supporting both type of methods.

The IEEE defines interoperability as the ability of two or more systems or components to exchange information and to use the information that has been exchanged [39]. The interoperability issues in cognitive radios can be grouped under two main categories: cognitive radio-cognitive radio interoperability and cognitive radio-legacy radio interoperability. For the first issue, both cognitive

radios can have the same or different waveforms. In the former case, they can exchange the information directly. However, in the latter case, both needs to agree on one of the waveforms in order to communicate, which is a current research topic. As a straightforward solution to the second issue, cognitive radio can switch its waveform to the waveform of legacy radio, since the latter radio does not have reconfigurability features. In addition, the type of sensed location information exposes another issue due to the diversity in location information format. For instance, the location information of a device can be in the format of WGS84 (used by the GPS) and this information can be converted to Tokyo Datum (TD) format by using reference datum conversion capability of cognitive radios [9]. As a result, cognitive radio is a promising technology to realize advanced seamless positioning and interoperability algorithms.

2.2.2.3 Security and Privacy

The prospect extensive utilization of location information in cognitive radios and networks brings two issues on the surface: security and privacy. The majority of the proposed location estimation and positioning techniques in the literature assume the absence of adversarial attacks. Nevertheless, positioning techniques are highly vulnerable to such attacks [40]. Of the many potential threats, tracking the position of a cognitive radio user without authorization and adversarial attacks are the two main ones. The first threat can violate the user privacy and the second one can result in catastrophic scenarios since LBSs highly depend on the location information. It is crucial to develop effective solutions to address these issues. For instance, local or global geolocation privacy protection methods can be developed to address privacy issue. Indeed, there is an effort in this line for mainly wired networks (e.g. world wide web), which is the formation of geographic location/privacy (Geopriv) working group under The Internet Engineering Task Force (IETF) [41]. The primary task of this working group is to assess authorization, security, integrity, and privacy requirements that must be met in order to transfer such information, or authorize the release or representation of such information through an agent. Similar geographic privacy methods can be developed for cognitive wireless networks. To address security issues in location aware applications, secure positioning systems that are robust to adversarial attacks (e.g. spoofing and cheating) can be developed. For instance, the proposed verifiable multilateration in [40] is a good example for secure positioning technique. Such secure positioning techniques can be developed for cognitive radios as well. In

summary, cognitive radios have a capability to support advanced geographic privacy and secure positioning methods.

2.2.2.4 Statistical Learning and Tracking

The location awareness engine can have a capability to track mobile CR users and it can be trained by the tracking data using statistical learning tools [42] such as neural networks and markov models to form user location profiles. These profiles can be used to predict the trajectory of the CR users and improve the positioning accuracy, especially in pattern matching based positioning methods. As a result, the location awareness engine can have a capability to track the users with history using statistical learning models as shown in Fig. 2.2.

2.2.2.5 Mobility Management

Utilization of location information in cognitive radios and networks for different applications will have a major impact on the system complexity. Introduction of such additional services and applications into cognitive wireless networks will exacerbate the mobility issues. Consequently, the system capacity and implementation cost can be affected by these issues. Therefore, it is desirable to develop an accurate mobility model during the network planning phase. Therefore, the location awareness engine has a mechanism to handle mobility tasks as shown in Fig. 2.2.

2.2.2.6 Adaptation of Location Aware Systems

The main objective of the adaptation block is to support location awareness engine in terms of adaptation of algorithms and parameters for the satisfaction of the user, consequently, cognitive engine requirements. These requirements stem from goal driven and autonomous location aware applications that are supported. The reported performance parameter or requirement of location aware applications in the literature are accuracy, integrity, continuity, and availability [37]. Nevertheless, range accuracy is one of the most important performance parameters or requirements of location aware applications, which is considered in this section. We refer to [37] for the details on the integrity, continuity, and availability requirements of positioning systems.

Goal driven and autonomous location aware applications (e.g. advanced LBS) can require different level of accuracy. For instance, indoor positioning systems demand higher precision accuracy compared to outdoor positioning systems. More specifically, asset management in industrial areas,

which is a local positioning application, can require typically $0.05 - 30$m accuracy. On the other hand, $E911$ services in the United States require $50 - 300$m accuracy in the most cases [12]. In order to address this issue, range accuracy adaptation methods can provide arbitrary accuracy to support goal driven and autonomous location aware applications. Moreover, as mobile cognitive radio moves, the channel environment can change and it is known that change of environment affects the range accuracy [17]. In order to keep the accuracy at desired level in spite of change of channel environment, the operational environment can be monitored by using environment awareness engine. The range accuracy can be adapted based on the input from the environment awareness engine regarding the environmental changes. In summary, supporting goal driven and autonomous location aware applications requires having range accuracy adaptation methods that can provide arbitrary accuracy anywhere and anytime. Therefore, a range accuracy adaptation method is proposed in Chapter 3.

2.2.3 Environment Awareness Engine

Environment awareness is one of the most substantial and complicated task in cognitive radios since channel environment is the bottleneck of wireless systems. Creatures with environment awareness capabilities such as human being and bats can be considered as models for the realization of environment awareness in cognitive radios. For instance, human being has different sophisticated senses such as observing and learning the surrounding environment and bats utilize their echolocation systems for object and environment identification, and target detection and tracking. As a result, similar environment awareness techniques can be developed for cognitive radios. The consequent essential questions that arise are:

- What type of information to acquire from environment?
- How to acquire such information?
- How to utilize the acquired environmental knowledge in cognitive radios and networks?

In this section, we address to these questions briefly. In order to achieve this goal, a conceptual model for environment awareness engine is introduced, which is shown in Fig. 2.4. The model consists of the following functionalities:

- Environment sensing,
- Environment awareness core,

- Topographical information,
- Object recognition and tracking,
- Propagation characteristics,
- Meteorological information,
- Environment aware applications.

These functionalities are described in the order to answer the aforementioned three questions as follows.

The answer to the first question is hidden in the definition of "environment". From the wireless systems point of view, an environment mainly consists of the following entities: topographical information, objects, propagation characteristics, and meteorological information. Although some sensing techniques for the aforementioned environmental information exist in the literature, there is not any structured foundation for environment sensing in cognitive radios to the best of author's knowledge. Therefore, development of environment sensing techniques is a current research topic as well. The same discussion is also valid for the adaptation of environment aware techniques. In what follows, we describe each entity along with some corresponding representative sensing, adaptation techniques and applications.

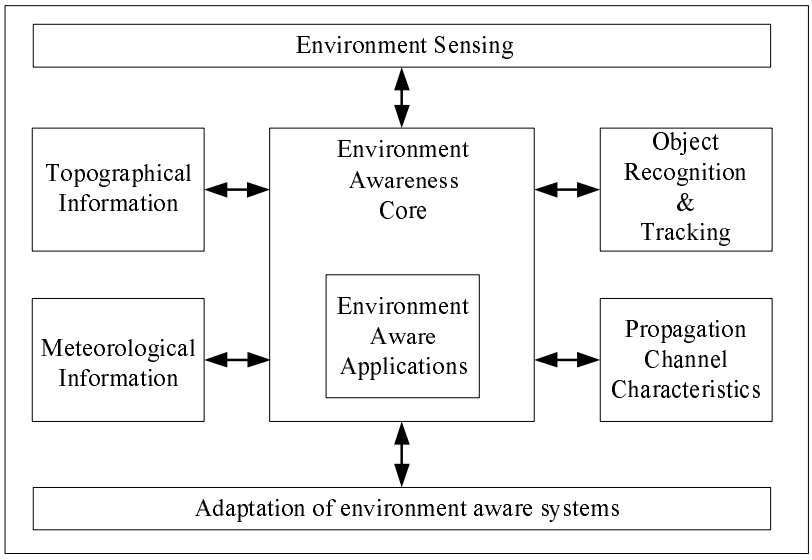

Figure 2.4 A conceptual model for environment awareness engine.

2.2.3.1 Topographical Information

According to *Oxford English Dictionary*, topography is defined as "the science or practice of describing a particular place, city, town, manor, parish, or tract of land; the accurate and detailed delineation and description of any locality". In other words, topography of a local region provides information about not only the relief (Earth's surface features), but also vegetation, human-made structures, history and culture of that particular area. Assuming that central environment awareness engine has topographical map including the aforementioned information, then numerous advanced LBS can be developed. There are some efforts towards the realization of topographical map such as the Google Maps^{TM}. Another example is the proposed vision enhanced object and location awareness method for mobile services in [29]. In the proposed method, mobile user (e.g. tourist) points the embedded camera towards to the object of interest (e.g. historical structure), captures the image. Consequently, the captured image is transmitted to a server to extract the information related to the image and then send this information to the mobile user.

2.2.3.2 Object Recognition and Tracking

Objects are defined as the human-made entities present in the target local environment temporarily or permanently in this study. The large and permanent human-made structures such as buildings and bridges are considered as part of topography of environment, hence, such human-made structures are included in the topographical information. On the other hand, relatively small and movable human-made entities such as vehicles, home and office appliances are considered as objects. Object detection, identification and tracking are important features of environment awareness engine since they can affect the dynamic of environment. For instance, cognitive radar and cognitive sonar are two promising technologies to embody such capabilities, which are the features of bat echolocation, in cognitive radios [21]. In [21], cognitive radar is introduced with the capability of target detection and tracking using Bayesian approach. The proposed cognitive radar architecture is based on dynamic closed-loop feedback system (e.g. a cognition cycle) encompassing the transmitter, environment, and receiver. We refer to [21] for further details.

2.2.3.3 Propagation Characteristics

This entity provides information on the characteristics of signal progression through a medium (channel environment). Basically, propagation characteristics of channel environment shows that

how the channel affects transmitted signal. The statistical characteristics of wireless channel are described mainly with two group of statistics: 1) Large-scale, 2) Small-scale. Large-scale statistics provide information on path loss behavior of channel environment. On the other hand, small-scale statistics determine the drastic variations of received signal in time and frequency due to short displacements. In addition, the selectivity of the channel provides important statistics related to multipath radio channel. Some representative channel statistics are delay spread, doppler spread, and angular spread [24]. Traditionally, these statistical parameters are obtained after performing extensive measurements and data post-processing, which is known as propagation channel modeling process in the literature [43]. Alternatively, the propagation statistics of local environment can be obtained in different ways using cognitive radios such as the proposed location-awareness based performance improvement of wireless systems in [24]. The proposed method consists of the following three main steps: environment recognition and classification, statistical propagation model parameters extraction, and channel environment adaptation. Various propagation characteristics acquisition methods can be developed and such information can be utilized for different applications by cognitive radios.

2.2.3.4 Meteorological Information

This entity provides information on the weather of target local region, which can affect the signal propagation. The current and future weather parameters such as rain, snow, temperature, humidity and pressure can be acquired either using radio auxiliary sensors or from central cognitive base station. By having current and forecasted meteorological information, cognitive radio can adapt itself accordingly. For instance, rain can have significant effects on the performance of broadband fixed wireless access links (e.g. Fixed WiMAX) [44], especially operating at higher carrier frequencies. One of the performance parameters that can be affected from rain is the carrier-to-interference ratio (C/I) and this performance metric depends on the rain intensity of the location of desired signal path and interferer signal paths. Some of the representative scenarios showing the rain effects on C/I performance of the broadband fixed wireless access links are given as follows [44]: rain-induced C/I degradation, rain-induced C/I improvement, and no C/I change. The details of these scenarios can be found in [44]. If cognitive radio or network has a capability to acquire rain intensity of local regions from a central meteorological server or Internet, then, C/I adaptation can be performed accordingly.

Inspiring from the definition of environment term, the main task of environment awareness engine in cognitive radios is having a complete knowledge of the surrounding environment by acquiring the information on topography, objects, propagation channel, and meteorology of the target local region. Environment awareness engine provides these information to other components of cognitive radios in order to support goal driven and autonomous systems. For instance, object and environment identification, seamless positioning, and LOS-NLOS identification are three potential environment aware systems that can be developed. In summary, cognitive radio is envisioned to have environment awareness capability, which can lead to the development of advanced cognitive radio applications.

2.3 Conclusions

A conceptual model for cognitive radios with location and environment awareness cycles is presented. Location awareness engine and environment awareness engine architectures are proposed. The detailed descriptions of the functionalities of the proposed cognitive radio and both engines are presented. The proposed cognitive radio is a promising underlying architecture for developing advanced and autonomous location and environment aware systems. Finally, each component of the model needs to be developed, which can be considered as active research topics.

CHAPTER 3

COGNITIVE POSITIONING SYSTEMS

3.1 Introduction

Location awareness is one of the fundamental characteristics of cognitive radio (CR) technology. Realization of location awareness requires incorporation of a location awareness engine into cognitive radios and networks. In Chapter 2, a system model for location awareness engine in cognitive radios and networks is introduced. By using location awareness capability of CR, numerous goal driven and advanced location aware applications can be developed, which are discussed in Chapter 7. These applications are fourfold: location-based services (LBSs), location-assisted network optimization, transceiver algorithm optimization, and environment characterization [24].

Applications of location awareness can require different level of ranging and positioning accuracy. For instance, generally, indoor positioning systems demand higher accuracy compared to outdoor positioning systems. More specifically, asset management in industrial areas, which is a local positioning application, can require typically $0.05 - 30$m accuracy depending on the specific applications [45]. On the other hand, $E911$ services in the United States require $50 - 300$m accuracy in the most cases [46]. For instance, when a CR device is located in the outdoor environment (e.g. in a public park), CR can adjust its accuracy level to 100m to satisfy E911 services requirements in the United States. In this case, lets assume that the current waveform of the CR is GSM and the CR user leaves from the park to office. After entering to the office, the CR device recognizes WLAN network at office using its interoperability capability and it switches its waveform to WLAN. Consequently, it can improve its positioning accuracy (e.g. $5m$) since it operates in the indoor environment. In order to support different location aware applications using CRs, an adaptive positioning system that can achieve accuracy adaptation is inevitable.

To the best of author's knowledge, there is not any solid study in the literature on the evaluation and comparison of the existing positioning technologies (e.g. GPS, UWB positioning) in the light

of realization of location awareness in CRs. Hence, in this chapter, a brief discussion on some of the existing positioning technologies such as GPS and UWB positioning is provided. There are different forms of GPS technology: standard GPS ($4-20m$ accuracy), Code-Phase GPS ($3-6$m accuracy), Carrier-Phase GPS ($3-4$mm accuracy), Differential GPS (sub-decimeter) [47], Assisted-GPS (less than 10m accuracy) [48], Indoor GPS [49], and Software GPS [50]. As it can be seen that each of these GPS technologies provide different level of accuracy. Even combining these different form of GPS in a single device to provide switched accuracy level (not adaptive) is impractical and costly. However, software GPS is a promising method to switch between different GPS forms. But, eventually, this approach will only provide a set of fixed accuracy levels that are provided by each form of GPS. Basically, the existing GPS technologies do not have a capability to achieve range accuracy adaptation. Moreover, GPS is not a low-cost and low-power solution [51] for some wireless networks (e.g. wireless sensor networks) where the cost and power are the major concerns.

Another alternative technology is UWB positioning, which has the capability to provide centimeter ranging accuracy due to the use of large bandwidth during the transmission [18]. However, this technology does not have a capability to achieve range accuracy adaptation either. Moreover, this technology provides such fixed and high positioning accuracy within only short ranges. In [52], a hybrid distance estimation technique for a legacy positioning system that is based on time-of-arrival (TOA) and signal strength methods is proposed. The technique provides flexibility to improve the accuracy using a priori distance information rather than achieving range accuracy adaptation.

The details of the existing location estimation (e.g. triangulation, proximity) and sensing (e.g. scene analysis) techniques in CR context are presented in [9]. Moreover, the details of some specific location estimation techniques such as TOA for CRs are provided in [53]. However, according to [9], legacy positioning techniques without enhancements do not provide the required cognition capability that a CR demands. As a result, deficiencies of the existing legacy positioning systems in terms of providing cognition features such as range accuracy adaptation in our case motivate us to develop a cognitive positioning system (CPS). Basically, CPS is a location sensing method for the location awareness engine presented in the Chapter 2. The CPS can have many cognition capabilities such as range accuracy adaptation and seamless positioning. However, in this chapter, our aim is to realize the range accuracy adaptation behavior of the bats in the CPS.

TOA, signal strength, and angle-of-arrival (AOA) legacy location estimation techniques can be considered as candidates for the proposed CPS, if they can be enhanced with cognition capabilities.

AOA techniques are mostly implemented by means of antenna arrays. But, angulation employing antenna arrays is not suitable for rich multipath environments such as indoor UWB propagation channel due to the cost and imprecise location estimation [54]. On the other hand, signal strength based methods provide high accuracy only for the short ranges since the Cramer-Rao Lower Bound (CRLB) for these methods depend on the distance [52]. Moreover, performance of the estimator for signal strength techniques depends on the channel parameters such as the path loss factor and standard deviation of the shadowing effects. Additionally, CR does not have much control over the channel parameters but to measure them in order to adjust the accuracy. Since the accuracy of TOA techniques mainly depends on the parameter that transceiver can control, it is the most suitable location estimation technique for the CPS. Therefore, TOA technique is adopted for the CPS in order to estimate location information.

The type of location information that needs to be sensed plays an important role to determine the complexity of positioning systems. Hence, location information is classified into three categories based on its dimension in Chapter 2: 1-dimensional (1-D), 2-D, and 3-D. In the majority of location sensing techniques, the dimension of location information that needs to be sensed determines minimum number of reference devices required and the geometric relationship between them. For instance, distance measurements from three devices (multi-lateration) that are located in a non-collinear manner are required to estimate the location of a device in 2-D. On the other hand, estimation of the 3-D location of a device requires the distance measurements from four non-coplanar devices [55]. As a result, CR can optimize the performance and complexity of the positioning algorithm by having a priori information about the dimension of the location information. For instance, the signal traffic and power consumption due to the positioning in CRs and networks can be reduced.

3.2 Range Accuracy Adaptation

Range accuracy is one of the most essential performance metrics of cognitive location and environment aware systems. In order to support such systems, range accuracy adaptation is inevitable. Furthermore, range adaptation is one of the main cognitive behaviors of bat echolocation system [21]. The bats using frequency modulation (FM-bats) for the emission make adjustments on the emitted-sound duration, bandwidth, and repetition rate during the target (e.g. insect) approach. For instance, as the FM-bat gets closer to its target, it decreases the transmitted signal duration and increases the burst repetition rate. This is accomplished by using the feedback information provided

by the receiver, which is the distance to the target. In this chapter, range accuracy adaptation for the CPSs is introduced, nevertheless, this method can be applied to cognitive radar to accomplish bat echolocation system with range accuracy adaptation capability in cognitive radios. The proposed range accuracy adaptation method utilizes Cramer-Rao Lower Bound (CRLB) information in the transmitter as the parameter optimization criterion since it shows the relationship between range accuracy, transceiver and channel environment parameters.

Before proceeding to the details of range accuracy adaptation algorithm, it is worth to mention the challenges related designing an ideal cognitive radio transceiver due to its dynamic nature. Since the spectrum utilization is dynamic and even random, the available spectrum parameters such as carrier frequencies and corresponding bandwidths and transmit power levels can be random. Consequently, the observed channel statistics between two cognitive radios can be random. In such scenarios, radio channel needs to be monitored and modeled. As a result, the receiver algorithms and parameters will be dynamic as well. As a result, it is a challenging task to design such dynamic cognitive radio transceivers, which is a current research topic.

3.2.1 Transmitter for Range Accuracy Adaptation

The cognitive engine sends the desired range accuracy to the location awareness engine. This engine optimizes the transmission parameters for achieving the given range accuracy using CRLB. In this section, we derive the CRLB that is used as the optimization criterion for the range accuracy adaptation. In order to simplify the analysis, additive white Gaussian noise (AWGN) channel is considered. The baseband representation of receive signal $r(t)$ is given by

$$r(t) = \alpha s(t-\tau) + n(t) \ , \tag{3.1}$$

where α and τ are the path coefficient and delay, respectively, $s(t)$ is transmit baseband signal, and $n(t)$ is independent white Gaussian noise with spectral density of σ^2.

Let $\boldsymbol{\theta} = [\tau \ \alpha]$ represent the vector of unknown signal parameters. Assuming that the signals in (3.1) are observed over the interval $[0, T]$, the log-likelihood function for $\boldsymbol{\theta}$ can be expressed as [19], [56],

$$\Lambda(\boldsymbol{\theta}) = c_1 - \frac{1}{2\sigma^2} \int_0^T \left[r(t) - \alpha s(t-\tau) \right]^2 \mathrm{d}t \ , \tag{3.2}$$

where c_1 represents a constant that is independent of $\boldsymbol{\theta}$. Then, the ML estimate for $\boldsymbol{\theta}$ can be obtained from (5.2) as

$$\hat{\boldsymbol{\theta}}_{\mathrm{ML}} = \arg\max_{\boldsymbol{\theta}} \Big\{ \frac{1}{\sigma^2} \int_0^T \alpha r(t) s(t-\tau) \mathrm{d}t - \frac{E\alpha^2}{2\sigma^2} \Big\} \ ,$$

where $E = \int_0^T [s(t-\tau)]^2 \mathrm{d}t$ is the signal energy[1]. From (5.2), the Fisher information matrix (FIM) [56] can be obtained, after some manipulation, as

$$I_\theta = \begin{bmatrix} I_{\tau\tau} & I_{\tau\alpha} \\ I_{\alpha\tau} & I_{\alpha\alpha} \end{bmatrix}, \tag{3.3}$$

where the elements of FIM are given by

$$I_{\tau\tau} = \gamma \tilde{E} \ , \tag{3.4}$$

$$I_{\tau\alpha} = I_{\alpha\tau} = -\frac{\alpha \hat{E}}{\sigma^2}, \tag{3.5}$$

$$I_{\alpha\alpha} = \frac{E}{\sigma^2}, \tag{3.6}$$

where $\gamma = \alpha^2/\sigma^2$, $\tilde{E}$ and $\hat{E}$ are defined as

$$\tilde{E} = \int_0^T \left[s'(t-\tau) \right]^2 \mathrm{d}t \ , \tag{3.7}$$

$$\hat{E} = \int_0^T s'(t-\tau) s(t-\tau) \mathrm{d}t \ . \tag{3.8}$$

From the first row and column element of the inverse FIM, i.e. $\left[I_\theta^{-1} \right]_{11}$, the CRLB for unbiased time delay estimators can be obtained as

$$\mathrm{CRLB} = \frac{1}{\gamma \left(\tilde{E} - \hat{E}^2/E \right)} \ . \tag{3.9}$$

[1] Although E_i is a function of τ in general, it is not shown explicitly for convenience. The same convention is also employed for the expressions in (3.4)-(3.8).

If the channel coefficient are known, the unknown parameter vector reduces to τ. Then, the CRLB can be obtained from (3.3) as

$$\text{CRLB} = \frac{1}{\gamma \tilde{E}} \ . \tag{3.10}$$

Note that (3.10) is CRLB for generic $s(t)$ waveform. In what follows, we obtain the CRLB in (3.10) for a specific waveform, which is impulse radio. Hence, let the baseband signal $s(t)$ in (3.1) consist of a sequence of modulated pulses as follows:

$$s(t) = \sum_{l} d_l p(t - lT_s) \ , \tag{3.11}$$

where d_l is the real data[2] for the lth symbol with symbol duration T_s, and $p(t)$ represents a pulse with duration T_p, i.e., $p(t) = 0$ for $t \notin [0, T_p]$. For simplicity of expressions, it is assumed that the observation interval T can be expressed as $T = NT_s$. Consequently, $\tilde{E}$ in (3.10) can be expressed as [19]

$$\tilde{E} = 4\pi^2 N d_l^2 E_p \beta^2 \ , \tag{3.12}$$

where $E_p = \int_{-\infty}^{\infty} p^2(t) \mathrm{d}t$ and β is the effective bandwidth of $p(t)$, given by

$$\beta^2 = \frac{1}{E_p} \int_{-\infty}^{\infty} f^2 |P(f)|^2 \mathrm{d}f \ , \tag{3.13}$$

with $P(f)$ denoting the Fourier transform of $p(t)$. Furthermore, assuming that the spectral density of $p(t)$ is constant over the B, then the relationship between β and B can be obtained from (3.13) as [57]

$$\beta^2 = \frac{B^2}{3} \ . \tag{3.14}$$

By using (3.14), (3.12) and (3.10), and after some manipulation, CRLB expression in (3.10) takes the following form,

[2]Since a data-aided time delay estimation scenario is considered, the data symbols are assumed to be known.

$$\text{CRLB} = \frac{1}{\frac{4\pi^2}{3}\text{SNR}B^2} \ , \tag{3.15}$$

where SNR is defined as

$$\text{SNR} = \frac{\alpha^2 N d_l^2 E_p}{\sigma^2} \ . \tag{3.16}$$

A similar approach can be followed to derive CRLB for highly resolvable multipath propagation channels [12].

3.2.2 Receiver for Range Accuracy Adaptation

Since the proposed range accuracy adaptation method utilizes CRLB in the transmitter, there is a need to develop a location estimator that can achieve the performance of CRLB in the receiver side. Maximum a posteriori (MAP) estimator using both line of sight (LOS) and non-line of sight (NLOS) signals and maximum likelihood (ML) estimator using only LOS signals achieve the CRLB [58]. In the following section, ML range accuracy adaptation algorithm is proposed.

3.2.3 Proposed ML Range Accuracy Adaptation

CR transceiver shown in Fig. 3.1 is proposed to implement the ML range accuracy adaptation algorithm. In this algorithm, it is assumed that both CRs involved in to the range accuracy adaptation are synchronized. Furthermore, we assume that spectrum awareness engine has already the available spectrum information and environment awareness engine has the complete knowledge of the channel environment, i.e. α channel fading coefficient. In addition, it is assumed that both CRs setup ranging parameters (e.g. SNR, B) through cognitive ranging protocol presented in Chapter 7. Finally, we assume that channel changes faster than the available spectrum. The steps for the proposed ML range accuracy adaptation can be summarized as follows:

- Location awareness engine obtains the desired range accuracy σ_d from the cognitive engine.
- Location awareness engine requests and receives the available spectrum information and channel parameters from spectrum and environment awareness engines, respectively.

- Location awareness engine performs the optimization to determine the transmission parameters, i.e. B (SNR is assumed to be fixed and known) for given $\tilde{B}$, where $\tilde{B}$ is the vector representing the available absolute bandwidth. The steps for the optimization algorithm are given as follows:
  - Determine all the candidate range accuracy $\sigma_{\hat{d}}$ for all the available bandwidths $\tilde{B}$ using the following equation (i.e. $\sqrt{\text{CRLB}}$)

$$\sigma_{\hat{d}} = \frac{c}{\sqrt{\frac{4\pi^2}{3}\text{SNR}\tilde{B}^2}} \ . \tag{3.17}$$

    where c is the speed of the light.
  - Select the optimal B for the whole and dispersed spectrum case, respectively using minimum square error (MSE) metric, i.e. $min(\sigma_{\hat{d}} - \sigma_d)^2$.
- CR transmitter sends the transmission parameters to the receiver in order receiver adapt itself to the parameters.
- Adaptive waveform generator generates the waveform based on the new parameters.
- CR transmitter transmits the signal and the CR receiver process the signal using adaptive waveform processor and then estimates the time delay using ML TOA estimator algorithm.

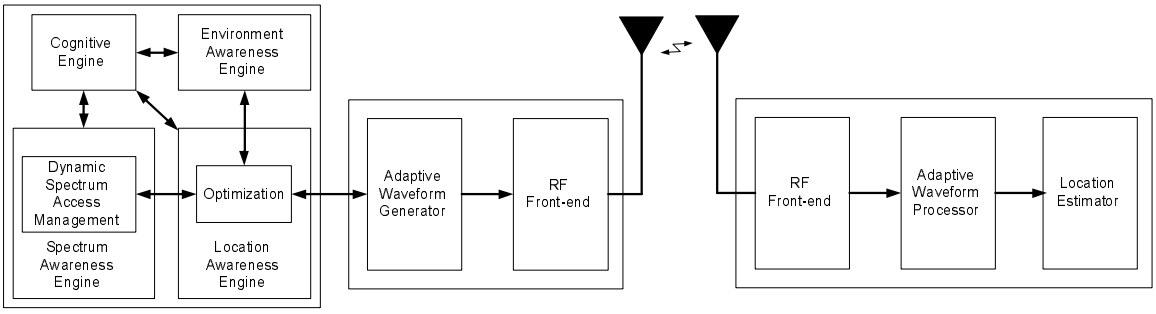

Figure 3.1 Block diagram of cognitive radio transceiver for range accuracy adaptation.

3.2.4 Main Error Sources

Any arbitrarily range accuracy is accomplished precisely using (3.15) if the parameters have infinite values. However, in practice, the value of the parameters and the corresponding resources

such as bandwidth and power are limited, which can affect the performance of range accuracy adaptation technique. In what follows, we emphasize the effects of the parameters and resources on the performance of range accuracy adaptation for the practical cases.

3.2.4.1 Dynamic Spectrum Effects

Bandwidth is one of the most important parameters that affects the performance of TOA-based range accuracy adaptation due to the randomness in the availability of bandwidth in the spectrum [17]. In other words, the distribution of available bandwidth affects the performance of range accuracy adaptation depending on the optimization method used to select the parameter values in (3.15). Furthermore, the resolution of available bandwidth also can affect the performance range accuracy adaptation. For instance, if the optimization criterion estimates the required bandwidth to be 10.335MHz and the bandwidth resolution of cognitive radio transceiver is 1 MHz, such residue in bandwidth resolution results in an additional range accuracy error.

Location of the selected available bandwidth in the spectrum, which is carrier frequency, also can affect the performance range accuracy adaptation. For instance, operating at higher carrier frequencies has some disadvantages such as higher propagation loss and lower range and penetration compared to low frequency bands [59]. In addition, weather-induced impairments and attenuation have impacts on the high frequency propagation as well [60], which can affect the performance of range accuracy adaptation. A mitigation technique to combat the aforementioned losses is to use advanced antenna systems (e.g. MIMO, beamforming) [53], [61], [62].

Another issue that can have impacts on the performance of range accuracy adaptation is the form of available bandwidth. The available bandwidth in the spectrum can be in the form of either whole or dispersed manner. For instance, if the required bandwidth is 10MHz, this bandwidth can be available mainly in two forms. The first form is 10MHz bandwidth as a chunk and the second one is the combination of multiple dispersed bandwidths that sums up 10MHz. An example to latter case is 10MHz = 3.3MHz at $f_c = 1900$MHz + 2.7MHz at $f_c = 2450$MHz + 4MHz at $f_c = 3550$MHz. The effects of these two forms of bandwidth availability on the performance of range accuracy adaptation is investigated in Chapters 4, 5, and 6.

3.2.4.2 Transceiver Effects

One of the transceiver parameters that affect the performance of range accuracy adaptation technique is the support of arbitrary bandwidth B and its resolution, which can be realized by the SDR capability of cognitive radio. Another parameter is the arbitrary transmit power level affecting SNR, which can be realized by adaptive transmit power level control feature of SDR. However, it is worth to note that the transmit power level across the spectrum is regulated by the local agencies. Another transceiver parameter in (3.15) is N, which is the length of observation symbols. The effects of this parameter on the performance of range accuracy adaptation are studied in Chapter 5. This parameter can easily be adapted by cognitive radio transceiver. However, increasing value of N improve the range accuracy with the cost of additional complexity such as overhead. Finally, the last transceiver parameter in (3.15) is d_l, which is the modulation type. The question that arise is how different modulation scheme affects the performance of range accuracy adaptation, which is investigated in Chapter 5.

3.2.4.3 Environmental Effects

The environmental parameter in (3.15) affecting the range accuracy is the channel tap coefficient α. This parameter represents the effect of channel distortion on the propagated signal and (3.15) includes this effect in order to estimate the resultant range accuracy at the receiver end. This parameter is conventionally estimated by the process known as channel estimation in the literature. However, in cognitive radios, channel environment parameters are sensed by environment awareness engine. Since (3.15) is derived for AWGN channel, the only channel propagation related parameter in the equation is α. Nevertheless, in realistic multipath channel, there are more channel environment related parameters that can affect the range accuracy such as frequency-dependency coefficient of channel [17], path loss coefficient [38], and LOS/NLOS condition [63]. For instance, the effects of frequency-dependency coefficient of channel on the range accuracy can be significant depending on the frequency-dependent feature of the radio channel, which is investigated in Chapter 4. In summary, there is a need to re-think these environmental problems from the cognitive radio perspective and develop effective solutions.

3.2.4.4 Interference Effects

Interference sources are mainly divided into two categories based on the origin of the interferers: external and internal. Multiuser interference and clutter are two examples for the external interference, and intersymbol interference and interframe interference are two examples for the internal interference. Moreover, external interference can be further split in two groups: object-oriented and device-oriented. As the names indicate that the object-oriented interference is the interference type that is originated from the objects in the surrounding environment. For instance, interference signal from the undesired objects (clutter) in the surroundings for the case of cognitive radar is an example for the object-oriented interference. Similarly, the interference originated from the undesired cognitive and non-cognitive device is referred as device-oriented interference. The aforementioned interference sources can affect the range accuracy [64]. Hence, interference avoidance, cancellation, or reduction techniques are needed to combat the interference sources.

3.2.5 Simulation Results for ML Range Accuracy Adaptation

The performance of the ML range accuracy adaptation algorithm is investigated through computer simulations. The CR transceiver shown in Fig. 3.1 is considered to obtain the simulation results in this section.

Assuming that we have a sequence of range accuracy requested by cognitive engine over a period of time. The desired range accuracy can be random due to goal driven and autonomous operation of cognitive radios. Therefore, we assume that range accuracy has a uniform distribution within $\sigma_{d,min}$ and $\sigma_{d,max}$ limits, i.e. $\mathcal{U}[\sigma_{d,min}, \sigma_{d,max}]$, where $\sigma_{d,min}$ and $\sigma_{d,max}$ are the minimum and maximum desired range accuracy, respectively. It is assumed that $\sigma_{d,min} = 8$m, and $\sigma_{d,max} = 17$m, i.e. $\mathcal{U}[8, 17]$ for the simulations.

Unlike to the conventional wireless systems, the utilized spectrum is random in addition to the channel. This implies that the transmission parameters (e.g. bandwidth, carrier frequency) are random in CR systems. Such randomness can introduce additional randomness into the channel. Consequently, the receiver needs to be adaptive to cope with the changes in transmitter and channel. For the evaluation of CR systems, there is a need to develop statistical modeling of the dynamic spectrum utilization as well as CR channel. To the best of authors' knowledge, there is not any solid study in the literature on statistical modeling of spectrum utilization and CR channel. Therefore, in

order to evaluate the performance of the proposed ML range accuracy adaptation, a simple statistical dynamic spectrum utilization model is assumed and generated in this study.

Theoretically, dynamic spectrum utilization can be modeled with four random variables, which are number of available band (R), carrier frequency (f_c), corresponding bandwidth (B), and power spectral density (PSD) or transmit power (P_{tx}). Without loss of generality, we assume that P_{tx} is constant and it is the same for the all available bands. Furthermore, we assume that all the bands have the same noise spectral density, which results in a fixed SNR value for all the bands. Since we consider baseband signal during analysis, the effect of f_c such as path loss are not incorporated into the simulations. In addition, R is assumed to be deterministic. Therefore, B is the only random variable considered during the generation of dynamic spectrum utilization in the simulation environment. As a result, B is assumed to be a uniform random variable within B_{min} and B_{max} limits, i.e. $\mathcal{U}[B_{min}B_{max}]$, where B_{min} and B_{max} are the minimum and maximum available absolute bandwidth, respectively. $B_{min} = 0.5$MHz and $B_{max} = 1$MHz are employed for the simulations. The rest of the dynamic spectrum utilization parameters are given as follows: $R = 100$, $N = 1$, and $SNR = 17$dB. The results are obtained over 3000 different channel realizations. Furthermore, we assume that $|\alpha| = 1$ provided by the environment awareness engine to the location awareness engine. For the pulse shape, the following Gaussian second order derivative is employed

$$p(t) = A\left(1 - \frac{4\pi t^2}{\zeta^2}\right) e^{-2\pi t^2/\zeta^2} \ , \tag{3.18}$$

where A and ζ are parameters that are used to adjust the pulse energy and the pulse width, respectively. A is selected in order to generate pulses with unit energy. For the given pulse shape, pulse width is defined as $T_p = 2.5\zeta$ [19]. During the transmission, the energy of transmitted signal is normalized to 1. Finally, ML TOA estimator is utilized to estimate time delay in the receiver side.

In Fig. 3.2, performance of the ML range accuracy adaptation is plotted and compared against the desired and theoretical cases. Note that (3.10) is described as exact CRLB in this section. On the other hand, the proposed ML range accuracy adaptation utilizes (3.17) as the optimization criterion, which is described as approximate CRLB. This approximation is due to the flat spectrum assumption that we made during the derivation of (3.17) from (3.10). For the sake of comparison, the performance of the proposed ML range accuracy adaptation is also compared to exact CRLB case.

In theory, if there is infinite number and value of available bandwidth and SNR, the approximate CRLB case follows the desired accuracy exactly. However, in practice, since the number and value of available bandwidth is finite, there can be a slight mismatch between the approximate CRLB case and desired accuracy as shown in Fig. 3.2. On the other hand, the ML case follows the approximate CRLB case with some margin, which is referred as correction factor. According to the results in Fig. 3.2, the first desired accuracy is 11m and the the estimated range accuracy for approximate CRLB case is 10.96m. On the other hand, the estimated range accuracy in the receiver side using ML range accuracy adaptation algorithm (i.e. ML case) is 10.06m. Moreover, the estimated range accuracy using for the exact CRLB case is 7.09m. As a result, the margin between the approximate CRLB and ML cases is 0.90m. This margin is due to the performance difference between the approximate CRLB and practical ML TOA estimator, which is investigated with details in Chapter 6. In addition, the margin between the exact and approximate CRLBs is due to the flat spectrum assumption that is made during the derivation, and this margin is also studied with details in Chapter 6. Note that the margin between the approximate CRLB and practical ML TOA estimator can be adjusted by adapting the SNR level, related parameters given by (3.16), and bandwidth. Three main approaches for improving the performance of ML range accuracy adaptation (i.e. reducing the margin between the approximate CRLB and practical ML cases) are investigated in the following sections.

Range accuracy adaptation is performed by adapting the bandwidth. Therefore, the corresponding bandwidth adaptation for the results in Fig. 3.2 is plotted in Fig. 3.3. For instance, the bandwidth is adapted from 755KHz to 916KHz in order to adapt range accuracy from 10.06m to 8.38m. The bandwidth adaptation can be implemented using software defined radio (SDR) feature of cognitive radios [9].

3.3 Performance Improvement Approaches for Range Accuracy Adaptation

The following are three potential ways for improving the performance of range accuracy adaptation method:

- Increasing the bandwidth availability through Hybrid Overlay and Underlay Dynamic Spectrum Access Systems,
- Dispersed spectrum utilization method,

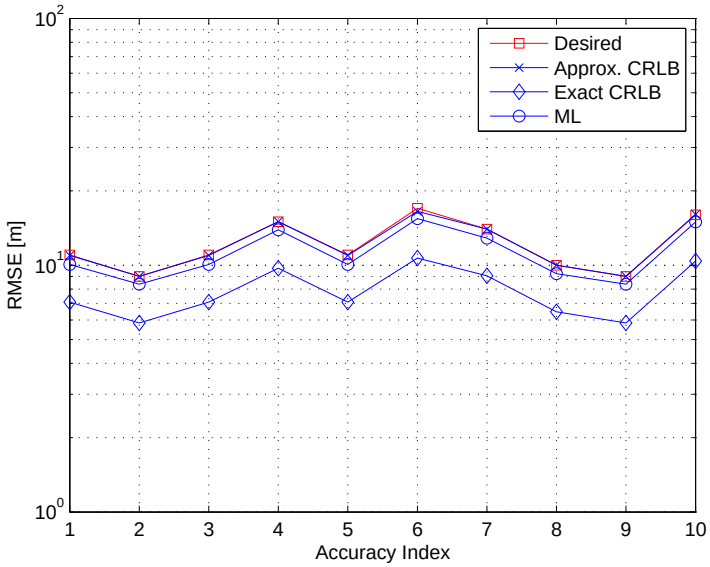

Figure 3.2 Performance of maximum likelihood range accuracy adaptation in whole spectrum utilization case.

- Using suboptimal lower bounds such as Ziv-Zakai lower bound (ZZLB) for the parameter optimization.

In this section, we emphasize on the first approach and the second approach is investigated with details in Chapters 5 and 6. The last option is not investigated in this dissertation, which can be considered as a future research topic.

3.3.1 Dynamic Spectrum Access Systems

The main task of dynamic spectrum access systems is to have complete knowledge of spectrum utilization and provides the available spectrum information to cognitive radio and its engines. There are two main approaches for spectrum access in the literature, which are overlay (opportunistic) and underlay [53], [65]. In the former approach, unlicensed users are allowed to utilize the licensed bands in opportunistic and non-interfering manners and temporarily in the absence of the associated licensed users. On the other hand, the basic idea behind the latter approach is permitting low power unlicensed users, which operate at the noise level of the licensed users, to utilize the licensed bands simultaneously with the associated licensed users.

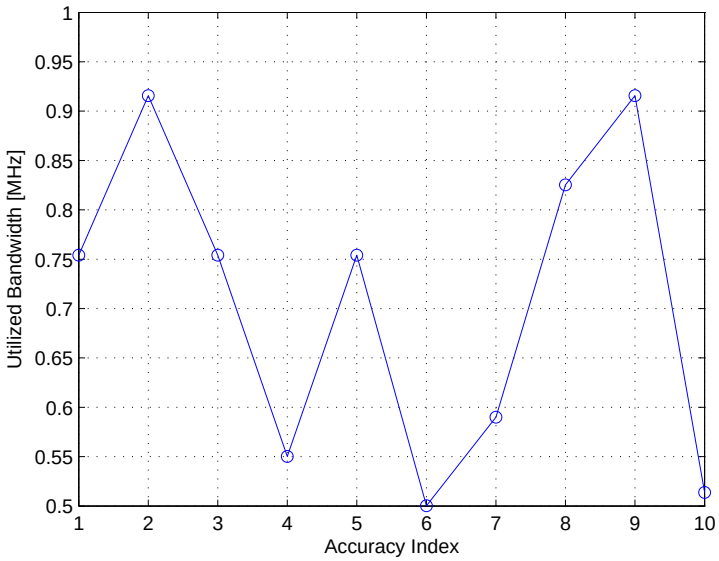

Figure 3.3 Bandwidth adaptation in maximum likelihood range accuracy adaptation.

Probability of finding unused bands in the spectrum is one of the main metrics behind the idea of dynamic spectrum access systems. Some measurement results on the utilization of spectrum are reported in the literature [66], [67]. In [66], a measurement campaign is conducted to determine the usage of $30 - 3000$MHz spectrum. The results show that only 13% of the this spectrum is utilized on average. Furthermore, similar measurement campaign is performed for $3 - 6$GHz frequency band. According to the results, the actual spectrum utilization in $3 - 4$GHz band is 0.4% and this drops to 0.3% in the $4 - 5$GHz band. These results imply that statistically more unused bands are available at higher frequencies (e.g. above 3GHz). However, operating at higher frequencies has some disadvantages such as higher propagation loss and lower range and penetration compared to low frequency bands [59]. Moreover, weather-induced impairments and attenuation have impacts on the high frequency propagation as well [60], which needs to be considered in the dynamic spectrum access systems. One of the methods to combat the aforementioned losses due to operating at high frequencies is to use advanced antenna systems (e.g. MIMO, beamforming) [61]. Especially, MIMO systems can be used to improve the spectrum efficiency in the dynamic spectrum access systems [53]. Furthermore, MIMO systems can be used to improve the accuracy of positioning systems [62]. In the cognitive positioning context, MIMO systems require less bandwidth than single-antenna systems for achieving a given accuracy, which is another way of improving the bandwidth efficiency in the

dynamic spectrum access systems. Although single-antenna systems are considered for the proposed CPS in this chapter, the analysis can be extended to the multiple-antenna systems case.

Achieving more approximate positioning accuracy comes with the cost of additional complexity. Therefore, overlay dynamic spectrum access systems (ODSAS) and hybrid overlay and underlay dynamic spectrum access systems (HDSAS) are two schemes that are presented in the context of the CPS to exhibit the trade-off between the positioning accuracy and the complexity of dynamic spectrum access systems.

3.3.1.1 Overlay Dynamic Spectrum Access Technique

ODSAS is the conventional way of accessing and utilizing the spectrum. Efficient usage of the spectrum depends on the performance of spectrum shaping technique that is employed. OFDM is one of the strongest candidate for spectrum shaping in CR technology. There are two type of OFDM-based spectrum shaping techniques, which are single band-OFDM (SB-OFDM) and multi band-OFDM (MB-OFDM) [9]. As the name implies, the former shapes the spectrum using single bandwidth, whereas the latter shapes the spectrum by dividing the total bandwidth into sub-bandwidths. Ideally, it is desirable that spectrum shaping techniques allocate bandwidths to the users in uncluttered manner where there are not much gaps between them. However, in reality, the bands can be cluttered resulting in the spectrum being full instantaneously or temporarily. As a worst case scenario where there is no any available bandwidth in the spectrum, the CPS declares that it can not estimate the location of the device at the moment.

3.3.1.2 Hybrid Overlay and Underlay Dynamic Spectrum Access Technique

The amount of available spectrum (e.g. bandwidth) can be increased if CR can access to the spectrum in both overlay and underlay manners, which is referred as hybrid overlay and underlay dynamic spectrum access systems (HDSAS). Since underlay dynamic spectrum access techniques provide limited coverage due to the power limitations, a priori rough information regarding the distance between the target and reference CR devices $\tilde{d}$ is required. Moreover, a priori information about threshold distance d_{th} that is used to manage the transition between the overlay and underlay spectrum access modes must be available. In this section, d_{th} is defined as the coverage radius that a CR can establish a link with another CR at acceptable QoS level. If $\tilde{d} \leq d_{th}$ condition is satisfied, the underlay as well as overlay dynamic spectrum access techniques (i.e. HDSAS) can

be used. Otherwise, only ODSAS can be employed. This mechanism is referred as the switching method to manage the transition between overlay and underlay dynamic spectrum access technique in the HDSAS. Two-slope model without any obstruction between two cognitive radios is considered to derive equations for the estimation of $\tilde{d}$ and d_{th}. Alternatively, $\tilde{d}$ can be estimated from RSSI information, which is readily available in the most of wireless systems. Approximate receive power as a function of distance is given by [68]

$$P_{rx}(\tilde{d}) = P_{tx}\left(\frac{\lambda}{4\pi\tilde{d}}\right)^2\left(\frac{d_o}{d_o+\tilde{d}}\right)^2 , \tag{3.19}$$

where P_{tx} is the transmit power, λ is the signal wavelength, and d_o is the breakpoint distance. The breakpoint distance can be determined approximately by [68],

$$d_o = \frac{12h_{tx}h_{rx}f}{v} , \tag{3.20}$$

where $v = 3 \times 10^8$m/s is the speed of light, h_{tx} and h_{rx} are the heights of the transmitter and receiver antennas from the ground, respectively. In this study, we assumed that h_{tx} and h_{rx} are equal and typical h_{tx} and h_{rx} values for mobile devices in indoor environments are assumed to be 1.5m [68]. The total received power P can be defined as,

$$P(\tilde{d}) = P_{rx}(\tilde{d}) + I + \eta , \tag{3.21}$$

where I and η represent the total interference seen by the target CR receiver and thermal noise, respectively. After manipulating (3.21), the following equation in unknown $\tilde{d}$ is obtained,

$$\tilde{d}^2 + d_o\tilde{d} - \sqrt{\frac{P_{tx}}{P(\tilde{d}) - I - \eta}}\left(\frac{\lambda d_o}{4\pi}\right) = 0 . \tag{3.22}$$

By solving (3.22), the following equation for the unknown $\tilde{d}$ is obtained,

$$\tilde{d} = \left| 0.5\left[d_o + \sqrt{d_o^2 + \sqrt{\kappa}\frac{v d_o}{f\pi}} \right] \right| , \tag{3.23}$$

where $\kappa = (P_{tx}/P_{rx})$ and it can be considered as the instantaneous dynamic range of a CR transceiver. The bounds on P_{tx} and f are determined by the regulatory agencies. For instance,

Table 3.1 A numerical example for determining $\tilde{d}$ and d_{th}.

Parameter	Value	Unit
d_o	11.25	m
h_{tx}	1.5	m
h_{rx}	1.5	m
f	125	MHz
P_{tx}	-42	dBm
P_{rx}	-70	dBm
$P_{tx,max}$	-41.3	dBm
$P_{rx,min}$	-80	dBm
κ	631	-
κ_{max}	7413	-
$\tilde{d}$	14.9	m
d_{th}	20.3	m

if UWB technology is considered for underlay spectrum shaping [5] maximum P_{tx} for indoor environments is determined by Federal Communications Commission (FCC) in the United States to be -41.3dBm/MHz [43]. The allocated frequency ranges for UWB devices are $3.1-10.6$GHz and $100-960$MHz. Maximum allowable P_{tx} mandated by the regulatory agencies is denoted by $P_{tx,max}$. P_{rx} level is mainly limited by the sensitivity of CR receiver, which is defined as the minimum power level that can be detected ($P_{rx,min}$). It is reported that acceptable minimum signal level at the mobile devices is typically -90dBm [68]. The following ratio is defined as maximum dynamic range of CR transceiver,

$$\kappa_{max} = \frac{P_{tx,max}}{P_{rx,min}} \ . \tag{3.24}$$

By substituting κ for κ_{max} in (3.23), the following equation that determines d_{th} is obtained,

$$d_{th} = \left| 0.5 \left[d_o + \sqrt{d_o^2 + \sqrt{\kappa_{max}} \frac{v d_o}{f \pi}} \right] \right| . \tag{3.25}$$

A numerical example for determining $\tilde{d}$ and d_{th} is shown in Table 3.1. According to these results, CR can switch to the underlay spectrum access mode since $\tilde{d} \leq d_{th}$ condition is satisfied.

Signal-to-interference and noise ratio (SINR) is an important parameter that is used to measure the reliability of the link and it is defined as,

$$SINR = \frac{P_{tx}\left(\frac{\lambda}{4\pi d}\right)^2\left(\frac{d_o}{d_o+d}\right)^2}{I+\eta} \ . \tag{3.26}$$

The link outage probability P_{out} is given by the following equation and it can be solved in a straightforward manner [69],

$$P_{out} = Pr\Big(SINR \leq SINR_{th}\Big) \ , \tag{3.27}$$

where $SINR_{th}$ is a given threshold SINR value and $Pr(.)$ represents the probability function. In this chapter, it is assumed that connectivity is lost when $SINR$ is below a given $SINR_{th}$.

3.3.1.3 Discussions

One way of exploiting the usage of spectrum in underlay manner is to increase d_{th}. According to (3.25), d_{th} depends on the d_o, K_{max}, v, and f. By assuming that h_{tx}, h_{rx}, and v are fixed parameters, K_{max} and f are the main controllable parameters that affects d_{th}. The parameter f has two main effects on d_{th}. According to the first effect, d_{th} is inversely proportional to f, which can be seen clearly in (3.25). This effect can be explained by the relationship between the frequency and radiated ("on the air") power. According to the second effect, which can be explained by f in (3.20), f is proportional to d_{th}. This implies that increasing f will increase breakpoint distance, which translates into an increase in d_{th}. As a result, it is recommended to consider these two effects during the estimation of the optimum f, which is out of scope of this chapter.

The second main parameter that affects the d_{th} is K_{max}, which consists of $P_{tx,max}$ and $P_{rx,min}$ parameters. The former one is determined by the regulatory agencies whereas the latter one is determined by the designer and it is limited by the hardware capabilities. The performance of CR transceiver are limited between these two bounds, but it can have a capability to operate adaptively between the bounds. Hence, the effects of K_{max} on d_{th} is studied and the results are plotted in Fig. 3.4 (h_{tx} = 1.5m, h_{rx} = 1.5m, f = 125MHz, $v = 3 \times 10^8$m/s). The results agree with the statement that K_{max} is proportional to the d_{th}.

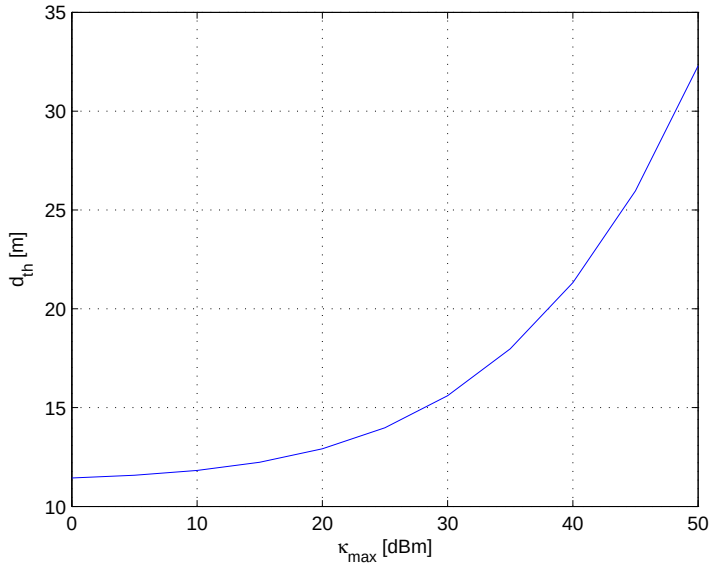

Figure 3.4 The effects of maximum dynamic range (κ_{max}) on the distance threshold (d_{th}).

CRLB, which provides optimum performance, is utilized for the parameter optimization in the proposed ML range accuracy adaptation. However, it is difficult (especially for multipath case) to approach to the lower bound in practice due to the non-linear characteristic of the devices in CR transceivers. Furthermore, samples at or above Nyquist rate are required since the CRLB are derived through ML estimation. Since the available B is dynamically changed in the CPS, sampling rate is not an issue for the small B, whereas it can be an issue for the large B. Either the signal can be downconverted to reduce the analog-to-digital converter (ADC) requirements or it can be assumed that CR has software defined radio (SDR) [9] capability to digitize the signal at high sampling rates. Dynamically changing the sampling rate and characteristics of the filters such as bandwidth and center frequency in both transmit and receive chains can also be realized by the SDR feature of CR.

There are several possible ways to improve the performance of range accuracy adaptation if stringent accuracy is required. One way of doing this is to employ the proposed HDSAS scheme. Of course, this advantage comes with additional complexity and a priori information requirements, which are $\tilde{d}$ and d_{th}. On the other hand, the ODSAS is suitable for the applications where the desired accuracy requirements are relaxed relative to the HSDAS. Another solution for bringing the accuracy to the desired level as much as possible is to change SNR, related parameters, and B parameters adaptively as well. However, this improvement also comes with the cost of additional

complexity. Using super-resolution algorithms for TOA estimation to improve the accuracy [70] is another alternative technique. But, the main drawback of this technique is that the accuracy improvement for $B \geq 120$MHz is negligible. It can be concluded that there is a trade-off between the positioning accuracy and the complexity.

In this section, it is assumed that the reference and target CR devices are perfectly synchronized. However, additional accuracy error due to the imperfect synchronization (which is a practical case) needs to be included when modeling the overall performance of the proposed CPS. As a result, joint or disjoint synchronization and CPS algorithms can be developed for CRs and consequently, the effects of imperfect synchronization on the CPS performance can be investigated and quantified further.

3.4 Conclusions

In this chapter, a location sensing method that is coined as cognitive positioning systems is introduced. Range accuracy adaptation capability of the CPS is emphasized by inspiring from the range adaptation feature of the bats. Therefore, an ML TOA range accuracy adaptation algorithm is proposed. The proposed method employs CRLB information in the receiver side to optimize transmission parameters for achieving a given range accuracy. In the receiver side, ML location estimator is used to estimate time of arrival of the path. Furthermore, the main error sources for range accuracy adaptation such as dynamic spectrum, transmission, channel environment, and reception effects are discussed.

Performance of the proposed ML TOA range accuracy adaptation is studied in dynamic spectrum access environment through computer simulations. The results show that ML TOA estimator can achieve the dynamic range accuracy requirement set by the transmitter with some margin. This margin are mainly depends on the (limited) available bandwidth, SNR and related parameters such as observation interval. Three main approaches, which are HDSAS, dispersed spectrum utilization, and practical lower bounds such as ZZLB, are presented for improving the performance of ML TOA range accuracy adaptation algorithm. In this chapter, only HSDAS approach is emphasized. For the HDSAS, a switching algorithm that is used to manage the transition between underlay and overlay spectrum usage modes is presented. In what follows, simulation results along with the discussions on challenges and complexity of the implementation of the proposed ML TOA range accuracy adaptation algorithm are provided. The results show that the proposed ML TOA range

accuracy adaptation is a promising underlying algorithm for the CPS to support goal driven and autonomous location and environment aware systems.

Note that performance of the proposed ML TOA range accuracy adaptation algorithm is studied for AWGN channel. The analysis is extended to the multipath channels considering large bandwidth assumption, where the multipaths are highly resolvable. Performance of the ML TOA range accuracy adaptation can be studied for multipath channel environments further. Finally, multipath channel analysis can be unified for all the types of band-limited signals, where the paths can be overlapped and/or non-overlapped depending on the transmission bandwidth and environment.

CHAPTER 4

TIME DELAY ESTIMATION USING WHOLE SPECTRUM UTILIZATION APPROACH

4.1 Ranging in Dynamic Spectrum Access Systems

Cognitive radio with dynamic spectrum access systems (DSAS) [71] are promising systems to keep up with constantly increasing quality-of-service (QoS) requirements that are demanded by both users and service providers. Ranging algorithms, which provide distance information of the users, can play a crucial role to improve the QoS of cognitive wireless networks. Although ranging information has traditionally been used for the network authorization and positioning systems, it can be utilized for network and transceiver algorithm optimization as well as location-based services (LBSs) in cognitive wireless networks [2], [9]. Hence, ranging algorithms with high-precision are desirable for cognitive wireless networks. One way of achieving high accuracy ranging (e.g. on the order of centimeter range) is to utilize large absolute bandwidth (e.g. 500MHz) during the transmission along with use of time-of-arrival (TOA) techniques at the reception [18], [54], [12]. The DSASs have an ability to utilize large absolute bandwidth at low and high frequency bands using hybrid underlay and overlay dynamic spectrum access techniques presented in Chapter 3, thanks to their agile capability of exploiting the spectrum usage. Furthermore, ranging accuracy in the dynamic spectrum access systems (DSAS) can be either dynamic or fixed and the former option is more suitable for the DSASs [12]. In order to perform an accurate analysis of high accuracy ranging algorithms, all the reported propagation characteristics of wireless channel, including the frequency-dependent feature (FDF) [43], [72], [73] and phase of multipath components (MPCs), need to be considered. In [54], [74], time-domain Cramer-Rao bound (CRB) is derived for ultrawideband (UWB) ranging. However, CRB is derived by considering only the (real) multipath gains and delays.

In this section, asymptotic frequency-domain CRB for TOA high accuracy ranging algorithms in the DSASs, which take the phase information and FDF of MPCs (FDF-MPCs) into account, is derived using Whittle formula [75], [76]. Due to the dynamic nature of the DSASs, the effects

of absolute bandwidth, operating center frequency, and FDF-MPCs on the ranging accuracy are investigated. The results along with remarkable conclusions are outlined.

4.1.1 System Model

TOA high accuracy ranging algorithm can be implemented either using Impulse-radio (IR) or Multiband-orthogonal frequency division multiplexing (MB-OFDM) technologies. However, IR provides better ranging accuracy than MB-OFDM [74]. Hence, IR is considered in this section where a pulse stream is transmitted. Moreover, single pulse system is adopted for the sake of analysis in which a single pulse $p(t)$ is transmitted over a symbol duration T_s. As a result, the transmitted signal is defined as $s(t) = \sqrt{\varepsilon}\sum_k b[k]p(t - kT_s)$, where $b[k]\epsilon\{+1, -1\}$ is the training sequence that is known by the receiver and ε is the symbol energy that is assumed to be unity for the sake of simplicity.

The CRB for the ranging algorithm can be derived in various ways and the selected method can affect the accuracy of the lower bound. Due to the inclusion of FDF-MPCs to the channel transfer function, a frequency-domain approach that is based on Whittle formula is adopted to derive the CRB in this section. Time-domain received signal $r(t)$, which is assumed to be stationary zero-mean Gaussian [76], is given by,

$$r(t) = h(t) \otimes s(t) + n(t) \ , \tag{4.1}$$

where $n(t)$ is noise signal that is statistically independent from the source signal, $\otimes$ is the convolution operation, and $h(t)$ is the channel impulse response including the FDF-MPCs. The corresponding channel transfer function including the FDF-MPCs is given by [73],

$$H(w) = \sum_{l=1}^{L} U_l(w) \ , \tag{4.2}$$

where L is the number of MPCs and $U_l(w)$ is defined as,

$$U_l(w) = \alpha_l e^{j\phi_l} e^{-jw\tau_l} F_l(w) \ , \tag{4.3}$$

where α_l, ϕ_l, and τ_l are the gain, phase, and delay of lth MPCs, respectively. The FDF-MPCs is denoted as $F_l(w)$ in (4.3). There exist two different models for FDF-MPCs [43], [73] to the best of the author's knowledge. Here, we adopt the model in [73] to derive the CRB since it is more

generic. According to this model, $F_l(w)$ is defined as $w^{-\beta_l}$, where β_l is the frequency-dependent path coefficient (FDPC) of lth MPCs. As a result, the frequency-domain received signal $R(w)$ is given by,

$$R(w) = H(w)S(w) + N(w) \ , \tag{4.4}$$

where $S(w)$ and $N(w)$ are the frequency-domain representation of $s(t)$ and $n(t)$, respectively.

4.1.2 The Asymptotic Frequency-domain Cramer-Rao Bound

To derive a general expression of CRB, Fisher Information Matrix (FIM) is formed first. In the sequel, let $4L \times 1$ unknown channel vector $\boldsymbol{\theta}$ be,

$$\boldsymbol{\theta} = [\tau_1, ..., \tau_L, \beta_1, ..., \beta_L, \alpha_1, ..., \alpha_L, \phi_1, ..., \phi_L] \ . \tag{4.5}$$

The corresponding FIM J_θ has the dimension of $4L \times 4L$ and it takes the following form,

$$J_\theta = \begin{bmatrix} J_{\tau\tau} & J_{\tau\beta} & J_{\tau\alpha} & J_{\tau\phi} \\ J_{\beta\tau} & J_{\beta\beta} & J_{\beta\alpha} & J_{\beta\phi} \\ J_{\alpha\tau} & J_{\alpha\beta} & J_{\alpha\alpha} & J_{\alpha\phi} \\ J_{\phi\tau} & J_{\phi\beta} & J_{\phi\alpha} & J_{\phi\phi} \end{bmatrix} \ , \tag{4.6}$$

where each entry of the FIM J_{xy} ($x = \{\tau, \beta, \alpha, \phi\}$, $y = \{\tau, \beta, \alpha, \phi\}$) is an $L \times L$ submatrix with the elements of $[J_{xy}]_{mn}$ ($m = 1, ..., L$, $n = 1, ..., L$). The elements of these submatrices are obtained asymptotically using Whittle formula [75], [76],

$$[J_{xy}]_{mn} = \frac{N}{4\pi} \int tr\Big(\frac{\partial P_R(w)}{\partial x_m} P_R^{-1}(w) \frac{\partial P_R(w)}{\partial y_n} P_R^{-1}(w) \Big) dw, \tag{4.7}$$

where $tr(.)$ is the matrix trace operation and $N = 2BT_o$ is the number of samples at Nyquist rate in which B and T_o are the bandwidth and observation interval, respectively. The observation interval T_o equals to KT_s, where K is the number observation symbols. In (4.7), $P_R(w)$ is the spectral density function of $R(w)$ and it is given by,

$$P_R(w) = P_H(w)P_S(w) + P_N(w) \ , \tag{4.8}$$

where $P_H(w)$, $P_S(w)$, and $P_N(w)$ are the spectral density function of $H(w)$, $S(w)$, and $N(w)$, respectively. These functions are given as follows,

$$P_H(w) = E[H(w)H^*(w)] \ , \tag{4.9}$$

$$P_S(w) = E[S(w)S^*(w)] \ , \tag{4.10}$$

$$P_N(w) = E[N(w)N^*(w)] \ , \tag{4.11}$$

where $E[.]$ and $*$ are the expected value and conjugate operators, respectively. It is assumed that $P_S(w)$ is known at the receiver. The closed-form of all elements of FIM J_{xy} are derived and given in the Appendix A[1]. It is known that the CRB is obtained by the inverse of FIM. Hence, the CRB of each $\hat{\tau}_l$, which are the parameters of interest, are obtained using (4.6) as follows,

$$CRB(\hat{\tau}_l) = \frac{[\boldsymbol{\gamma}]_{l,l}}{|J_\theta|} \ , \tag{4.12}$$

where $\boldsymbol{\gamma}$ is the cofactor (matrix) for $J_{\tau\tau}$ that is given in the Appendix A and $|.|$ is the determinant operator. Based on (4.12) and $\hat{\tau} = \hat{d}/c$ formula, where $\hat{d}$ is the estimated distance and c is the speed of light that is assumed to be 3×10^8m/s, the standard deviation of distance estimation error for each lth MPCs $\sigma_{\hat{d}_l}$ is obtained as follows,

$$\sigma_{\hat{d}_l} = c\sqrt{\frac{[\boldsymbol{\gamma}]_{l,l}}{|J_\theta|}} \ . \tag{4.13}$$

4.2 Ranging Related Channel Statistics

Impulse radio-ultrawideband (IR-UWB) is one of the leading technologies for high accuracy ranging applications and it has the capability to provide centimeter ranging accuracy due to high time resolution of UWB signaling [54]. Popular localization techniques typically use time-of-arrival (TOA), direction-of-arrival (DOA), or signal-strength (SS) information which are estimated from the received signal. Time-based approaches, especially TOA algorithms, are more suitable for UWB ranging systems among these techniques [54].

Appropriate ranging algorithm development for TOA IR-UWB systems requires a good understanding of the ranging related channel statistics. A limited number of such statistics are identified

[1]For the sake of simplicity, 'w' is dropped.

for specific algorithms and modeled using measurement data in [77], [78], [79] and some of IEEE 802.15.4a channel models in [80]. In [77], a TOA ranging scheme using UWB radio link is proposed. Relative path strength and the delay between the strongest and direct paths are two critical parameters used for the proposed algorithm. These parameters are modeled statistically using a set of propagation measurements. In [78], some frequency domain measurements are performed for indoor geolocation applications (especially for WLAN applications) to measure the TOA of the first path. By using the data from the measurements, the effects of sampling period of radio channel (in both time and frequency domain), multipath and filtering on the accuracy of the distance estimation are studied.

In [79], the impact of some of the standard channel parameters on the performance of various UWB transmission schemes such as Rake receivers and Transmitted-reference (TR) systems are discussed briefly without providing analytical or simulation results. Furthermore, the effects of different receiver structures such as Stored-reference (SR) systems, TR and Energy detectors (ED) on the performance of TOA IR-UWB systems are analyzed and evaluated for CM1 and CM2 channel models of IEEE 802.15.4a standard in [81].

The previous studies motivate us to develop and study a unified list of TOA ranging related channel parameters and their statistics. Hence, in this section, we identify and investigate such parameters that have an impact on TOA IR-UWB ranging and obtain their statistics using computer simulations. The effects of the IEEE 802.15.4a channel models that represent different channel environments are discussed and impact of different type of receivers on these parameters are studied.

The discrete-time complex baseband channel impulse response (CIR) of IEEE 802.15.4a channel models is given in general as [82]

$$h[n] = \sum_{l=0}^{L} \sum_{k=0}^{K} a_{k,l} e^{j\phi_{k,l}} \delta[n - T_l - \tau_{k,l}] \ , \tag{4.14}$$

where $a_{k,l}$ is the tap coefficient of the kth multipath component (MPC) in the lth cluster, T_l is the delay of the lth cluster, $\tau_{k,l}$ is the delay of the kth multipath component relative to the lth cluster arrival time T_l. The phases are denoted as $\phi_{k,l}$ and it is a uniformly distributed random variable within the range of $[0, 2\pi]$. The number of clusters and MPCs are denoted as L and K, respectively.

In order to obtain the distance between a transmitter and a receiver in TOA ranging techniques, time delay information of the first arriving path is used. The algorithms that search for the first

arriving path typically start the search from the strongest path [77, 80]; therefore, the paths prior to the strongest path are candidates for the leading edge of the signal. For the sake of discussion, let the discrete-time representation of the first arriving path and strongest path be denoted as the leading edge sample (LES) and peak sample (PS), respectively. It is assumed that the CIR has finite number of taps ($n = 0, 1, ..., N-1$). The index of the LES (n_{le}), which is the index of the first tap, is then given by

$$n_{le} = \min\left\{n \middle| h[n] \neq 0\right\}, \tag{4.15}$$

The PS is defined as the tap with maximum coefficient. Consequently, the index of PS is given by

$$n_p = \underset{n}{\text{argmax}}\{h[n]\}. \tag{4.16}$$

4.2.1 IEEE 802.15.4a Channel Models

Detection of the first arriving path and the ranging accuracy highly depends on the multipath channel characteristics. Extensive research have been carried out in the past in order to model the UWB CIR in (4.14) for different environments. While IEEE802.15.3a channel models [83] are the first standardized channel models for UWB systems, a more comprehensive set of channel models was recently developed under the IEEE 802.15.4a standardization group [82]. The latter standard provides nine different channel models for different environments including LOS and NLOS scenarios [82], which are shown in Table 4.2. A comparison of both channel models can be found in [79] and a more detailed information for each IEEE 802.15.4a channel model such as range coverage and frequency range is reported in [82].

The IEEE 802.15.4a standard channel models have few important characteristics that are very critical for UWB ranging applications [84]. One of these characteristics is the frequency-dependent path loss, which indicates that the distortion of each separate multipath component depends on the frequency. Hence, the operating frequency used at transmitter affects the ranging related channel statistics. Another important characteristics that is specific to the office NLOS (CM4) and industrial NLOS (CM8) channel models is the "soft" onset concept. Due to the "soft" onset, the first arriving paths can be significantly weaker than the later MPCs in a power delay profile [84]. This implies that the detection of the first arriving path can be very challenging in such scenarios.

4.2.2 The Effects of Receiver Architectures

Although numerous types of receiver architectures are proposed for UWB communications systems in the literature, non-coherent receivers are suitable for *low-complexity* UWB ranging applications [81].

The statistics of ranging related parameters are affected by the employed receiver type. In this section, we consider the following three cases to study ranging related channel statistics:

- Channel impulse response (CIR): The statistics of ranging related parameters can be obtained directly from the CIR in (4.14) (i.e. sampled at Nyquist rate). Such an analysis may be particularly useful for coherent ranging such as using Rake receivers.

- Energy block (EB): In order to analyze the ranging related statistics when using TR (differentially coherent) and ED (non-coherent) types of receivers, the CIR in (4.14) can be passed through a square-law device and sampled at a practical sampling rate (i.e. path energies are aggregated within energy blocks). In this case, the sampling rate is much lower than that of CIR case.

- Energy block with waveform effects (EBWF): In order to model a more practical case, the CIR in (4.14) can be convolved with a practical pulse shape before passing the signal through a square-law device and sampling it. This captures the inter-pulse interference between the different multipath components and resulting statistics depend on the employed pulse shape.

Apart from the employed receiver type, there are few other receiver-related factors that may have impacts on ranging-related channel statistics.

- Antenna has an impact on the statistical parameters of ranging applications due to frequency dependence of the antenna characteristics.

- Filtering operations in the receiver chain may also affect the ranging related channel statistics. Since filtering introduces side-lobes prior to the leading edge of the signal (in time domain), the filtering effects may yield additional distance estimation errors [78]. Hence, mitigation of filtering effects is required at the receiver in order to improve TOA ranging accuracy.

Noise level and multiuser interference [54] are some other parameters that may have effects on ranging related channel statistics.

4.2.3 Channel Statistics for Practical TOA Ranging Algorithms

The illustration of channel statistics for practical TOA estimation is shown in Fig. 4.1. The following ranging related channel statistics are identified based on three parameters in (4.14), which are amplitude, phase and delay of MPCs.

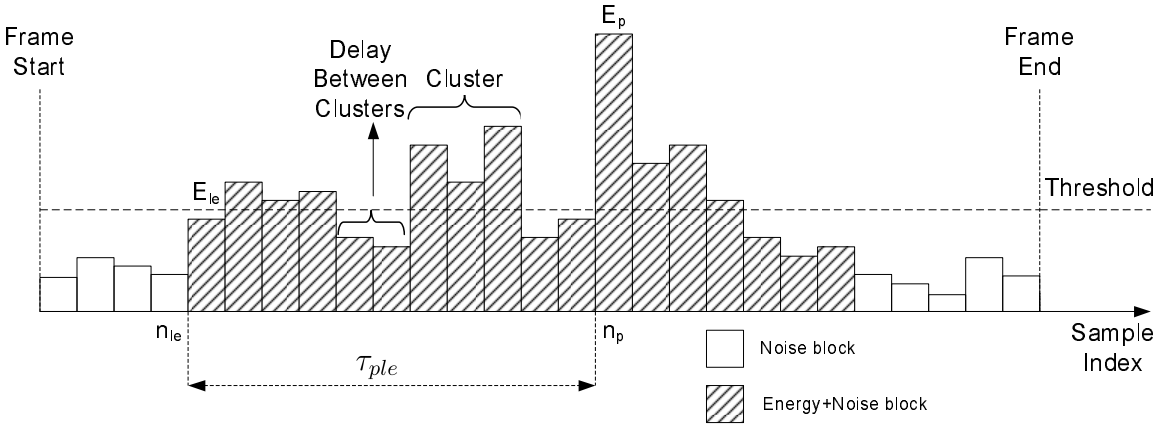

Figure 4.1 Illustration of time of arrival (TOA) ranging related channel statistics.

4.2.3.1 Statistics of Amplitude and Phase of the Leading Edge and Peak Samples

These statistics are helpful for setting a threshold to detect LES and for the identification of line-of-sight (LOS) and non-line-of-sight (NLOS) environments. The accuracy of the ranging algorithm can be improved with the knowledge of these statistics since the leading edge detection threshold and searchback window length [80] (or the search stopping rule [77]) can be determined more accurately. The phase statistics can be useful for coherent ranging systems.

The energy of the LES (E_{le}) and PS (E_p) are two important parameters that affect ranging accuracy. In this section, we will analyze the mean energy of the LES ($\overline{E_{le}}$) and PS ($\overline{E_p}$) rather than the complete statistics of the amplitude and phase.

4.2.3.2 Statistics of the Delay Between the Leading Edge and Peak Samples

Delay between the peak and the leading edge samples (τ_{ple}) can be useful for determining the complexity and accuracy of search algorithms and for identifying the LOS and NLOS environments.

4.2.3.3 Statistics of Number of Clusters Prior to the Peak Sample

Number of clusters prior to the peak sample (Λ) is an important statistical parameter, since it determines the number of noise-only clusters between signal clusters and thus may have an impact on threshold selection. This may affect the performance of certain searchback algorithms [85].

4.2.3.4 Statistics of Number of Delays Between Clusters that are Prior to the Peak Sample

Number of delays between clusters that are prior to the peak sample (γ) is also important for setting a threshold in certain searchback algorithms. The statistical information of the noise samples prior to the LES can also affect the performance of search algorithms [85].

In addition to above statistics, the power delay profiles (PDP) of different channel models, and the probability density function (PDF) of the energy within different samples are other important statistics which may have effects on the ranging algorithms (however, they will not be analyzed further in this dissertation).

4.2.4 Results and Discussions

Due to the nature of DSASs, the utilized spectrum parameters such as absolute bandwidth B and operating center frequency f_c can be dynamic. Furthermore, channel environment can be dynamic as well. Therefore, the effects of these parameters on $\sigma_{\hat{d}}$ are investigated in this section. Since the channel models developed by IEEE 802.15.4a standard group [82] take the FDF-MPCs into account, the parameters (α, ϕ, β) of these channel models are used to obtain the results in this section. In this standard, $F_l(w)$ is modeled as $w^{-2\kappa}$, where κ is the frequency dependency of the channel environment. In this model, it is assumed that all the MPCs in a channel environment (e.g. indoor residential LOS) have the same FDPC, which is $\beta_l = -2\kappa$. However, each channel environment has different κ, which is shown in Table 4.1. Moreover, Gaussian second derivative pulse shape with the duration of 2ns is considered.

The impacts of B on $\sigma_{\hat{d}}$ is studied and the results are plotted in Fig. 4.2 (Top figure: $\kappa = 1.12$, $f_c = 6$GHz, CM1 channel model parameters [82]). According to the results, increasing B improve the ranging accuracy even in the presence of FDF-MPCs. For instance, increasing B from 600MHz to 1000MHz improves the ranging accuracy from 5.53m to 46cm at -8dB SNR level. Similarly, the effects of f_c on $\sigma_{\hat{d}}$ is investigated and the results are shown in Fig. 4.2 (Bottom figure: $\kappa = 0.12$,

Table 4.1 The measured κ values of some UWB channels.

Channel Models	κ
CM1 (Residential Indoor LOS)	1.12
CM2 (Residential Indoor NLOS)	1.53
CM3 (Office Indoor LOS)	0.03
CM4 (Office Indoor NLOS)	0.71
CM5 (Outdoor LOS)	0.12
CM6 (Outdoor NLOS)	0.13
CM7 (Industrial LOS)	-1.103
CM8 (Industrial NLOS)	-1.427

$B = 500$MHz, CM5 channel model parameters [82]). The results show that increasing f_c deteriorates the ranging accuracy. For instance, ranging accuracy degradation due to operating at $f_c = 3.5$GHz rather than $f_c = 2.5$GHz is approximately 1.75m at the SNR level of -8dB. The additional path loss that occurs at higher center frequencies due to the FDF-MPCs reduces the probability of detection of the first arrival paths and this causes a degradation in the ranging accuracy.

The effects of FDF-MPCs on the $\sigma_{\hat{d}}$ are investigated as well and the results are shown in Fig. 4.3 ($B = 500$MHz, $f_c = 6$GHz, CM1 channel model parameters [82]). According to the results, the parameter κ is inversely proportional to $\sigma_{\hat{d}}$. This implies that the ranging accuracy in

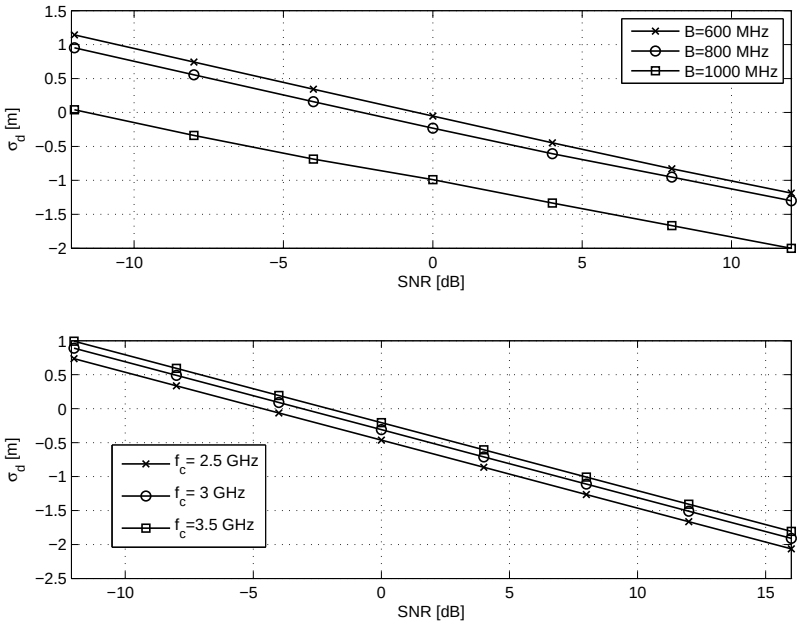

Figure 4.2 The effects of absolute bandwidth (top figure) and center frequency (bottom figure) on the standard deviation of the distance estimation error in log scale.

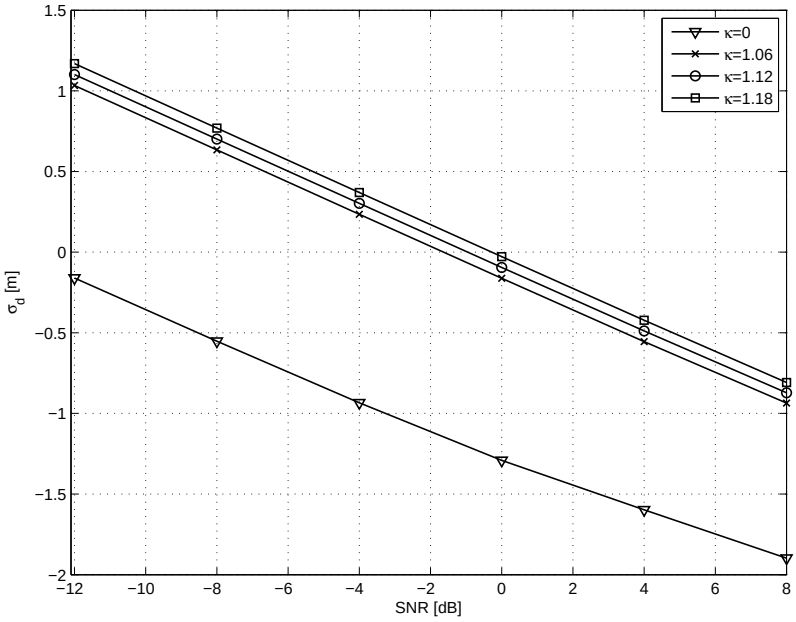

Figure 4.3 The effects of frequency dependency of the channel environment on the standard deviation of the distance estimation error in log scale.

highly frequency-dependent channel environments is worse than that of low frequency-dependent channel environments under the same conditions. For instance, the ranging accuracy is 5.88m for the channel with $\kappa = 1.18$ whereas the ranging accuracy is 4.3m for the channel with $\kappa = 1.06$ at -8dB SNR level. The reason behind this result is the reduction in the detection probability of the first arrival MPCs due to the frequency dependency of the channel. Moreover, Fig. 4.3 contains a curve for $\kappa = 0$ case that represents the propagation channel without FDF-MPCs. As it can be seen clearly, FDF-MPCs shifts up the bound significantly (5.6m for $\kappa = 1.18$ at -8dB SNR level). Hence, the effects of FDPG on the accuracy of TOA ranging algorithms can be significant depending on the frequency-dependent feature of the radio channel. Note that the results in all three figures have a common trend, which is the proportionality between the ranging accuracy and the SNR level.

We investigate the statistics of $\overline{E_p}$, $\overline{E_{le}}$, τ_{ple}, Λ, and γ through computer simulations. The results are obtained over 2000 different channel realizations for each channel model. Center frequency of 6GHz is used during the generation of all channel models. The sampling times that are used during simulations for CIR, EB, and EBWF cases are 0.1265ns, 3.79ns, and 3.79ns, respectively. For the third case, a root raised cosine (RRC) pulse with parameters $\alpha = 0.5$, $B = 500$MHz, and pulse

Table 4.2 The τ_{ple} values in ns for different channel models that have a probability of $5 \cdot 10^{-4}$.

Channel Models	CIR	EB	EBWF
CM1 (Residential Indoor LOS)	59	61	55
CM2 (Residential Indoor NLOS)	83	87	91
CM3 (Office Indoor LOS)	42	34	53
CM4 (Office Indoor NLOS)	38	38	44
CM5 (Outdoor LOS)	127	91	99
CM6 (Outdoor NLOS)	380	342	380
CM7 (Industrial LOS)	27	23	46
CM8 (Industrial NLOS)	228	154	213
CM9 (Open Outdoor NLOS)	228	222	228

Table 4.3 The values of $\overline{E_p}$ and $\overline{E_{le}}$ for different channel models.

Channel	CIR		EB	
	E_p	E_{le}	E_p	E_{le}
CM1	$164 \cdot 10^{-3}$	$129 \cdot 10^{-3}$	$419 \cdot 10^{-3}$	$338 \cdot 10^{-3}$
CM2	$73.6 \cdot 10^{-3}$	$0.76 \cdot 10^{-3}$	$304 \cdot 10^{-3}$	$68 \cdot 10^{-3}$
CM3	$131 \cdot 10^{-3}$	$63 \cdot 10^{-3}$	$449 \cdot 10^{-3}$	$422 \cdot 10^{-3}$
CM4	$52 \cdot 10^{-3}$	$11 \cdot 10^{-3}$	$230 \cdot 10^{-3}$	$139 \cdot 10^{-3}$
CM5	$114 \cdot 10^{-3}$	$55 \cdot 10^{-3}$	$368 \cdot 10^{-3}$	$317 \cdot 10^{-3}$
CM6	$76 \cdot 10^{-3}$	$0.11 \cdot 10^{-3}$	$182 \cdot 10^{-3}$	$7.9 \cdot 10^{-3}$
CM7	$181 \cdot 10^{-3}$	$104 \cdot 10^{-3}$	$739 \cdot 10^{-3}$	$725 \cdot 10^{-3}$
CM8	$782 \cdot 10^{-5}$	$2.3 \cdot 10^{-5}$	$4098 \cdot 10^{-5}$	$325 \cdot 10^{-5}$
CM9	$398 \cdot 10^{-3}$	$1.1 \cdot 10^{-3}$	$654 \cdot 10^{-3}$	$60.6 \cdot 10^{-3}$

duration of 4ns are used. The effects of antennas, filters, and noise level are not included in the simulations.

The $\overline{E_p}$ and $\overline{E_{le}}$ values for all nine channel models and for CIR and EB cases are tabulated in Table 4.3. For all channel models, the $\overline{E_p}$ and $\overline{E_{le}}$ values of EB case are larger than those of CIR case due to aggregation of path energies within the block duration. Although using energy blocks increases the energy of both LES and PS, the noise energy also increases in practice. Nevertheless, aggregation of path energies within block duration may increase the probability of detection of both LES and PS. This advantage comes with the cost of an additional error in accuracy of distance estimation due to decrease in the path resolution. $\overline{E_p}$ and $\overline{E_{le}}$ values of all LOS channels for both CIR and EB cases are larger than those of corresponding NLOS channels. These results indicate that detection of both LES and PS in LOS environments are easier than NLOS ones. The CM7-EB and CM8-CIR cases have the largest and lowest $\overline{E_{le}}$ values, respectively.

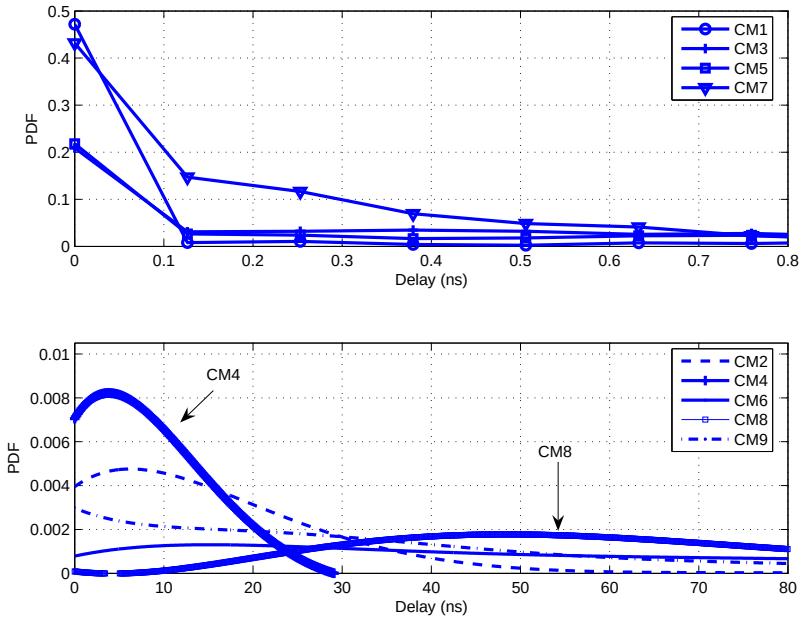

Figure 4.4 The statistics of the delay between the peak and leading edge sample (τ_{ple}) based on channel impulse response for line of sight (LOS) and non-line of sight (NLOS) environments.

The PDFs of τ_{ple} for CIR and EB for all the channel models are presented in Fig. 4.4 and 4.5 where we used 10^{th} order polynomial curve fits to smooth the results. Also, the values of τ_{ple} that has a probability of $5 \cdot 10^{-4}$ for all the cases are tabulated in Table 4.2. According to Fig. 4.4, minimum value of τ_{ple} is 0ns for all channels. For the CIR case, CM1 and CM8 are the channels that have the highest and lowest probability for $\tau_{ple} = 0$ (i.e. PS is the LES), respectively. This implies that CM1 has the highest probability that the first arriving path is the strongest path, which is desirable for ranging applications. For CM8 channel, the probability of the first arriving path to be the strongest path is about zero. This is due to the first arriving paths of CM8 being very weak (soft onset effects). For the CIR case, maximum and minimum upper limit of τ_{ple} are observed for CM6 (380ns) and CM7 (27ns), respectively. It is concluded that the most complex and the least complex search algorithms (in terms of timing estimation) will be required most likely for CM8 and CM7 channels, respectively.

According to Fig. 4.5, the probability of τ_{ple} being zero for all channels in EB case are larger than those in CIR case. This is due to the reduction of delays during the aggregation of path energies within the blocks. This also comes with an additional error in accuracy.

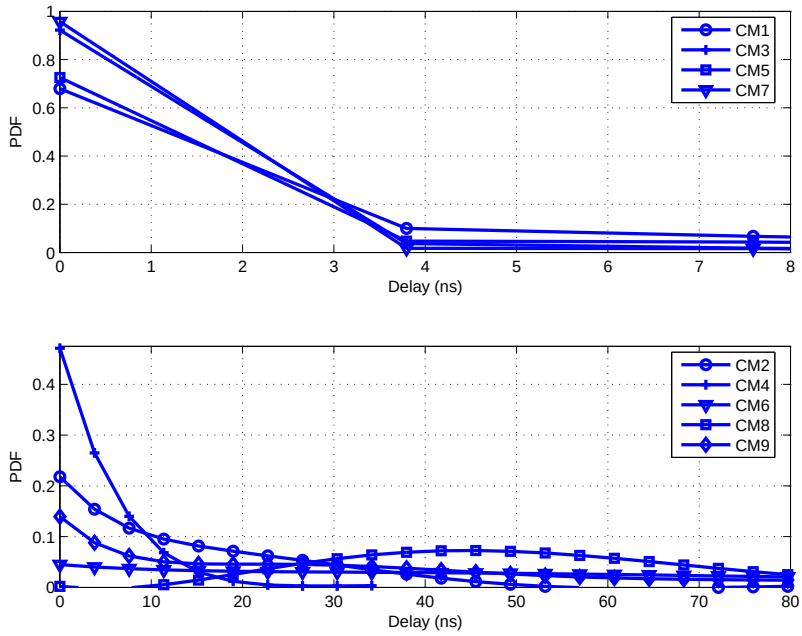

Figure 4.5 The statistics of the delay between the peak and leading edge sample (τ_{ple}) based on energy block for line of sight (LOS) and non-line of sight (NLOS) environments.

For the EB case, maximum and minimum values of τ_{ple} that has a probability of $5 \cdot 10^{-4}$ are for CM6 (342ns) and CM7 (23ns) channels, respectively. The results suggest that the block length affects the τ_{ple} statistics and consequently the complexity of the search algorithm.

Results obtained for EBWF are similar to those in EB case. The probability of τ_{ple} being zero for all channels in EBWF case are slightly lower than those in EB case. In the case of EBWF, maximum and minimum upper limit of τ_{ple} are observed for CM6 (380ns) and CM4 (44ns), respectively. Therefore, the effects of waveform on the τ_{ple} statistics is not significant.

The PDFs of Λ and γ for all LOS and NLOS channels are plotted in Figs. 4.6 and 4.7, respectively. The probability of Λ being zero for CM3, CM4, CM7, and CM8 are approximately 100%. According to [82], CM4 and CM8 channels have a single power delay profile (single cluster), which agree with our results. Maximum value of Λ for CM1, CM2, CM5, CM6, and CM9 channels are 1, 2, 1, 5, and 3, respectively. Overall, the number of clusters for the LOS channels are equal or less than those for the NLOS channels. For all channels except CM8 channel, the γ value with the highest probability is 3.79ns. In the case of CM8 channel, the probability of γ statistics for all possible delay values is zero. Maximum possible delay value for CM1, CM2, CM3, CM4, CM5, CM6, CM7, CM8, and CM9 channels are 22.74, 18.95, 18.95, 18.95, 37.9, 41.69, 18.95, 0, and 56.85ns, respectively.

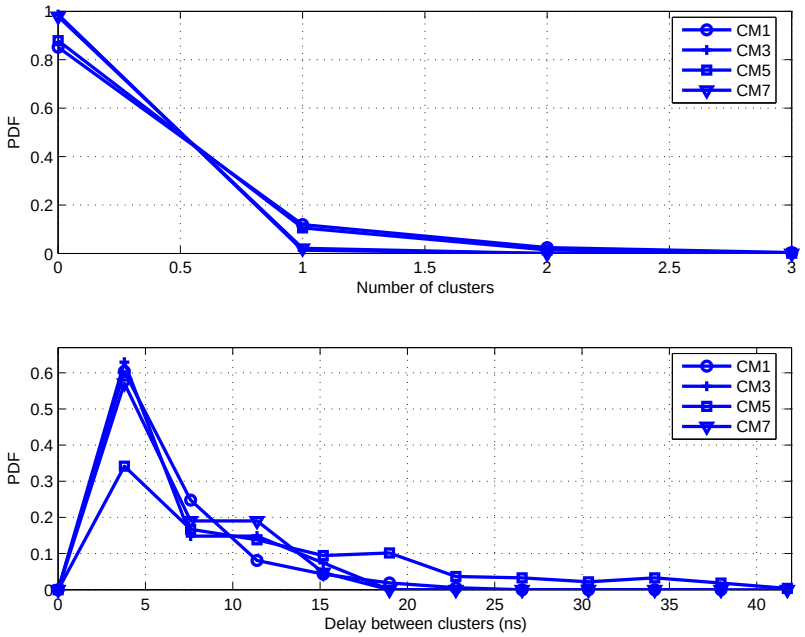

Figure 4.6 Number of clusters prior to the peak sample (Λ) and number of delays between clusters that are prior to the peak sample (γ) statistics for line of sight (LOS) environments.

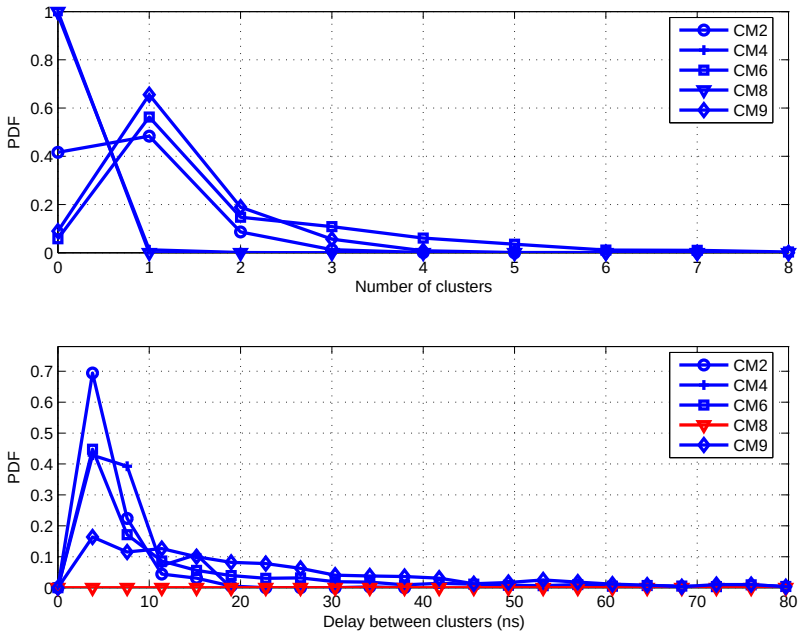

Figure 4.7 Number of clusters prior to the peak sample (Λ) and number of delays between clusters that are prior to the peak sample (γ) statistics for non-line of sight (NLOS) environments.

4.3 Conclusions

The performance analysis of TOA IR-UWB high accuracy ranging algorithm for the DSASs is carried out. The general expression of asymptotic frequency-domain CRB for the ranging algorithm, which takes the FDF-MPCs and phase information into account, is derived through Whittle Formula. The impacts of the FDF-MPCs, absolute bandwidth, and operating center frequency on the ranging accuracy are investigated. The results reveal the necessity of including FDF-MPCs into the performance analysis of TOA ranging algorithms and it is suggested to utilize as large absolute bandwidth as possible at low center frequencies in order to achieve high precision ranging in the DSASs.

In addition, a list of channel statistics specific to the ranging applications employing TOA IR-UWB systems are presented. The statistics are obtained via computer simulations by considering the impacts of different channel environments and as well as receiver structures. The results suggest that different channel environments and receivers affect the ranging related channel statistics significantly. The effects of operating frequency, antenna, filtering, and noise level on the statistics can be studied further.

CHAPTER 5

TIME DELAY ESTIMATION USING DISPERSED SPECTRUM UTILIZATION APPROACH

5.1 Introduction

One of the prominent characteristics of cognitive radio [9], [10], [20] is location awareness [2], [15], [24]. Cognitive radios with location awareness cycle [15] can support goal driven and autonomous location aware systems such as location-based services (e.g., package tracking), location-assisted network optimization (e.g., dynamic spectrum management), location-assisted transceiver optimization (e.g., adaptive beamforming), and location-assisted environment identification (e.g., propagation channel characterization), which are discussed in Chapter 7.

A conceptual architecture for cognitive radio with a location awareness cycle, which consists of a location awareness engine, sensing interface and environment loop, is presented in Chapter 2 [15]. In the same chapter [2], a conceptual model for the location awareness engine, which is the main component of a location awareness cycle, is introduced. The main tasks of the location awareness engine are location sensing, seamless positioning and interoperability, security and privacy, statistical learning and tracking, mobility management, adaptation of location aware systems, and location aware applications [2], [15]. In order to develop a location sensing method for the location awareness engine, a cognitive positioning system (CPS) along with range accuracy adaptation method is proposed in Chapter 3 [12], [16]. The CPSs use Cramer-Rao lower bound (CRLB) information at the transmitter side to optimize the transmission parameters for achieving goal driven range and position accuracy requirements. In Chapter 3, the CRLB for time delay estimation in both AWGN and multipath channels are derived, where the path delays and coefficients are assumed to be unknown. This analysis is extended in Chapter 4 by deriving the frequency-domain CRB in dynamic spectrum access systems. In Chapter 4, it is assumed that path delays, distance-dependent coefficients, phases and frequency-dependent coefficients are unknown. Furthermore, the effects of bandwidth, carrier frequency, and path frequency dependence on the CRLB in dynamic spectrum access systems are

investigated. Note that the studies in Chapters 3 and 4 are based on the fact that the available bandwidth is in the form of a single piece (i.e., the whole bandwidth). Since the available bandwidths in the dynamic spectrum access systems are dispersed [86], a single cognitive radio user can transmit and receive over multiple dispersed bands. Such method is referred as dispersed spectrum utilization systems and developed in the context of time delay estimation in this chapter.

In this chapter, fundamental limits of time delay estimation are studied in dispersed spectrum utilization systems, where the available dispersed bandwidths are assumed to be narrow. The limits are quantified in terms of the CRLBs and the effects of both unknown channel coefficients and carrier frequency offsets (CFOs) are taken into account. After deriving a generic expression, specific CRLB formulas are obtained for various modulation schemes[1]. It is shown for linear modulation schemes that the same fundamental limits can be achieved for the cases of known and unknown CFOs. In addition, it is proven that the effects of unknown channel coefficients are mitigated as well for linear modulations with constant envelopes. Finally, numerical results are presented to verify the theoretical analysis.

5.2 Signal Model

Consider a cognitive radio system that occupies K different frequency bands as shown in Fig. 5.1. The cognitive transmitter sends a signal occupying all the K bands, and the receiver wishes to calculate the time delay of the incoming signal. One way to implement such a system is to consider the received signal as an orthogonal frequency division multiplexing (OFDM) signal with zero coefficients at the sub-carriers corresponding to the unused bands [87], [88], [89]. Then, the signal can be processed as in a conventional OFDM receiver. However, the available spectrum can be very dispersed in some cases, which requires processing of very large bandwidths if the signal is considered as a single OFDM signal. In such cases, it can be more practical to process the signal in multiple branches, as shown in Fig. 5.2. Each branch considers one available band, and down-converts the signal according to the center frequency of that band. In this way, signals with narrower bandwidths can be processed at each branch. Then, the question is to determine the accuracy of time delay estimation for such a receiver structure, considering practical issues such as CFO due to the use of multiple down-conversion units.

[1]The author thanks to Dr. Sinan Gezici for his contributions to this chapter, especially for the development of Sections 5.3 and 5.4.

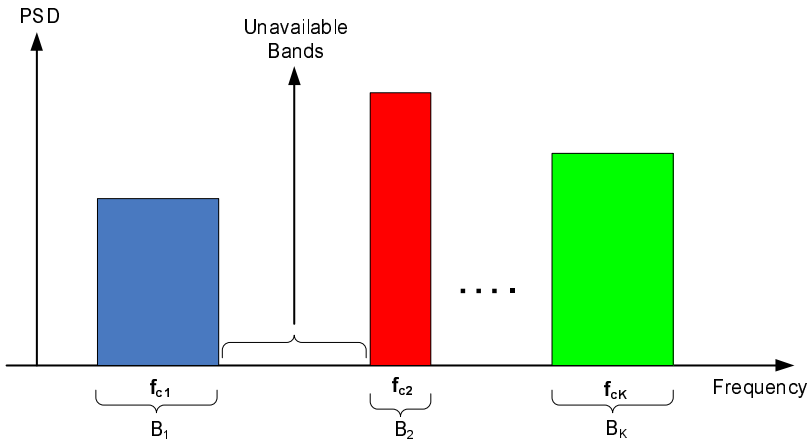

Figure 5.1 Illustration of dispersed spectrum utilization in cognitive radio systems.

The baseband representation of the received signal in the ith branch can be expressed as

$$r_i(t) = \alpha_i e^{-j\omega_i t} s_i(t-\tau) + n_i(t) \ , \tag{5.1}$$

for $i = 1, \ldots, K$, where $\alpha_i = a_i e^{j\phi_i}$ and ω_i represent, respectively, the channel coefficient and the CFO for the signal in the ith branch, $s_i(t)$ is the baseband representation of the transmitted signal corresponding to the ith band, τ is the time delay, and $n_i(t)$ is complex Gaussian noise with independent and white components, each having spectral density σ_i^2.

For the signal model in (5.1), it is assumed that the signal at each branch can be modeled as a narrowband signal. Therefore, a single complex channel coefficient is used to represent the fading of each signal.

Note that, in addition to the cognitive radio framework, the signal model in (5.1) can also represent a multiple-input multiple-output (MIMO) system, in which transmitter i sends $s_i(t)$ to receiver i, in the presence of synchronization among the transmissions, or when the receiver knows the relative delays between transmissions.

5.3 CRLB Calculations

Let $\boldsymbol{\theta} = [\tau \ a_1 \cdots a_K \ \phi_1 \cdots \phi_K \ \omega_1 \cdots \omega_K]$ represent the vector of unknown signal parameters. If the signals in (5.1) are observed over the interval $[0, T]$, the log-likelihood function for $\boldsymbol{\theta}$ is given

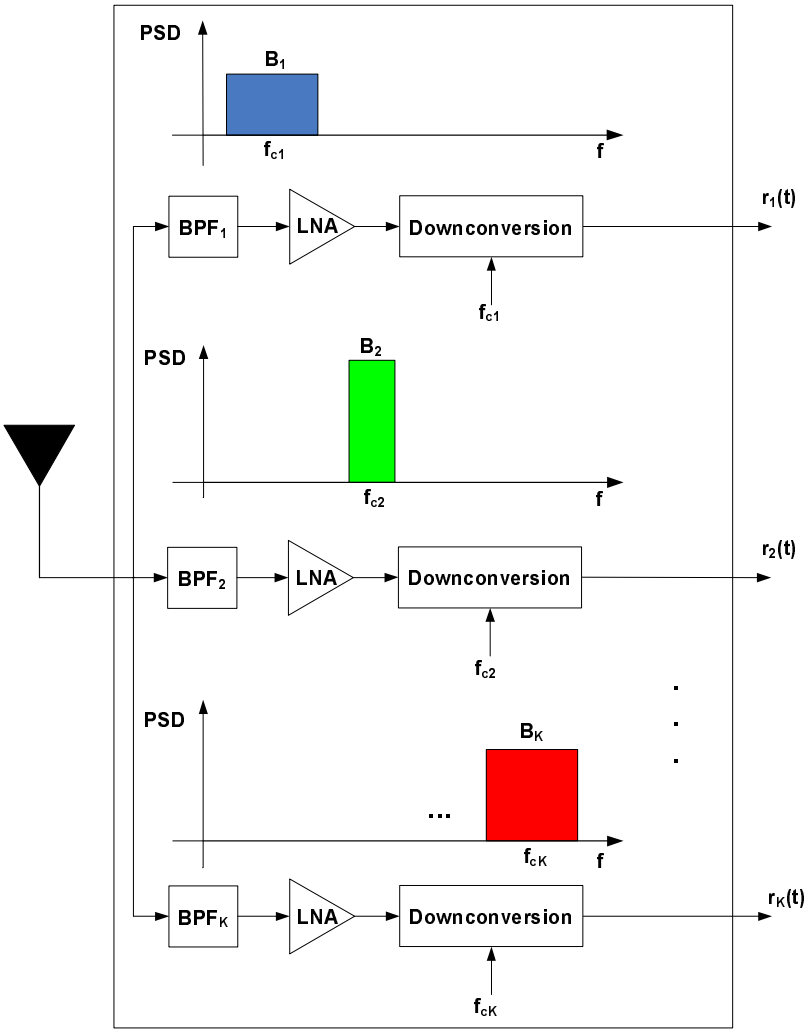

Figure 5.2 Block diagram of a cognitive radio receiver.

by [56]

$$\Lambda(\boldsymbol{\theta}) = c - \sum_{i=1}^{K} \frac{1}{2\sigma_i^2} \int_0^T \left| r_i(t) - \alpha_i \mathrm{e}^{j\omega_i t} s_i(t-\tau) \right|^2 \mathrm{d}t \ , \tag{5.2}$$

where c is a constant that is independent of $\boldsymbol{\theta}$. Then, the maximum likelihood (ML) estimate for $\boldsymbol{\theta}$ can be obtained from (5.2) as[2]

$$\hat{\boldsymbol{\theta}}_{\mathrm{ML}} = \arg\max_{\boldsymbol{\theta}} \left\{ \sum_{i=1}^{K} \frac{1}{\sigma_i^2} \int_0^T \mathcal{R}\left\{ \alpha_i^* \mathrm{e}^{-j\omega_i t} r_i(t) s_i^*(t-\tau) \right\} \mathrm{d}t - \sum_{i=1}^{K} \frac{E_i |\alpha_i|^2}{2\sigma_i^2} \right\} \ , \tag{5.3}$$

[2]For a complex number z, $\mathcal{R}\{z\}$ and $\mathcal{I}\{z\}$ represent its real and imaginary parts, respectively.

where $E_i = \int_0^T |s_i(t-\tau)|^2 \mathrm{d}t$ is the signal energy[3]. From (5.2), the Fisher information matrix (FIM) [56] can be obtained, after some manipulation, as

$$\mathbf{I} = \begin{bmatrix} \mathrm{I}_{\tau\tau} & \mathbf{I}_{\tau a} & \mathbf{I}_{\tau\phi} & \mathbf{I}_{\tau\omega} \\ \mathbf{I}_{\tau a}^T & \mathbf{I}_{aa} & \mathbf{0} & \mathbf{0} \\ \mathbf{I}_{\tau\phi}^T & \mathbf{0} & \mathbf{I}_{\phi\phi} & \mathbf{I}_{\phi\omega} \\ \mathbf{I}_{\tau\omega}^T & \mathbf{0} & \mathbf{I}_{\phi\omega}^T & \mathbf{I}_{\omega\omega} \end{bmatrix}, \tag{5.4}$$

with

$$\mathrm{I}_{\tau\tau} = \sum_{i=1}^{K} \gamma_i \tilde{E}_i \ , \tag{5.5}$$

$$\mathbf{I}_{aa} = \mathrm{diag}\left\{ \frac{E_1}{\sigma_1^2}, \ldots, \frac{E_K}{\sigma_N^2} \right\}, \tag{5.6}$$

$$\mathbf{I}_{\phi\phi} = \mathrm{diag}\left\{ E_1\gamma_1, \ldots, E_K\gamma_K \right\}, \tag{5.7}$$

$$\mathbf{I}_{\omega\omega} = \mathrm{diag}\left\{ F_1\gamma_1, \ldots, F_K\gamma_K \right\}, \tag{5.8}$$

$$\mathbf{I}_{\tau a} = -\left[\hat{E}_1^{\mathrm{R}} \frac{|\alpha_1|}{\sigma_1^2} \ \cdots \ \hat{E}_K^{\mathrm{R}} \frac{|\alpha_K|}{\sigma_K^2} \right], \tag{5.9}$$

$$\mathbf{I}_{\tau\phi} = -\left[\hat{E}_1^{\mathrm{I}}\gamma_1 \ \cdots \ \hat{E}_K^{\mathrm{I}}\gamma_K \right], \tag{5.10}$$

$$\mathbf{I}_{\tau\omega} = -\left[G_1\gamma_1 \ \cdots \ G_K\gamma_K \right], \tag{5.11}$$

$$\mathbf{I}_{\phi\omega} = \mathrm{diag}\left\{ \hat{F}_1\gamma_1, \ldots, \hat{F}_K\gamma_K \right\}, \tag{5.12}$$

where $\gamma_i = |\alpha_i|^2/\sigma_i^2$, $\mathrm{diag}\{x_1, \ldots, x_K\}$ represents an $K \times K$ diagonal matrix with its ith diagonal being equal to x_i, $\tilde{E}_i$ is the energy of the first derivative of $s_i(t)$; i.e., $\tilde{E}_i = \int_0^T |s_i'(t-\tau)|^2 \, \mathrm{d}t$, and $\hat{E}_i^{\mathrm{R}}$, $\hat{E}_i^{\mathrm{I}}$, F_i, $\hat{F}_i$ and G_i are given, respectively, by

$$\hat{E}_i^{\mathrm{R}} = \int_0^T \mathcal{R}\left\{ s_i'(t-\tau) s_i^*(t-\tau) \right\} \mathrm{d}t \ , \tag{5.13}$$

$$\hat{E}_i^{\mathrm{I}} = \int_0^T \mathcal{I}\left\{ s_i'(t-\tau) s_i^*(t-\tau) \right\} \mathrm{d}t \ , \tag{5.14}$$

$$F_i = \int_0^T t^2 \left| s_i(t-\tau) \right|^2 \mathrm{d}t \ , \tag{5.15}$$

$$\hat{F}_i = \int_0^T t \left| s_i(t-\tau) \right|^2 \mathrm{d}t \ , \tag{5.16}$$

$$G_i = \int_0^T t\, \mathcal{I}\left\{ s_i^*(t-\tau) s_i'(t-\tau) \right\} \mathrm{d}t \ . \tag{5.17}$$

[3]Although E_i is a function of τ in general, it is not shown explicitly for convenience. The same convention is also employed for the expressions in (5.13)-(5.17).

The CRLB for unbiased time delay estimators can be obtained from the element in the first row and first column of the inverse of the FIM in (5.4), i.e., $\left[\mathbf{I}^{-1}\right]_{11}$. Based on the formulas for block matrix inversion, the CRLB can be obtained as (Appendix B)

$$\mathrm{CRLB}_1 = \frac{1}{\sum_{i=1}^{K} \gamma_i \left(\tilde{E}_i - (\hat{E}_i^{\mathrm{R}})^2 / E_i \right) - \xi} \ , \tag{5.18}$$

where

$$\xi = \sum_{i=1}^{K} \gamma_i \frac{(\hat{E}_i^{\mathrm{I}})^2 F_i + E_i G_i^2 - 2\hat{E}_i^{\mathrm{I}} G_i \hat{F}_i}{E_i F_i - \hat{F}_i^2} \ . \tag{5.19}$$

In order to investigate the effects of unknown CFOs, the CRLB for time delay estimation can be obtained for known CFOs. In that case, the unknown parameter vector reduces to $\tilde{\boldsymbol{\theta}} = [\tau \ a_1 \cdots a_K \ \phi_1 \cdots \phi_K]$, and the CRLB can be obtained, similarly to the previous derivations, as

$$\mathrm{CRLB}_2 = \frac{1}{\sum_{i=1}^{K} \gamma_i \left(\tilde{E}_i - \hat{E}_i^2 / E_i \right)} \ , \tag{5.20}$$

where

$$\hat{E}_i = \left| \int_{-\infty}^{\infty} s_i'(t-\tau) s_i^*(t-\tau) \mathrm{d}t \right| = \sqrt{(\hat{E}_i^{\mathrm{R}})^2 + (\hat{E}_i^{\mathrm{I}})^2} \ . \tag{5.21}$$

Note that CRLB_2 in (5.20) is smaller than or equal to CRLB_1 in (5.18) in general, since more unknown parameters exist for the latter.

If both the channel coefficients and the CFOs are known, the unknown parameter vector reduces to τ. Then, the CRLB can be obtained from (5.5) as

$$\mathrm{CRLB}_3 = \frac{1}{\sum_{i=1}^{K} \gamma_i \tilde{E}_i} \ . \tag{5.22}$$

5.4 Special Cases

Although the CRLB can be obtained from (5.13)-(5.19) in general, its evaluation for specific signal structures can provide more intuition related to the effects of CFOs.

Let consider the baseband signal $s_i(t)$ in (5.1) to be composed of a sequence of modulated pulses as follows:

$$s_i(t) = \sum_l d_{i,l}(t) p_i(t - lT_i) \ , \tag{5.23}$$

for $i = 1, \ldots, K$, where $d_{i,l}(t)$ denotes the complex data[4] for the lth symbol of signal i, and $p_i(t)$ represents a pulse with duration T_i, i.e., $p_i(t) = 0$ for $t \notin [0, T_i]$. To simplify notation, it is assumed that the observation interval T can be expressed as $T = N_i T_i$ for an integer N_i for $i = 1, \ldots, K$.

- Proposition 1: For any linear modulation of the form $s_i(t) = \sum_l d_{i,l} p_i(t - lT_i)$, the CRLBs in (5.18) and (5.20) are equal, and are given by

$$\text{CRLB}_1 = \text{CRLB}_2 = \frac{1}{\sum_{i=1}^{K} \gamma_i \left(\tilde{E}_i - (\hat{E}_i^{\text{R}})^2 / E_i \right)} \ . \tag{5.24}$$

- Proof: When the complex data $d_{i,l}(t)$ is not time-dependent, as stated in the proposition, $s_i'(t) s_i^*(t)$ can be calculated from (6.5) as

$$s_i'(t) s_i^*(t) = \sum_l |d_{i,l}|^2 p_i(t - lT_i) p_i'(t - lT_i) \ . \tag{5.25}$$

  Since $s_i'(t) s_i^*(t)$ is a real quantity, it can be shown that $\hat{E}_i^{\text{I}}$ in (5.14) and G_i in (5.17) are equal to zero. Therefore, it can be observed from (5.19) and (5.21) that CRLB_1 in (5.18) and CRLB_2 in (5.20) reduce to the expression stated in the proposition. □

  Proposition 1 states that for most modulation types, such as pulse amplitude modulation (PAM), phase shift keying (PSK) and quadrature amplitude modulation (QAM) [90], the CRLB of time delay estimation for the case of unknown CFOs is the same as that for the case of known CFOs[5]. For non-linear modulation types, the statement in the proposition cannot be employed. For example, for FSK modulation with $d_{i,l}(t) = \exp\left\{ j2\pi \tilde{d}_{i,l} \Delta_i t \right\}$, where $\tilde{d}_{i,l}$ is the modulation data and Δ_i is the amount of frequency shift, $\hat{E}_i^{\text{I}}$ in (5.14) and G_i in (5.17) are not zero in general.

[4] Since a data-aided time delay estimation scenario is considered, the data symbols are assumed to be known.
[5] Unknown channel coefficients are considered for both cases.

- Proposition 2: For linear modulations of the form $s_i(t) = \sum_l d_{i,l} p_i(t - lT_i)$, with $|d_{i,l}| = |d_i|$ $\forall l$ and $p_i(t)$ satisfying $p_i(0) = p_i(T_i)$ for $i = 1, \ldots, K$, the CRLBs in (5.18), (5.20) and (5.22) are given by

$$\text{CRLB}_1 = \text{CRLB}_2 = \text{CRLB}_3 = \frac{1}{4\pi^2 \sum_{i=1}^{K} \text{SNR}_i \beta_i^2} \ , \tag{5.26}$$

where $\text{SNR}_i = N_i |d_i|^2 \frac{|\alpha_i|^2 E_{p_i}}{\sigma_i^2}$ with $E_{p_i} = \int_{-\infty}^{\infty} p_i^2(t) \mathrm{d}t$, and β_i is the effective bandwidth of $p_i(t)$, given by

$$\beta_i^2 = \frac{1}{E_{p_i}} \int_{-\infty}^{\infty} f^2 |P_i(f)|^2 \mathrm{d}f \ , \tag{5.27}$$

with $P_i(f)$ denoting the Fourier transform of $p_i(t)$.

- Proof: Since $|d_{i,l}| = |d_i|$ $\forall l$, $\hat{E}_i^{\text{R}}$ in (5.13) can be obtained from (5.25) as

$$\hat{E}_i^{\text{R}} = |d_i|^2 \sum_l \int_0^T p_i(t - \tau - lT_i) p_i'(t - \tau - lT_i) \mathrm{d}t \tag{5.28}$$

$$= N_i |d_i|^2 \int_{-\infty}^{\infty} p_i(t) p_i'(t) \mathrm{d}t = 0 \ , \tag{5.29}$$

for $i = 1, \ldots, K$. Note that the second equality is obtained from the fact that $T = N_i T_i$, and the final equality is due to the facts that $p_i(t)$ is non-zero only over $t \in [0, T_i]$ and satisfies $p_i(0) = p_i(T_i)$.

Since $\hat{E}_i^{\text{R}} = 0$ for $i = 1, \ldots, K$, the CRLB expression in (5.24) becomes

$$\text{CRLB}_1 = \text{CRLB}_2 = \frac{1}{\sum_{i=1}^{K} \gamma_i \tilde{E}_i} \ , \tag{5.30}$$

which is the same as the CRLB in (5.22) for the case of known CFOs and channel coefficients. In addition, $\tilde{E}_i$ can be calculated, from (6.5) and the fact that $|d_{i,l}| = |d_i|$ $\forall l$, as

$$\tilde{E}_i = \int_0^T |s_i'(t - \tau)|^2 \mathrm{d}t = |d_i|^2 \sum_l \int_0^T \left(p_i'(t - \tau - lT_i)\right)^2 \mathrm{d}t = N_i |d_i|^2 \tilde{E}_{p_i} \ , \tag{5.31}$$

where $\tilde{E}_{p_i} = \int_{-\infty}^{\infty} \left(p_i'(t)\right)^2 \mathrm{d}t$. From Parseval's relation, $\tilde{E}_{p_i}$ can be expressed as $4\pi^2 \beta_i^2 E_{p_i}$, where E_{p_i} is the energy of $p_i(t)$ and β_i is the effective bandwidth of $p_i(t)$ [56]. In what

follows, it is observed from (5.31) that (5.30) is equal to (5.26) for $\text{SNR}_i = N_i|d_i|^2\gamma_i E_{p_i}$ and $\gamma_i = |\alpha_i|^2/\sigma_i^2$. □

From Proposition 2, it is observed that for linear modulations with constant envelope, such as PSK, the CRLB for time delay estimation is the same whether the CFOs and/or channel coefficients are known or unknown for pulses satisfying $p(0) = p(T)$, which is usually the case in practice. This implies that in such cases, the ML estimators in the absence of any information on CFOs and channel coefficients can asymptotically achieve the same CRLB as the ones in presence of CFO and/or channel coefficient information [56].

5.5 Numerical Results

In this section, numerical studies are described that illustrate the CRLBs discussed in Sections 5.3 and 5.4. It is assumed that all the K bands in the system have the same bandwidth and the same pulse is employed for all of them; i.e., $p_i(t) = p(t)$ for $i = 1, \ldots, K$ (c.f. (6.5)). For the pulse shape, the following Gaussian second order derivative is employed

$$p(t) = A\left(1 - \frac{4\pi t^2}{\zeta^2}\right) e^{-2\pi t^2/\zeta^2} \ , \tag{5.32}$$

where A and ζ are parameters that are used to adjust the pulse energy and the pulse width, respectively. In the following, $\zeta = 1$ μs is employed, for which the pulse width becomes approximately 2.5 μs, and A is selected in order to generate pulses with unit energy. In addition, it is assumed that the spectral density of the noise is the same for all the K branches; i.e., $\sigma_i = \sigma$ for $i = 1, \ldots, K$, and the system SNR is defined as the sum of the SNRs in the various branches.

In Fig. 5.3, the CRLB expressions in (5.18), (5.20) and (5.22), labeled as CRLB_1, CRLB_2 and CRLB_3, respectively, are plotted versus SNR for three different modulation types, namely 16FSK[6], 16QAM, and 16PSK. For all cases, it is assumed that the same modulation sequence is used at different branches; i.e., $d_{i,l}(t) = d_l(t)$ for $i = 1, \ldots, K$, and that the channel amplitudes are normalized to unity; i.e., $|\alpha_i| = 1$ for $i = 1, \ldots, K$. In addition, the modulation sequence for each modulation type is scaled appropriately so that the sequences have the same energy in all cases. Also, there are $K = 3$ branches in the system, and $N = 2$ symbols are received at each branch. From the figure, it is first observed that for all the modulations, $\text{CRLB}_3 \leq \text{CRLB}_2 \leq \text{CRLB}_1$ is satisfied, since CRLB_1 corresponds to the case of unknown delay, channel coefficients and CFOs, CRLB_2

[6]The amount of frequency shift is selected as 190 kHz for the FSK modulation.

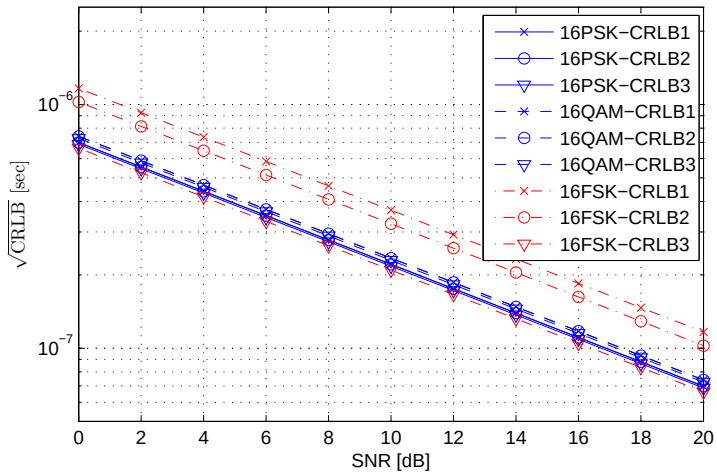

Figure 5.3 $\sqrt{\text{CRLB}}$ versus SNR for $K = 3$ and $N = 2$.

corresponds to the case of unknown delay and channel coefficients, and CRLB_3 corresponds to the case of unknown delay only. In other words, for the cases with fewer unknown parameters, lower CRLBs are observed. For the 16FSK modulation, all three bounds are distinct, which is possible because 16FSK is a non-linear modulation and the result of Proposition 1 does not apply in this case. For the 16QAM case, $\text{CRLB}_1 = \text{CRLB}_2$ as expected from Proposition 1. However, CRLB_3 is lower than both, which is due to the fact that 16QAM is not a constant envelope modulation, for which the equivalence of all the CRLBs is not guaranteed as can be deduced from Proposition 2. Finally, the results for the 16PSK case show that all the three bounds are the same, which verifies the statement in Proposition 2.

In Fig. 5.4, $N = 16$ symbols are considered and the rest of the system parameters are the same as in the previous case. It is observed that the results are similar to those in Fig. 5.3, except that the gap between the CRLBs is decreased, and lower CRLBs are attained when more symbols are employed. Also, the reduction of the gaps between CRLB_1, CRLB_2 and CRLB_3 implies that using a larger number of observation symbols can mitigate the effects of unknown CFOs and/or channel coefficients.

Next, the CRLBs for different numbers of branches, which represent the numbers of available dispersed bands in the spectrum, are investigated for various SNR values. The parameters are the same as in the previous scenario, except that only 16PSK is considered here for simplicity, and the CRLB is evaluated for $K = 1, 2, 3, 4, 5$ branches and for SNR $= 5, 10, 15$ dB. It is observed from

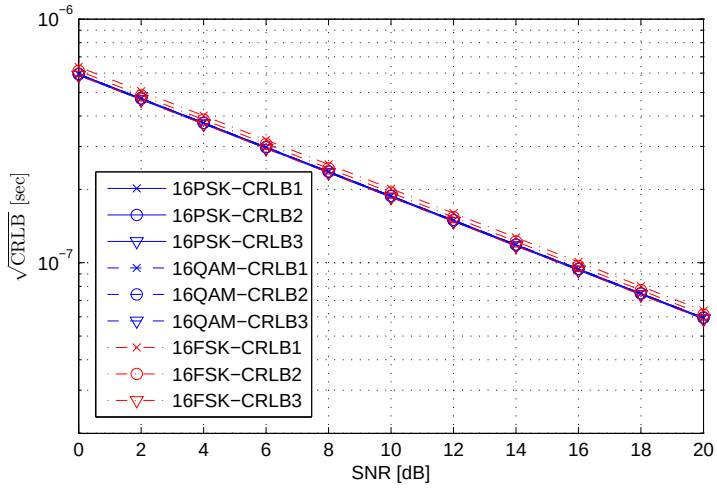

Figure 5.4 $\sqrt{\text{CRLB}}$ versus SNR for $K = 3$ and $N = 16$.

Fig. 5.5 that the CRLBs decrease as the SNR increases but they stay the same for different numbers of branches. This is due mainly to the fact that the SNR is defined as the sum of the SNRs in the different branches; hence, the SNR per branch is reduced as more branches are considered (c.f. (5.22)). However, in many practical cases, as more bands become available for the system, higher SNR can be achieved. For Fig. 5.6, the previous constraint on the SNR is removed, which is now defined per branch and the total SNR can increase as K increases. Therefore, it is observed that as more bands become available, lower CRLBs can be achieved.

5.6 Concluding Remarks

In this chapter, a new idea called dispersed spectrum utilization systems, where signal is transmitted and received over multiple dispersed bands, is proposed. CRLBs for time delay estimation have been obtained for dispersed spectrum utilization systems in the presence of unknown channel coefficients and CFOs. In addition, various modulation schemes have been considered and the effects of unknown channel coefficients and CFOs have been investigated.

The CPSs employ CRLB information at the transmitter side for achieving range accuracy adaptation as discussed in Chapter 3. The results of the study in this chapter indicate that range accuracy can be adapted by selecting an appropriate number (K) of dispersed bands in the spectrum, modulation type, number of observation symbols, and/or SNR levels. This can be achieved by using the adaptive waveform generation/processing feature of cognitive radios. Moreover, in order for the

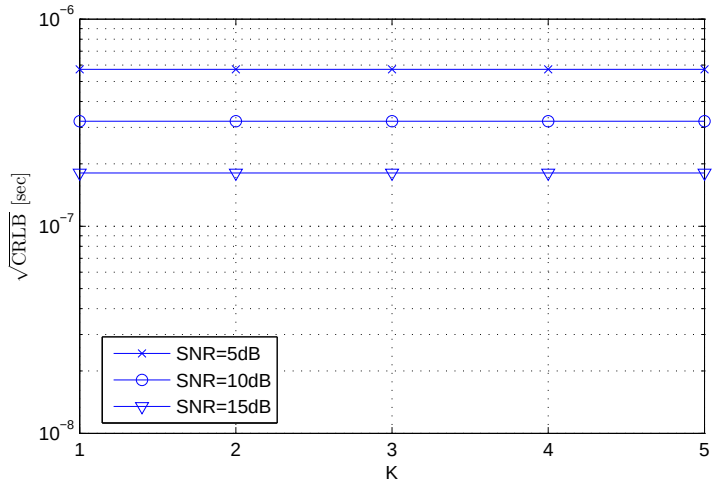

Figure 5.5 $\sqrt{\text{CRLB}}$ versus K for $N = 16$ and 16PSK modulation when the SNR is defined as the sum of the SNRs at different branches.

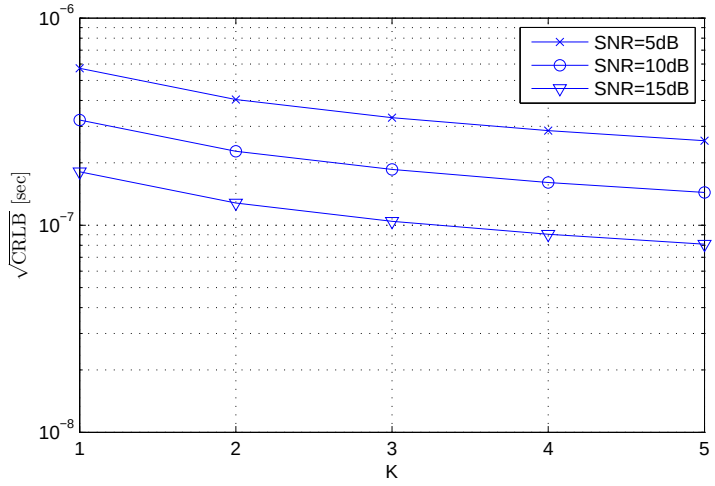

Figure 5.6 $\sqrt{\text{CRLB}}$ versus K for $N = 16$ and 16PSK modulation when the SNR is defined per branch.

CPSs to achieve a given accuracy, it needs to include all impairments in the transmitter-channel-receiver chain. The results in the existing study (i.e., Fig. 5.4) suggests that the impairments such as CFOs can be compensated for by selecting the appropriate modulation type, the number of observation symbols, and the SNR levels.

CHAPTER 6

COMPARISON OF WHOLE AND DISPERSED SPECTRUM UTILIZATION FOR TIME DELAY ESTIMATION

6.1 Introduction

Cognitive radio (CR) has a capability to exploit the spectrum utilization due to its spectrum agility. The available spectrum can be mainly in two forms: single band, i.e. whole spectrum, and multiband, i.e. dispersed spectrum [15], [19], [86]. In the whole spectrum utilization approach, transmit signal occupies single band as illustrated in Fig. 6.1, whereas, in the dispersed spectrum utilization approach, transmit signal occupies multiple bands (e.g. K number of adjacent or non-adjacent bands) simultaneously as illustrated in Fig. 6.2.

Since whole spectrum utilization is the conventional way of transmitting signal numerous technologies and transceiver architectures have been developed for such approach. For instance, Cognitive Positioning Systems (CPSs) along with range accuracy adaptation and fundamental limits of time delay estimation are studied considering whole spectrum utilization approach in Chapters 3 and 4, respectively.

The dispersed spectrum utilization approach is discussed and investigated in Chapter 5. A CR receiver architecture for the dispersed spectrum utilization based on the idea of processing the receive signal at multiple branches is proposed. Each branch considers one available band, and down-converts the signal according to the center frequency of that band. By this way, signals with narrower bandwidths can be processed at each branch. Note that another way to implement dispersed spectrum utilization approach is to employ orthogonal frequency division multiplexing (OFDM) technology, where the sub-carriers corresponding to the used and unused bands are activated and nulled, respectively [19,87,88,91,92]. However, such approach has some drawbacks, which are discussed in Chapter 5. In this chapter, the performance of whole and dispersed spectrum utilization systems are compared considering time delay estimation problem in the CPSs. Since combining signals received over multiple dispersed bands play an important rule on the performance

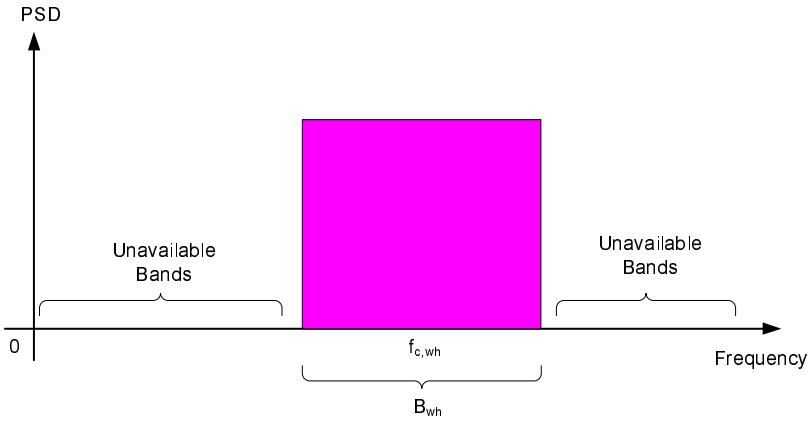

Figure 6.1 Illustration of whole spectrum utilization in cognitive radio systems.

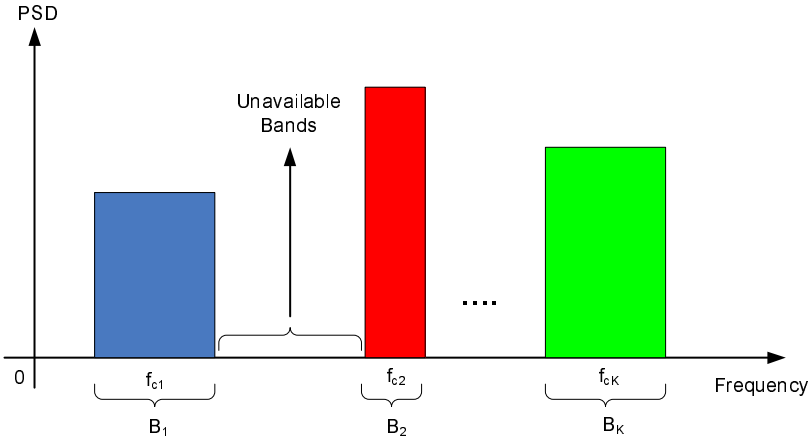

Figure 6.2 Illustration of dispersed spectrum utilization in cognitive radio systems.

of dispersed spectrum utilization systems, a combining technique based on maximizing SNR criterion is proposed. Cramer-Rao lower bound (CRLB) over AWGN channel for both approaches are presented. Furthermore, the performance of both approaches are compared for both theoretical and practical scenarios considering maximum likelihood (ML) time of arrival (TOA) estimator.

6.2 System and Signal Model

The CR transceiver architecture shown in Fig. 6.3 is considered. In this architecture, cognitive engine along with location awareness engine wish to satisfy goal driven range accuracy requirements. In this chapter, range information is estimated using time of arrival (TOA) method. In the transmitter side, cognitive engine provides transmission parameters for achieving range accuracy

requirements to the adaptive waveform generator. The adaptive waveform generator generates the corresponding transmit signal. CR can activate K number of branches depend on the K number of band that is utilized. For instance, the transmit signal is processed over single branch (i.e. $K = 1$) for the whole spectrum case and multiple branches (i.e. $K > 1$) for the dispersed spectrum case. The signal at each band are combined and transmitted over a single antenna. In the receiver side, the receive signal is processed over K number of branches. The receive baseband signal at the output of each branch is processed using adaptive waveform processor and combined in the case of dispersed spectrum utilization method. This is followed by the location estimator to estimate range information.

To the best of author's knowledge, there is not any solid study on channel behavior of dispersed spectrum utilization method in the literature. In practice, the observed channel at each band can be different depending on how dispersed bands are located in the spectrum. As a result, for the sake of simplifying the analysis and exploring the fundamental considerations and problems in the dispersed spectrum utilization methods, we assume that all the dispersed bands experience different AWGN channel. In other words, we perform the theoretical analysis of both approaches considering AWGN channel. In the following sections, we provide the details of CR transceiver for both approaches.

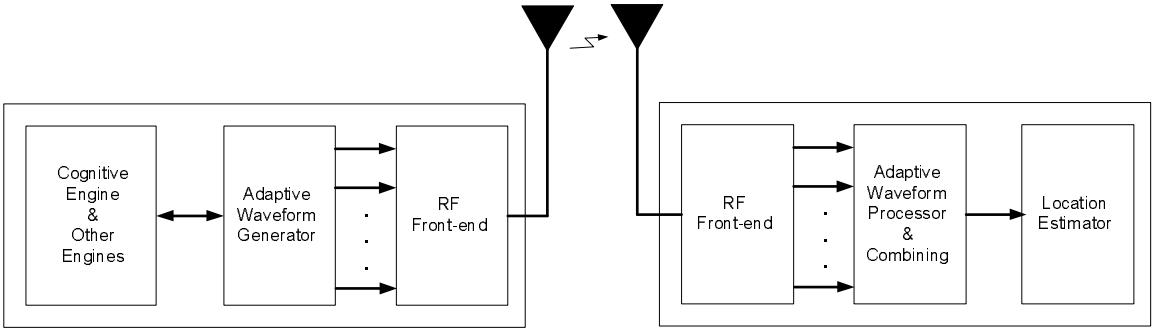

Figure 6.3 Block diagram of cognitive radio transceiver for whole and dispersed spectrum utilization.

6.2.1 Cognitive Radio Transceiver for Whole Spectrum Utilization

For the whole spectrum utilization systems, the signal is processed over a single branch (i.e. $K = 1$) using the RF front-end shown in Fig. 6.4. The baseband transmit signal $s(t)$ with absolute bandwidth of B_{wh} in whole spectrum utilization method occupies a whole band as shown in Fig. 6.1. The baseband signal $s(t)$ is upconverted to the carrier frequency $f_{c,wh}$, amplified, filtered and then

transmitted over channel. At the receiver side, the receive signal is filtered out using a bandpass filter (BPF) with bandwidth of B_{wh} and downconverted to the baseband. We assume that there is not any impairments in the transceiver such as out-of-band radiation. The baseband representation of receive signal $r(t)$ is given by

$$r(t) = \alpha s(t - \tau) + n(t) \ , \tag{6.1}$$

where α and τ are the path coefficient and delay, respectively, and $n(t)$ is independent white Gaussian noise with spectral density of σ^2.

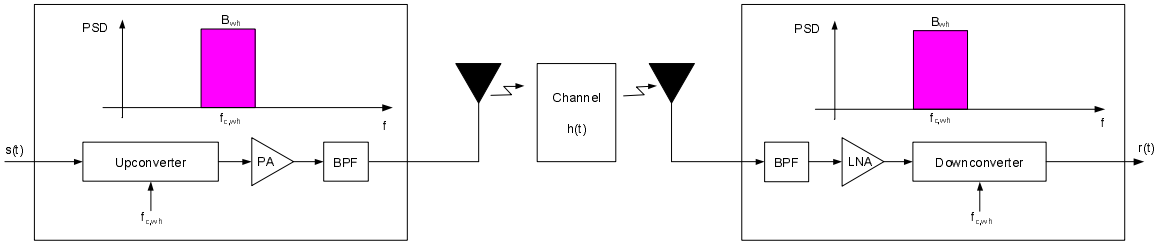

Figure 6.4 Block diagram of cognitive radio transceiver for the whole spectrum utilization.

6.2.2 Cognitive Radio Transceiver for Dispersed Spectrum Utilization

In this architecture, the same baseband signal $s(t)$ as previous case is transmitted over the dispersed spectrum occupying K available bands illustrated in Fig. 6.2. Various RF transceiver can be developed for the implementation of dispersed spectrum utilization method. One way to implement this approach is using the CR transceiver illustrated in Fig. 6.5, which is considered in this chapter. Similar to whole spectrum utilization case, we assume that there is no any impairments in the transceiver for the sake of simplicity. In the transmitter side, the transmit baseband signal at ith branch $s_i(t)$ is upconverted to the corresponding carrier frequency f_{ci} and then amplified and filtered out. The RF signal at each branch is combined and transmitted through a single antenna as shown in Fig. 6.5. In the receiver side, the receive signal is split into K branches and the signal in each band is processed by the corresponding branch. In other words, each branch filters, amplifies, and downconverts the signal to the baseband. The baseband representation of receive signal at ith branch $r_i(t)$ is given by

$$r_i(t) = \alpha_i s_i(t - \tau) + n_i(t) \ , \tag{6.2}$$

where α_i and τ are the path coefficient and delay for ith branch, respectively, and $n_i(t)$ is independent white Gaussian noise with spectral density of σ_i^2.

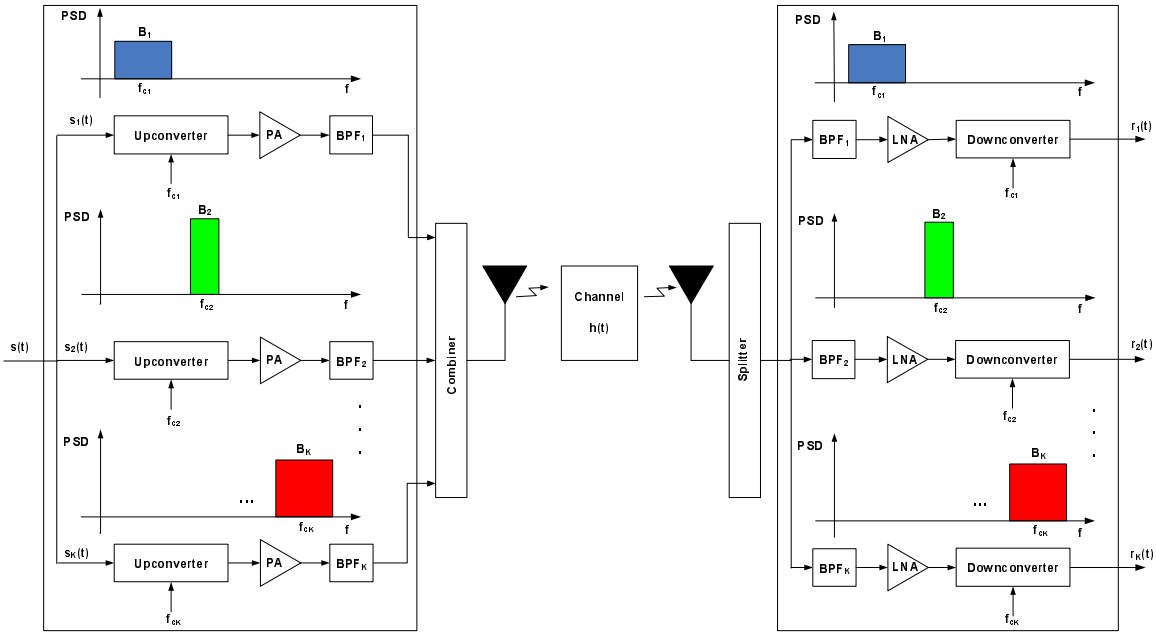

Figure 6.5 Block diagram of cognitive radio transceiver for the dispersed spectrum utilization.

6.3 CRLB for Whole and Dispersed Spectrum Utilization Systems

In this section, approximate CRLB of time delay estimation for both whole and dispersed spectrum utilization cases are presented. Let $\boldsymbol{\theta} = [\tau]$ represent the vector of unknown signal parameters, where α and α_i are assumed to be known for whole and dispersed spectrum utilization systems, respectively. The observation interval $[0, T]$ is considered. Since the approximate CRLB for the whole spectrum utilization approach considering AWGN channel is derived in Chapter 3, we only derive approximate CRLB for the dispersed spectrum utilization approach over AWGN channel in this section. For the sake of convenience and comparison, we re-write the approximate CRLB of time delay estimates for the whole spectrum utilization over AWGN channel here in this section, which is given by

$$\text{CRLB}_{wh} = \frac{1}{\frac{4\pi^2}{3}\text{SNR}_{wh}B_{wh}^2} \ , \tag{6.3}$$

The exact CRLB for dispersed spectrum utilization systems is derived in Chapter 5, which has the following form,

$$\mathrm{CRLB}_{disp} = \frac{1}{\sum_{i=1}^{K} \gamma_i \tilde{E}_i} \ . \tag{6.4}$$

In what follows, we derive the approximate CRLB for the dispersed spectrum utilization approach. Let the baseband signal $s_i(t)$ in (6.2) consist of a sequence of modulated pulses as follows

$$s_i(t) = \sum_{l} d_{i,l} p_i(t - lT_s) \ , \tag{6.5}$$

for $i = 1, \ldots, K$, where $d_{i,l}$ is the real data for the lth symbol of signal i, and $p_i(t)$ represents a pulse with duration T_{pi}, i.e., $p_i(t) = 0$ for $t \notin [0, T_{pi}]$. Here, we assume that $d_{i,l} = d_l$, which implies that d_l data in case of whole band is transmitted over each dispersed band. It is also assumed that the observation interval T can be expressed as $T = NT_s$, where $N_i = N$ is considered for an integer N_i for $i = 1, \ldots, K$. Consequently, $\tilde{E}_i$ in (6.4) can be written in the following form

$$\tilde{E}_i = 4\pi^2 N_i d_l^2 E_{p_i} \beta_i^2 \ , \tag{6.6}$$

where

$$E_{p_i} = \int_{-\infty}^{\infty} p_i^2(t) \mathrm{d}t \ , \tag{6.7}$$

and β_i is the effective bandwidth of $p_i(t)$, given by

$$\beta_i^2 = \frac{1}{E_{p_i}} \int_{-\infty}^{\infty} f^2 |P_i(f)|^2 \mathrm{d}f \ , \tag{6.8}$$

with $P_i(f)$ denoting the Fourier transform of $p_i(t)$. Similar to the whole spectrum utilization case, it is assumed that the spectral density of $p_i(t)$ is constant over the B_i, then the relationship between β_i and B_i can be obtained from (6.8) as [57]

$$\beta_i^2 = \frac{B_i^2}{3} \ . \tag{6.9}$$

By using (6.6) and (6.4), and after some manipulation, CRLB expression for the dispersed case in (6.4) takes the following form,

$$\mathrm{CRLB}_{disp} = \frac{1}{\frac{4\pi^2}{3}\sum_{i=1}^{K} \mathrm{SNR}_i B_i^2} \ , \tag{6.10}$$

where SNR_i is defined as

$$\mathrm{SNR}_i = \frac{\alpha_i^2 N_i d_l^2 E_{p_i}}{\sigma_i^2} \ . \tag{6.11}$$

By examining (6.3) and (6.10), the performance comparison of whole and dispersed spectrum utilization in terms of CRLB depends on the values of SNR_{wh}, B_{wh}, SNR_i, and B_i. The following are three possible cases for the CRLB performance comparison of both approaches,

$$\begin{cases} \mathrm{CRLB}_{disp} > \mathrm{CRLB}_{wh}, & \textit{If } \sum_{i=1}^{K} \mathrm{SNR}_i B_i^2 < \mathrm{SNR}_{wh} B_{wh}^2 \ , \\ \mathrm{CRLB}_{disp} < \mathrm{CRLB}_{wh}, & \textit{If } \sum_{i=1}^{K} \mathrm{SNR}_i B_i^2 > \mathrm{SNR}_{wh} B_{wh}^2 \ , \\ \mathrm{CRLB}_{disp} = \mathrm{CRLB}_{wh}, & \textit{If } \sum_{i=1}^{K} \mathrm{SNR}_i B_i^2 = \mathrm{SNR}_{wh} B_{wh}^2 \ , \end{cases} \tag{6.12}$$

Note that the above conditions hold theoretically. However, this may not be the case for the practical scenarios, which is investigated in a later section through computer simulations.

From the third condition in (6.12), it can be observed that the same CRLB can be achieved theoretically by selecting the appropriate SNR levels and absolute bandwidths B for both technique. Some representative applications of (6.12) are given as follows. This equation is useful for the selection of the K, SNR_i, B_i parameters in dispersed spectrum utilization techniques that can provide the same performance as whole spectrum utilization techniques with SNR_{wh} and B_{wh} parameters. It also can be useful to quantify the equivalent of K number of dispersed bandwidth B_i as a whole bandwidth B_{wh} for given SNR_i and SNR_{wh}, respectively. Finally, the conditions in (6.12) is useful for the optimization mechanism in range accuracy adaptation [12], [15], [19], which is a feature of the CPSs. During the optimization of spectrum parameters, range accuracy adaptation algorithm can select the optimal spectrum parameters (e.g. B, SNR) using the conditions in (6.12).

6.4 A Combining Technique for Dispersed Spectrum Utilization Systems

Combining signals received over dispersed bands at the receiver side is a crucial process and it affects the performance of dispersed spectrum utilization systems. The signals at each branch can be combined using different criterion. In this section, we propose an energy combining technique based on maximizing total SNR criterion for dispersed spectrum utilization systems as shown in Fig. 6.6. In this method, receive signal in each branch is correlated with the corresponding template signal and the resultant signals are combined in such a way to maximize SNR. This is followed by performing time delay estimation process.

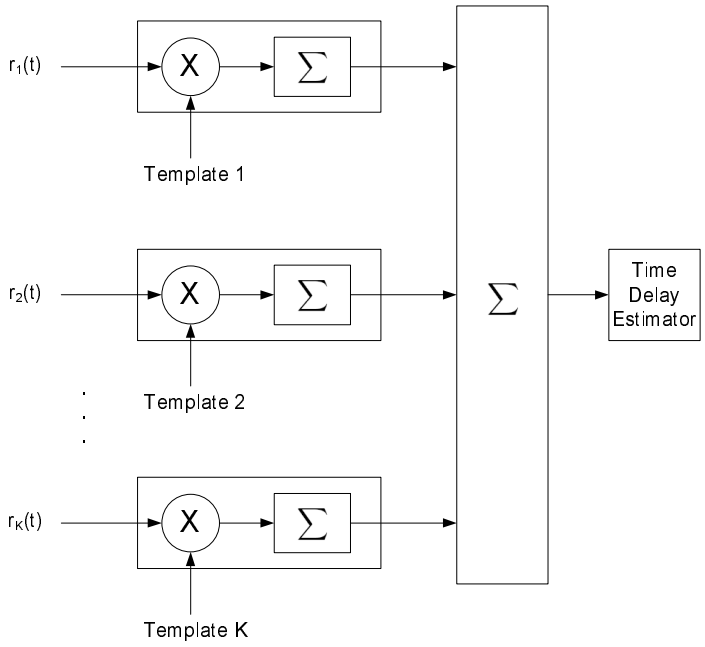

Figure 6.6 Energy combining technique for dispersed spectrum utilization systems.

6.5 Results and Discussions

In this section, performance of both exact and approximate CRLB is compared considering whole spectrum utilization systems. This is followed by performance comparison of both whole and dispersed spectrum utilization approaches for theoretical and practical cases.

The following simulation parameters are used for comparing the exact and approximate CRLB and ML TOA estimator. For the pulse shape, Gaussian second order derivative is employed

$$p(t) = A\left(1 - \frac{4\pi t^2}{\zeta^2}\right) e^{-2\pi t^2/\zeta^2} \ , \tag{6.13}$$

where A and ζ are parameters that are used to adjust the pulse energy and the pulse width, respectively. A is selected in order to generate pulses with unit energy. For the given pulse shape, pulse width is defined as $T_p = 2.5\zeta$ [19]. The signal bandwidth that is considered is 1MHz. Moreover, uniformly distributed delay $T_a = 5T_p$ is considered, i.e. $U[0, T_a]$. The number of training symbol N that is considered is 1 and $d_l = [1]$. The results are obtained over 3000 channel realizations with channel fading coefficient $\alpha = 1$ and are plotted in Fig. 6.7. According to the results, exact CRLB performs better than approximate CRLB by approximately 3.7dB. This is due to the flat spectrum assumption made during the derivation of B from β.

ML approach can be implemented by cross-correlating the received signal with template signal and computing the minimum square error (MSE) of time delay estimates. The time delay estimates are subject to ambiguity errors caused by the oscillatory nature of the signal correlation function [93]. The results in Fig. 6.7 as well as the results in the literature [93] indicates that MSE is a function of SNR exhibiting threshold phenomenon. The SNR threshold for the results in Fig. 6.7 is 16dB and it divides the SNR region into two distinct regimes [93], which are low and medium SNR regions.

Note that the SNR point where the transition from low to medium SNR regimes occurs is referred as SNR threshold. MSE demonstrates a nonlinear behavior in the low SNR regime, whereas this behavior becomes linear after the SNR threshold. This behavior is formulated by Barankin bound [93]. An alternative definition of SNR threshold is developed from the results in Fig. 6.7, which is the SNR point where the noise effects become negligible. As a result, bandwidth effects also begin to contribute to the overall MSE performance. In other words, SNR is the dominant parameter in the low SNR region and both SNR and B contributes to the overall MSE performance after the SNR threshold. This definition is also useful to explain the performance gap between ML and CRLB in the low SNR (or nonlinear) region. This is because of CRLB takes both SNR and B (see (6.3)) into account during time delay estimate over the entire SNR region. Therefore, CRLB performs better than ML in the low SNR region and it converges to approximate CRLB after the

SNR threshold. Moreover, ML performs better than approximate CRLB by 0.5dB according to the results in Fig. 6.7.

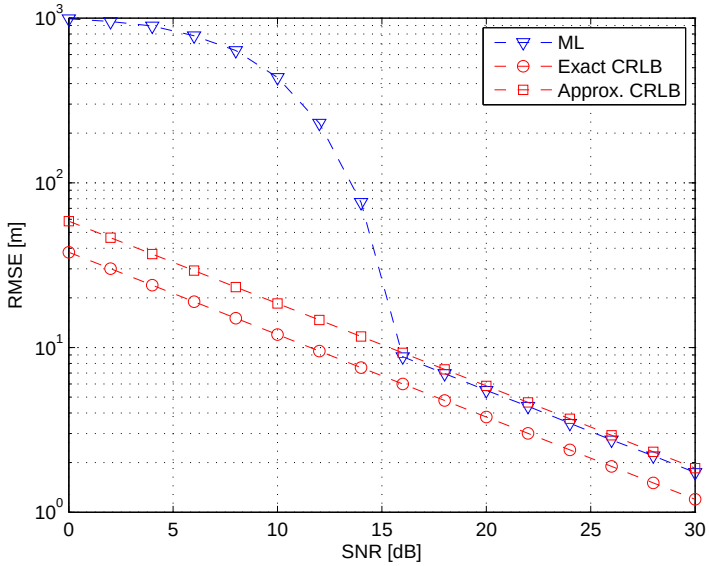

Figure 6.7 Comparison of exact and approximate CRLB for whole spectrum utilization systems.

Performance of whole and dispersed spectrum utilization systems are compared considering approximate CRLB and ML TOA estimator. Performance comparison of both approaches are conducted for three cases. The number of available dispersed bandwidth for all three cases is considered to be 2, i.e. $K = 2$. In case 1, $SNR_1 + SNR_2 = SNR_{wh}$, $B_i = 1$MHz and $B_{wh} = 2$MHz. For case 2, $SNR_i = SNR_{wh}$, $B_i = B_{wh} = 2$MHz. Finally, the parameters for case 3 are given as follows: $SNR_1 + SNR_2 = SNR_{wh}$, $B_i = B = 2$MHz. The remaining system parameters for all three cases are common and they are given as follows. Training data $d_l = 1$ is considered, where the number of observation symbols for both whole and dispersed spectrum is 1, i.e. $N_i = N = 1$. In addition, it is assumed that the spectral density of the noise is the same for the whole spectrum and all the K branches of the dispersed spectrum techniques; i.e., $\sigma_i = \sigma$ for $i = 1, \ldots, K$. The Gaussian second order derivative pulse shape is used. Therefore, the pulse shape for the whole and dispersed spectrum methods are generated using $T_p = 2.5\zeta_{wh}$, where $\zeta_{wh} = 1/2.5B_{wh}$, and $T_{pi} = 2.5\zeta_i$, where $\zeta_i = 1/2.5B_i$, respectively. For the practical cases, ML TOA estimator is employed. The combining technique shown in Fig. 6.6 is used for dispersed spectrum utilization systems. Furthermore, the root

mean square error (RMSE) metric is considered to measure the performance of ML TOA estimator. Note that all the results in this section are obtained over 10000 channel realizations.

For the theoretical case, (6.3) is denoted as CRLB-Whole and (6.10) is denoted as CRLB-Dispersed. Similarly, ML TOA estimator for the whole and dispersed spectrum cases are denoted as ML-Whole and ML-Dispersed, respectively. The results for case 1 are plotted in Fig. 6.8. CRLB-Whole performs better than CRLB-Dispersed by 6dB for the entire SNR region. Since combined total SNR for dispersed case is equal to SNR_{wh}, this performance difference is due to $B_{wh}^2 = 4B_i^2$. This result is justified by the first condition in (6.12). On the other hand, ML-Whole performs similar to ML-Dispersed in the low SNR (nonlinear) region since combined total SNR for dispersed case is equal to SNR_{wh}. However, in the linear region (after the SNR threshold of 17dB), ML-Whole and ML-Dispersed converges to CRLB-Whole and CRLB-Dispersed, respectively. In other words, ML-Whole performs better than ML-Dispersed by 6dB in this region. Furthermore, the SNR threshold for dispersed is less than the SNR threshold for whole case and this is due to noise reduction obtained from combining process in the dispersed spectrum utilization case.

The results for case 2 are plotted in Fig. 6.9. According to the results, CRLB-Dispersed performs better than CRLB-whole by 3dB for the entire SNR region. This is due to SNR gain obtained from combining process in the dispersed case since $B_i = B = 2$MHz. This result is justified with the second condition in (6.12). On the other hand, ML-Dispersed performs better than ML-Whole by 3dB in the low SNR region due to the SNR gain obtained from the combining process. The same result is observed in the linear region since $B_i = B$. In other words, bandwidth does not cause any performance difference.

In Fig. 6.10, the results for case 3 are shown. CRLB-Whole and CRLB-Dispersed performs same for all the SNR values. This result is justified by the third condition in (6.12). Similarly, ML-Whole and ML-Dispersed performs same over all SNR region since the combined SNR in dispersed case is equal to SNR_{wh} and $B_i = B$.

6.6 Conclusions

In this chapter, performance of whole and dispersed spectrum utilization approaches are compared considering time delay estimation problem in cognitive positioning systems. A combining technique based on maximizing SNR criterion is proposed for dispersed spectrum utilization systems. The CRLB for both approaches over AWGN channel are presented. Furthermore, performance

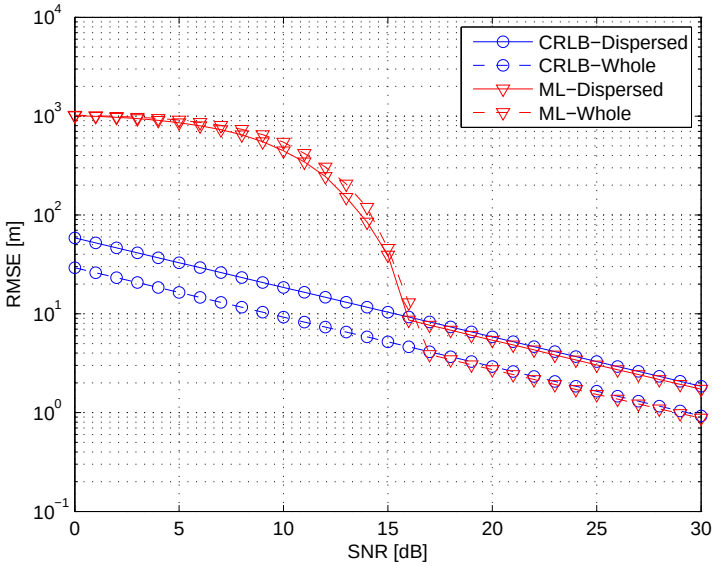

Figure 6.8 RMSE of ML TOA estimator and $\sqrt{\text{CRLB}}$ versus SNR for dispersed and whole spectrum utilization techniques considering simulation parameters in case 1.

of both approaches are compared for both theoretical and practical cases considering ML TOA estimator. The results suggest that dispersed spectrum utilization is a promising approach for exploiting the efficiency of the spectrum utilization as well as supporting goal driven and autonomous cognitive radio systems. Especially, dispersed spectrum utilization approach has a capability for achieving dynamic range accuracy requirements of cognitive location and environment aware systems.

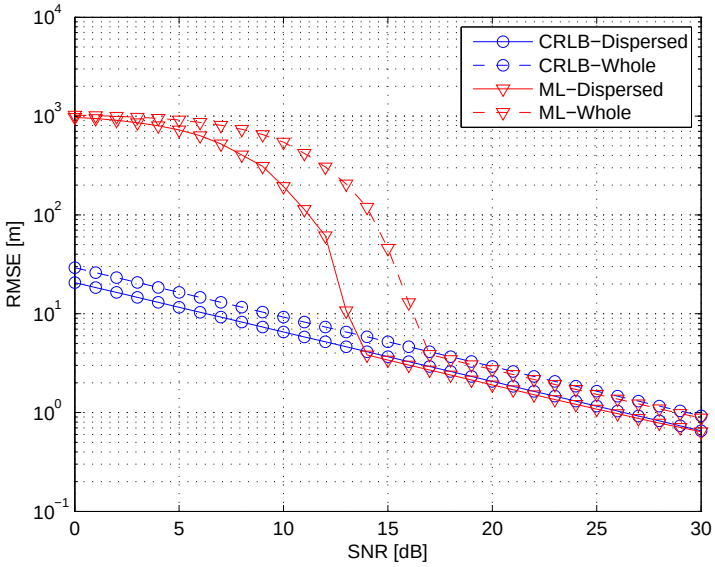

Figure 6.9 RMSE of ML TOA estimator and $\sqrt{\text{CRLB}}$ versus SNR for dispersed and whole spectrum utilization techniques considering simulation parameters in case 2.

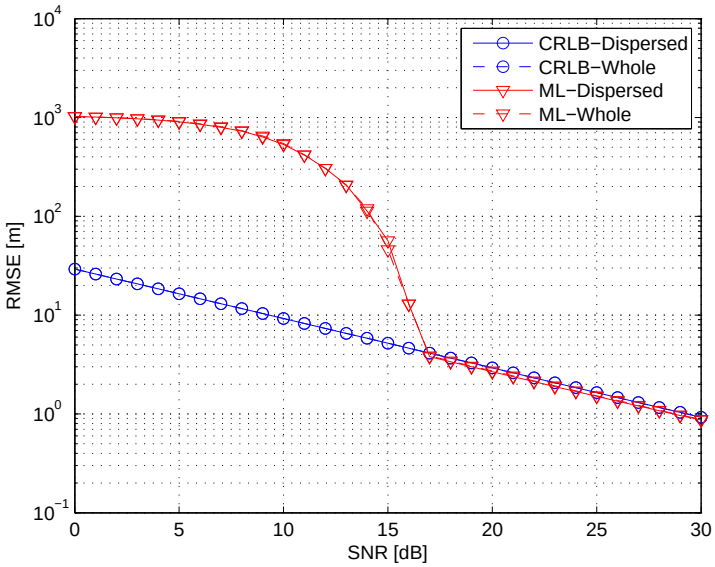

Figure 6.10 RMSE of ML TOA estimator and $\sqrt{\text{CRLB}}$ versus SNR for dispersed and whole spectrum utilization techniques considering simulation parameters in case 3.

CHAPTER 7

LOCATION AWARE SYSTEMS IN COGNITIVE WIRELESS NETWORKS

7.1 Introduction

One of the most prominent features of cognitive radio (CR) technology is its location awareness. Incorporation of this capability to CR brings challenges and opportunities such as location sensing, seamless positioning and interoperability, statistical learning and tracking, security and privacy, mobility management, adaptation of location aware systems, and location aware applications. Some of these issues and applications have been studied for the legacy radios and wireless networks in some extent. However, all of these issues need to be revisited in the CR and cognitive wireless network (CWN) domains. Therefore, a location awareness engine handling all these issues and applications in CWNs is proposed in Chapter 2. The focus of this chapter is to present some representative applications of the location awareness engine that it can support.

Applications of the location awareness engine are folded under four major groups: location-based services (e.g. monitoring real-time traffic), location-assisted network optimization (e.g. location-assisted dynamic spectrum access systems), location-assisted transceiver optimization (e.g. location-assisted link adaptation), and location-assisted environment identification (e.g. location-assisted channel environment characterization). Only some representative applications of location-assisted network optimization are presented in this chapter to demonstrate the utilization of location information for different applications in CWNs.

In this chapter, a brief taxonomy of CWNs based on cognition, collaboration, and node diversity criteria is presented. Implementation options of location awareness in cognitive radios and networks are discussed. Furthermore, several location-assisted network optimization applications for CWNs such as location-assisted dynamic spectrum access management, network planning and expansion, and handover along with preliminary results are presented.

7.2 Cognitive Wireless Network Model

Cognition, collaboration, and node diversity are the main criteria that can be used to classify CWNs. These networks consist of two major parts, which are central cognitive engine and nodes. One can think of a central cognitive engine in CWNs like a mobile switching center with more intelligence in cellular networks. We consider both CR base station and mobile station as a node in this chapter.

Partitioning cognition features between the central cognitive engine of a network and cognitive engine of nodes plays a key role to classify CWNs. In theory, various type of CWNs can be developed between two extreme cognition limits, which are absolute centralized and distributed (non-centralized) cognition [14]. In the former limit, central cognitive engine has full cognition capabilities whereas nodes possess limited cognition capabilities. Basically, central cognitive engine can be considered as the brain and nodes are members. On the other hand, the structure is totally opposite in the absolute distributed cognition case, where the full cognition capability is embedded into the cognitive engine of each node. Note that this type of network will always have a central cognitive engine to maintain network organization regardless of the cognition level of CR nodes. Indeed, nodes will have more cognition capabilities as the technology advances. On the other hand, ad-hoc CR network [94] can be considered as a network type between these two cognition limits.

CWNs can be classified under three types from the perspective of collaboration within a network [95]. Collaboration can be between a node and central cognitive engine of network and/or between nodes. Since there is a natural collaboration between central cognitive engine and nodes, the following classification is based on the collaboration between nodes. The first type is so called cooperative network, in which all the nodes agree on performing predefined (i.e. cooperative spectrum sensing) or ideally goal driven tasks collectively. Non-cooperative network is the second type of network, in which there are no collaborations between nodes. On the other hand, if a group of nodes do and the rest of them do not agree to collaborate, then this forms the third type of network that is so called partially cooperative network. Ideally, CWNs can have a capability to transit from one type to another dynamically depending on the collaboration of nodes. It is worth to note that CR nodes and CWNs can have a capability to cooperate with the satellites such as in the case of assisted-global positioning system (A-GPS).

Based on the node diversity criteria, CWNs can be grouped under two main categories: pure cognitive wireless networks and mixed cognitive and non-cognitive wireless networks. As the names imply, the former consists of only cognitive radio nodes and the latter composed of both cognitive and non-cognitive radio nodes. Pure cognitive wireless networks can be divided further into two subgroups, which are homogeneous and heterogeneous networks. For a given geographical area or cell, all cognitive radio nodes are identical (they use same waveform) in the homogeneous networks. For instance, a network consisting of only cognitive Worldwide Interoperability for Microwave Access (WiMAX) nodes is an example for the homogeneous networks, which is illustrated in Fig. 7.1. On the other hand, if the given geographical area or cell consists of mixture of different cognitive radio nodes (i.e. WiMAX base stations, Ultrawideband (UWB) nodes), this type of network is called as heterogeneous network [2]. In this type of network, a mobile device can roam across the cell borders of the other networks and inter-operate with the other wireless devices. A representative example of mixed cognitive and non-cognitive wireless networks is illustrated in Fig. 7.2. Notice that in this type of networks interoperability is an issue. Although cognitive radios can communicate among themselves and with non-cognitive radios, non-cognitive radio nodes may not be able to communicate among themselves. Location information of mobile cognitive radio nodes play important roles to achieve global mobility and seamless connectivity in CWNs. For instance, mobile cognitive radio node can switch from WLAN to WiMAX networks as the user leaves home by tracking the location of the user. Note that, in reality, the heterogeneity of CWNs can change dynamically as well.

7.3 Implementation Options

Learning through interactions of cognitive radio with the surrounding environment can be accomplished mainly in one of three ways: cooperative, self, and composite. Without loss of generality, the details of each implementation option are provided in the context of location awareness in the sequel.

In cooperative location awareness approach, (at least) two cognitive radios collaborate on learning the distance between them by estimating the ranging information. In this approach, one of the cognitive radios transmits signal (e.g. RF or acoustic) through channel environment and the other cognitive radio extracts the ranging information from the received signal as illustrated in Fig. 7.3. In other words, the transmitter and receiver are not co-located. Cooperative location awareness can be accomplished by using cognitive positioning systems [12]. Both cognitive radios negotiate on the

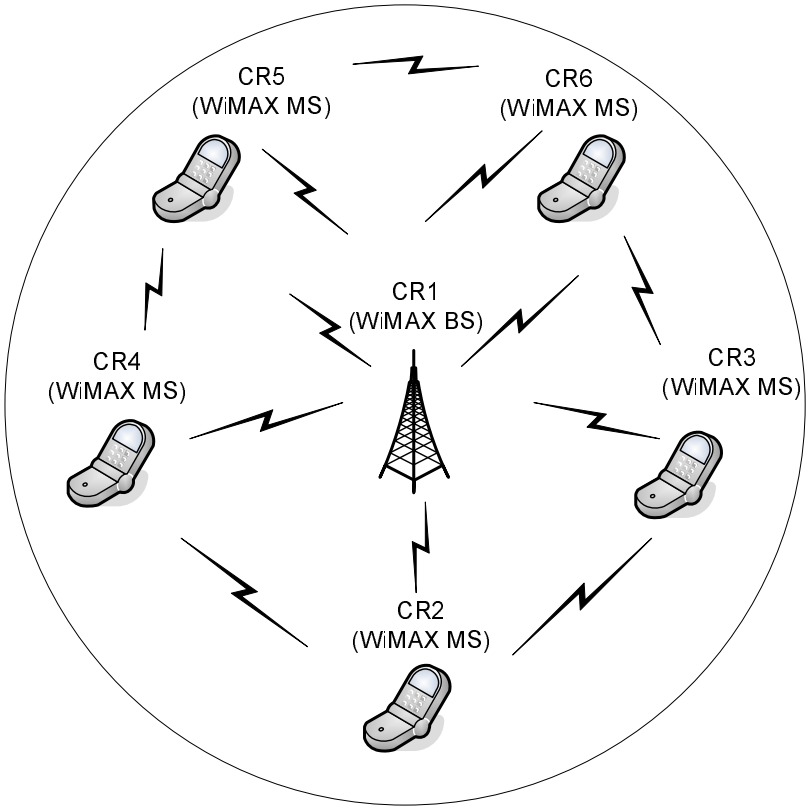

Figure 7.1 Illustration of the homogeneous pure cognitive wireless networks; text in the parentheses show the instantaneous waveform of each cognitive radio node (CR: cognitive radio node).

ranging parameters that achieves given accuracy through cognitive ranging protocol illustrated in Fig. 7.4. This protocol consists of three stages: ranging parameter setup, two-way TOA ranging, time-stamp report. Both cognitive radios negotiate or provide feedbacks to each other during the ranging parameter setup stage (loop). Once both agree on the parameters, the next two stages are initiated. The last two stages are parts of conventional two-way TOA ranging protocol, which the details of these steps can be found in [96].

Unlike to cooperative location awareness approach, self location awareness method enables a cognitive radio to perform location awareness without the need of another cognitive radio or infrastructure. The self location awareness can be achieved in one of two ways, which are active and passive manners as illustrated in Fig. 7.5. In active self location awareness methods, simply, both transmitter and receiver are utilized and they are co-located. A perfect example for this approach in the nature is bat echolocation system. Such system can be accomplished in cognitive radios by using

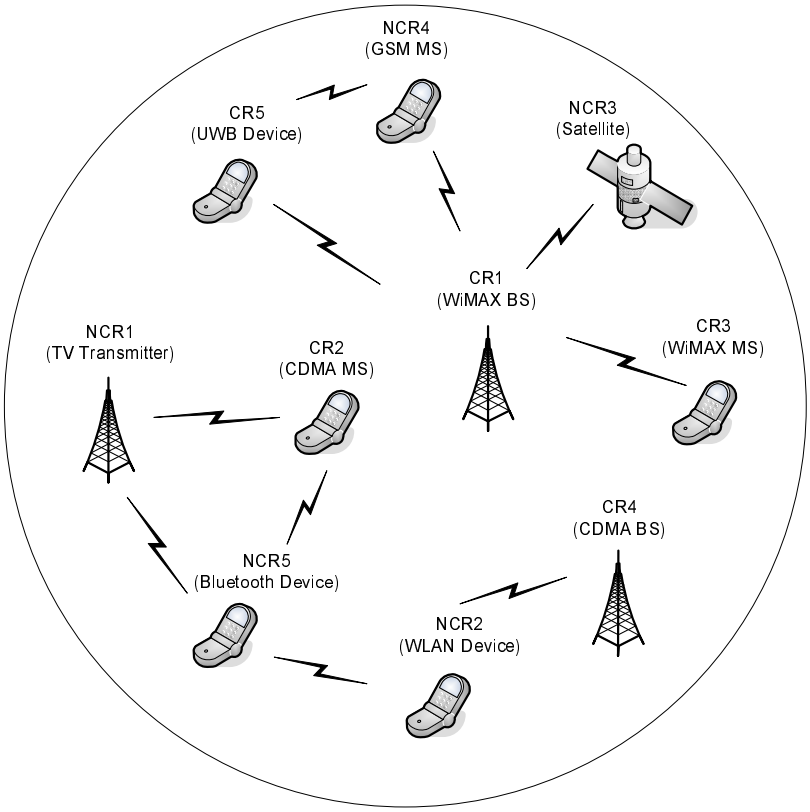

Figure 7.2 Illustration of the mixed cognitive and non-cognitive wireless networks (NCR: non-cognitive radio nodes).

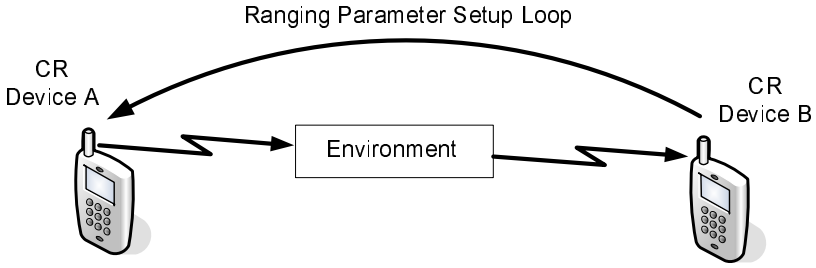

Figure 7.3 A conceptual model for cooperative location awareness between two cognitive radios.

cognitive radar [21] or cognitive sonar techniques. On the other hand, passive self location awareness methods observe and acquire the signals (e.g. optic or acoustic) from the environment without transmitting any signal. Basically, this approach requires only receptor such as image sensors. Human vision and hearing are two natural examples of passive self location awareness technique. Such capabilities can be embodied into cognitive radios using aforementioned location sensing methods.

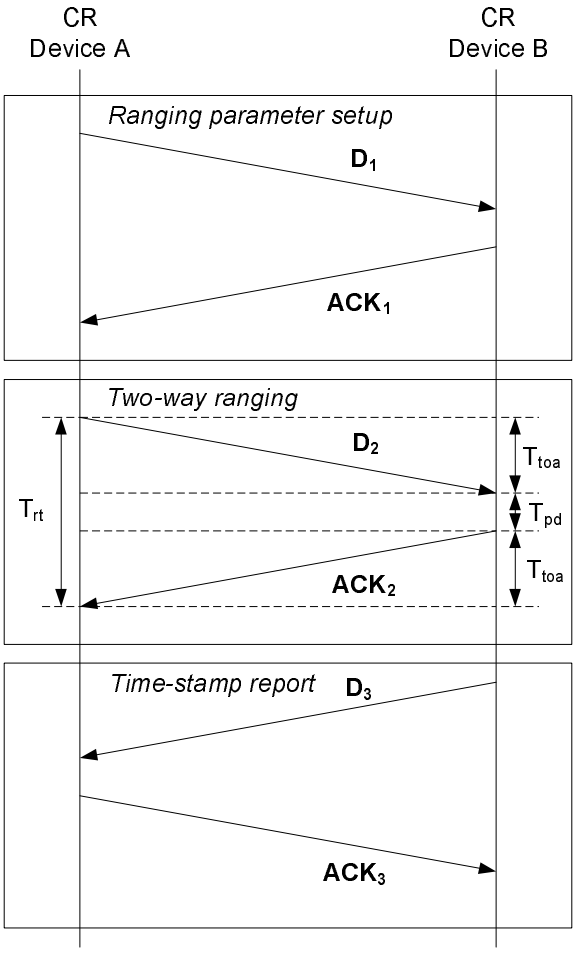

Figure 7.4 Illustration of cognitive ranging protocol.

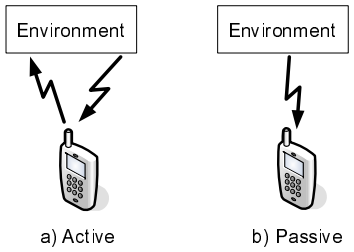

Figure 7.5 A conceptual model for self location awareness: a) active, b) passive.

Both cooperative and self location awareness methods have some strengths and weaknesses. For instance, cooperative methods have capability to provide absolute and relative ranging and positioning information whereas the self techniques can provide only relative ranging information.

Furthermore, the implementation of closed-loop feedback (receiver-transmitter-environment) in self location awareness architectures is less complex than that in cooperative location awareness architectures since the transmitter and receiver are co-located in the former architectures. Cognitive radio can leverage the strengths of both cooperative and self location awareness methods, which is referred as composite location awareness for supporting advanced and autonomous location aware applications.

7.4 Location-based Services

Location-based services (LBSs) are well known location aware systems. By using the location awareness capability of cognitive radios and networks, numerous location aware applications can be developed. Therefore, some representative location aware applications are provided in Table 7.1. Nevertheless, the focus of this chapter are location assisted network optimization methods, which are discussed in the following sections.

7.5 Location-assisted Network Optimization

Various location-assisted network optimization algorithms can be developed for CWNs such as location-assisted spectrum management, network plan and expansion, handover, dynamic channel allocation, routing, power control, internetworking, and adaptive coverage system. However, only the first three applications are discussed in this section.

7.5.1 Location-assisted Dynamic Spectrum Management

Under-utilization of the licensed bands and scarceness in the license-exempt bands prompt the concept of efficient usage of spectrum. Basically, in the absence of the licensed users that have the privileges to use their bands, unlicensed users can utilize these bands temporarily. This can be achieved by using overlay and/or underlay spectrum access techniques. There are many different proposals for dynamic spectrum management in CWNs. However, we consider three potential approaches proposed by the Federal Communications Commission (FCC) in the United States, which are Listen-before-talk, Geolocation-database, and Local beacon techniques [97]. These schemes are proposed for allowing unlicensed operations in the TV bands while preventing interference to TV receptions. Moreover, a recently formed IEEE 802.22 working group for the Wireless Regional Area Networks has the same vision as the FCC. The main goal of this group is to establish a CR-based

Table 7.1 Some representative location aware applications for cognitive radios and networks.

Application Type	Applications
Location-based Services (LBS)	• Public safety (e.g. police, fire), • E911, E112, • Package tracking, • Child finder, • Patient tracking, • Real-time traffic services, • Roadside assistance.
Location-assisted Network Optimization	• Dynamic spectrum management, • Network plan and upgrade, • Handover, • Dynamic channel allocation, • Routing, • Power management, • Internetworking, • Adaptive coverage system.
Location-assisted Transceiver Optimization	• Adaptive beamforming • Interference avoidance, • Link adaptation,
Location-assisted Environment Identification	• Channel environment characterization, • LOS/NLOS identification.

standard that allows unlicensed users to utilize the bands allocated to TV broadcast services in a non-interfering fashion. It is worth to mention that low frequency analog TV bands ($54 - 862$MHz) has some attractive features for wireless broadband services such as achieving long-distance trans-

mission. Since the Geolocation-Database and Local Beacon techniques utilize location information, the other technique is out of scope of this section.

According to Geolocation-database approach, licensed users (e.g. TV transmitter) are equipped with the location sensing device to estimate their current location information. The licensed users provide their spectrum and location information to the FCC central database. The FCC database broadcasts available channel information along with the location information of the licensed users. On the other hand, unlicensed users are also equipped with the location sensing device to estimate their current locations. Unlicensed users cross-check their locations with the location of licensed users in order to obtain the channel information that they can use locally. Two major concerns regarding this scheme are the reliability of the current geolocation technologies and the performance of FCC central database. For instance, some TV broadcasters point out that the GPS does not provide reliable location information of a user that is located in indoor environments. However, some deficiencies of GPS such as low accuracy and indoor inoperability are addressed with the recent advances in this technology such as A-GPS and Indoor GPS. Alternatively, the licensed users and unlicensed users can utilize more reliable positioning techniques such as the CPSs to obtain their current location information. The other concern is that the current FCC central databases are slow to catch up the frequency changes and they are not 100 % reliable. This is a valid concern and the FCC is aware of this issue. As a solution, the FCC can upgrade its database technology in order to be used for the spectrum sensing and allocation purposes.

Local beacon method is pretty similar to geolocation-database scheme except that the database will be placed in a local cell to manage the spectrum. Cognitive base station within a cell broadcasts local geolocation-database at predefined time intervals. A snapshot of local geolocation-database example is illustrated in Table 7.2. Unlicensed CR nodes within local cell receive the geolocation-database and cross-check with their own location information. Consequently, they can determine their prospective spectrum plans (e.g. center frequency and absolute bandwidth). In the US, the FCC states that short-range signals will be used to broadcast the available channel information. Since the FCC does not specify the "short-range signals" term, long-range signals can be used and they can introduce interferences to the neighbor cells. Consequently, such signals can degrade the performance of this scheme significantly and even it can shut down the system. Although these two location-assisted dynamic spectrum management approaches are recommended, there are many challenges to implement them, which are open research areas.

Table 7.2 An illustrative snapshot of local geolocation-database.

	CR1	CR2
User Type	Unlicensed	Licensed
Waveform	WLAN AP	WiMAX MS
Location estimation method	GPS	GPS
Datum	WGS-84	WGS-84
Date format	mmddyyyy	mmddyyyy
Date	12012006	12012006
Time source	GPS	GPS
Local time format	hhmmss AM/PM Zone	hhmmss AM/PM Zone
Local time	092307 AM US EST	092307 AM US EST
Dimension accuracy unit	meter	meter
Altitude unit	meter	meter
Frequency unit	MHz	MHz
Longitude	82 24 34 W	82 24 34 W
Longitude accuracy	4	4
Latitude	28 31 16 N	28 31 16 N
Latitude accuracy	3	3
Altitude	10	14
Altitude accuracy	3	1
Center Frequency	2415	3475
Absolute Bandwidth	20	10

7.5.2 Location-assisted Network Plan and Expansion

Network design is usually thought of as the initial phase of network build out, but it is an ongoing work that is needed to improve and optimize network performance. From a design point of view, revenue, license, capacity, and performance are the main criteria that are used to make decisions for network expansion. Last two criteria are considered in this section since they possess technical merits.

Current wireless network operators plan and expand their networks in a semi-computerized manner. They have a group of engineers that are responsible for the network plan and expansion. The network expansion is determined based on the measurement data that are collected from target geographical areas. Such data are generally collected by driving a vehicle equipped with the measurement instruments within target areas. The engineers map the collected data to the morphology tables, which are used to help them to predict the traffic intensity and consequently the capacity in various areas. The engineers carefully study the tables and perform area visits regularly to achieve an optimal capacity prediction. This is a critical part in the initial design and expansion phases of

the network. Over-prediction can cause an inefficient use of resources (e.g. hardware and spectrum) whereas under-prediction can degrade the quality of service (QoS) provided by network.

CWNs have a potential to perform the network plan and expansion procedure automatically. In this approach, CR nodes are equipped with the location sensing devices. Central cognitive engine can request or CR nodes can report back the information that is beneficial for the network plan, expansion and optimization along with their location information. This information can be also incidents for the drop calls and deep fading.

Table 7.3 An example of geographic table that is formed by location-assisted network plan and expansion method.

Area	Number of Samples	Ave. RSSI (dBm)	Priority Factor
A	77865	-107	1
B	65750	-105	2

For the coverage prediction case, central cognitive engine can construct geographic table such as illustrated in Table 7.3[1] using information (e.g. average received signal strength indicator (RSSI)) reported back from the CR nodes. Table 7.3 is constructed based on the measurement results. Two target areas are considered, which are labeled as A and B. In this measurement campaign, the vehicle equipped with test equipments to collect data represents CR nodes. RSSI metric is used to predict coverage level in these two target areas. The collected data are tabulated in Table 7.3. According to the measurement results, number of samples (RSSI values) collected in target area A is 77865 and resulting average RSSI is -107dBm. In real CWN scenarios, the RSSI samples can be reported by single or multiple CR nodes existed in the target area along with their instantaneous location information. In the target area B, 65750 RSSI samples are collected and the resulting average RSSI is -105dBm. Based on the average RSSI level, central cognitive engine can determine that the coverage in target area A is poorer than that of target area B. As a result, central cognitive engine can give priority to the target area in terms of improving the coverage. Having network plan and expansion capability in CWNs comes with an additional overhead. Hence, such capability of CWNs can be activated whenever there is a need. Alternatively, CR nodes can store the required information in their memories and the central cognitive engine can collect the information periodically.

[1]The author thanks to Mohammad Juma for providing these measurement results

7.5.3 Location-assisted Handover

Handover is an important mechanism in CWNs likewise in legacy cellular networks. In [98], a location-based handover algorithm is proposed for the GSM networks and the performance of conventional handover and the proposed handover algorithms are compared. The measurement results show that the location-based handover algorithm provides 30 % reduction in the number of handovers compare to the conventional RSSI-based handover for a given call. In this section, a set of measurement results (without detailed performance analysis) are presented to demonstrate the impact of handover mechanism on the network performance. Furthermore, a location-assisted handover mechanism is proposed for CWNs to reduce number of handovers and consequently network load.

The majority of the current handover mechanisms are based on only signal strength, signal quality and cell traffic parameters due to the complexity limitations. As the QoS requirements increase, the current handover algorithms such as RSSI-based handover start to lag. Therefore, they can be replaced with more efficient handover algorithms such as location-assisted handover method, which is based on use of the location information of mobile stations. In this algorithm, the handover zones in which all mobile stations are served by the predetermined candidates are defined. Mobile stations are equipped with the location sensing devices to report their locations back to mobile switching center. Once a mobile station enters into a handover zone, mobile station can be served by one of the predetermined candidates. Moreover, these candidates can be prioritized in the case of congestion, site outages or exceptions. The location-assisted handover algorithm can reduce the number of handovers along the intended road, release the signaling load on the network, and maintain the handover pattern between the serving sites in other areas.

A measurement campaign is conducted in a live cellular network to obtain the performance of RSSI-based handover and location-assisted handover in the presence of ping pong effects. The experiment is performed as follows: the first drive test is performed to obtain the performance of RSSI-based handover and it is conducted between two cells to capture the handover pattern along one stretch (5 miles) of a highway. The signal strength, signal quality, and handover pattern of the test phone (MS2) in the dedicated mode are shown in Fig. 7.6a and 7.6b, and 7.6c[2], respectively. The dedicated mode is the mode of the test phone when a call is in progress. During this trial, the

[2]The author thanks to Mohammad Juma for providing these measurement results

phone is allowed to handover from cell 200C to cell 201B. It is clear from the results that neither RSSI nor the signal quality is affected from the handover process.

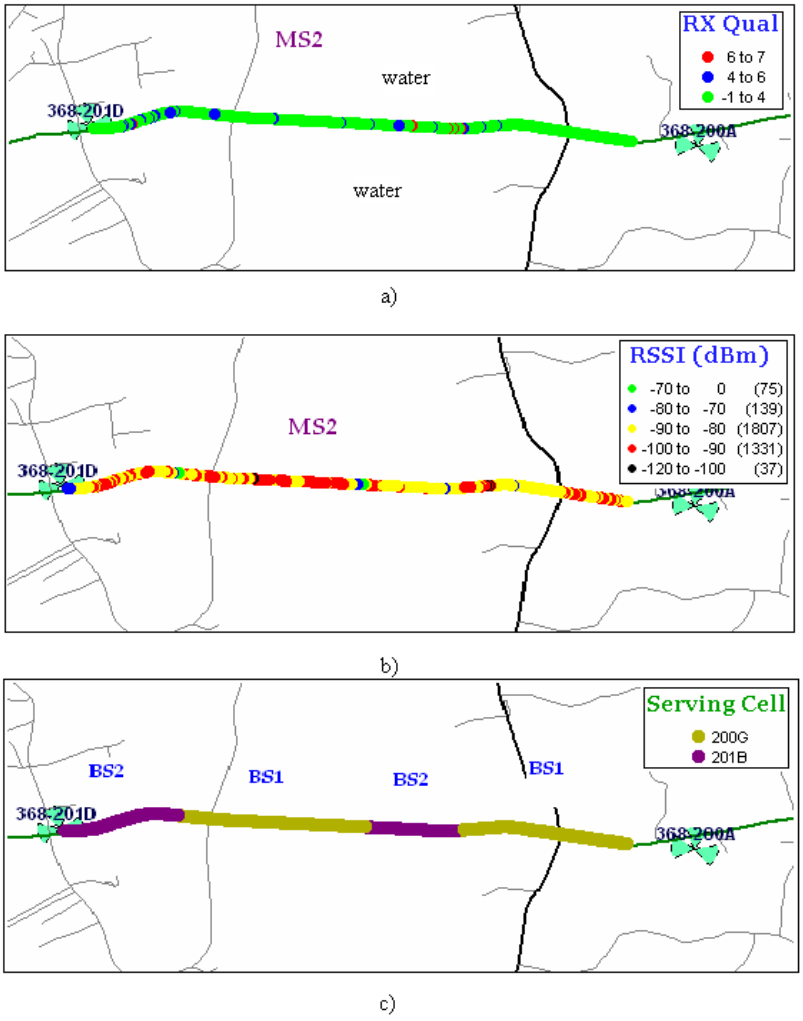

Figure 7.6 Test phone (MS2) in the dedicated mode: a) signal quality, b) signal strength, c) handover pattern.

In the second part of the experiment, the performance of location-assisted handover algorithm is observed. Since the test phone does not have the location estimation capability, the performance of location-assisted handover mechanism is obtained using a priori location information. Basically, we have the information about the boundaries of actual cell, in which the part of the highway that is used during the experiment resides. This a priori information is used to eliminate the need for the location sensing device. As a result, the test phone (MS1) is locked to the actual cell prior to

driving the test vehicle in the opposite direction of the same part of highway. The test phone is set to not accept any handover offer from any cells in the surrounding areas. The signal strength and signal quality profiles of the test phone are measured and the results are shown in Fig. 7.7a and 7.7b[3], respectively. It is observed that the drop call does not occur and the signal quality as well as the signal strength are preserved in the handover region as shown in Fig. 7.7. In the case of RSSI-based handover, the handover decision is initiated too early, which resulted in excessive number of handovers. Although the handover did not occur during the location-assisted handover experiment due to the restriction that we set in the test phone, the handover occurrence is inevitable in reality for this case. In such case, the proposed range accuracy adaptation can be utilized to reduce number of handovers. This can be accomplished to improve range accuracy adaptively in handover zone. In summary, we can conclude that the number of handovers can be reduced significantly by employing the location-assisted handover algorithms along with range accuracy adaptation method. As a result, it is recommended to incorporate the location-assisted handover algorithms into CWNs to optimize handover mechanism.

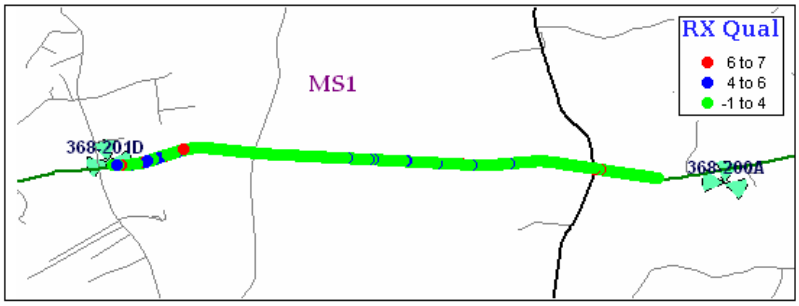

a)

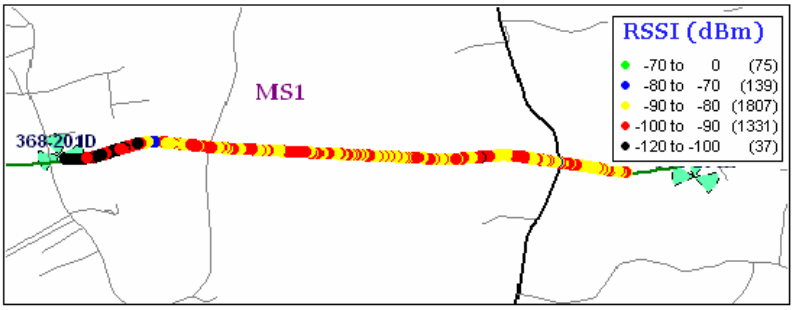

b)

Figure 7.7 Test phone (MS1) in the locked mode: a) signal quality, b) signal strength.

[3]The author thanks to Mohammad Juma for providing these measurement results

7.6 Conclusions

A classification of cognitive wireless networks based on the cognition, collaboration, and node diversity criteria is provided. Implementation options and challenges for the location awareness in cognitive radios and networks are discussed. Several representative examples of location-assisted network optimization are discussed to demonstrate applications of location awareness in cognitive radios. The preliminary results show that location information plays an important role in network optimization and we strongly recommend to balance the utilization of location information in the cognitive wireless networks and the protection of user privacy. Detailed performance analysis of the location-assisted optimization algorithms can be investigated further.

CHAPTER 8

CONCLUSIONS AND FUTURE WORKS

In this dissertation, we investigated the following topics: development of conceptual model for cognitive radio with location and environment awareness engines, cognitive positioning systems along with range accuracy adaptation, time delay estimation for whole spectrum utilization considering practical challenges, dispersed spectrum utilization method and its performance for time delay estimation problem, comparison of whole and dispersed spectrum utilization approaches in the context of time delay estimation, and some representative location aware systems in cognitive wireless networks. In what follows, the summary of the contributions are presented. Then, potential directions of our future work are provided.

In Chapter 2, a cognitive radio architecture with location and environment awareness engines and cycles is developed in order to support goal driven, autonomous, and advanced location aware systems. The architecture consists of engines (cognitive, location awareness, environment awareness, and spectrum awareness engines), adaptive waveform generation/processing, and sensing interface (radiosensing, radiovision, radiohearing sensors). The functionalities of location and environment awareness engines are identified and presented with details. Finally, the details of radiovision, radiohearing, and radiosensing sensors are presented.

In Chapter 3, cognitive positioning systems (CPS) for the location awareness engine is developed. One of the main features of the CPS is range accuracy adaptation, which is developed by inspiring from the range adaptation behavior of bats. Therefore, ML range accuracy adaptation algorithm is proposed to achieve arbitrarily given range accuracy requirements. The proposed ML range accuracy adaptation employs CRLB information at the transmitter side to optimize transmission parameters for the given range accuracy requirements and ML location estimator in the receiver side. Therefore, CRLBs for both AWGN and multipath channels are derived. The performance of ML range accuracy adaptation is simulated in dynamic spectrum access environment and compared to the theoretical bound. The results show that there is a margin between the practically achieved and desired range

accuracy. Therefore, three potential approaches are introduced in order to improve the performance of the proposed method (i.e. reducing the margin). These approaches are hybrid overlay and underlay dynamic spectrum access systems (HDSASs), dispersed spectrum utilization, and employing suboptimal lower bounds such as Ziv-Zakai lower bound (ZZLB) for the parameter optimization. In this chapter, we only emphasize on the HDSASs. In addition, a switching mechanism that manages the transition between overlay and underlay dynamic spectrum access schemes for the HDSASs is proposed.

In Chapter 4, we investigate the performance of time delay estimation using whole spectrum utilization approach in dynamic spectrum access systems. Therefore, asymptotic frequency domain CRB is derived through Whittle formula. The effects of dynamic spectrum access systems, especially bandwidth and carrier frequency, on the performance of time delay estimator are investigated. In addition, the effects of different channel environment on the performance of time delay estimator considering frequency dependence feature of channel environment as metric are studied. Furthermore, for the practical considerations, a generic list of TOA ranging related channel statistics are identified and quantified through computer simulations.

In Chapter 5, a new method for exploiting the spectrum utilization that is referred dispersed spectrum utilization is introduced. A cognitive radio transceiver for this new method is developed. The performance of this transceiver is studied in the context of time delay estimation. Hence, a generic CRLB is derived considering unknown channel coefficients and carrier frequency offsets. Then, the effects of various modulation and unknown channel coefficients and carrier frequency offsets on the accuracy of time delay estimation are quantified. Finally, numerical results are obtained to verify the theoretical analysis.

In Chapter 6, the performance of whole and dispersed spectrum utilization approaches are compared in the context of time delay estimation for theoretical and practical scenarios. Hence, cognitive radio transceivers for both approaches are proposed. A combining technique based on maximizing signal to noise ratio (SNR) criterion is proposed for the dispersed spectrum utilization approach. Consequently, CRLBs for both approaches are presented as well considering AWGN channel. For the practical considerations, ML TOA estimator is considered. Finally, the performance of both approaches are compared by providing theoretical (i.e. CRLBs) and practical (i.e. ML TOA estimator) results.

In Chapter 7, a taxonomy for cognitive wireless network is presented. This is followed by the discussion of implementation options challenges of cognitive radios and networks. Then, several potential cognitive location aware systems are presented with preliminary results in order to demonstrate the utilization of location information in cognitive radios and networks. These systems are categorized under four group:

- Location-based services (LBS),
- Location-assisted network optimization,
- Location-assisted transceiver optimization,
- Location-assisted environment identification.

For each group, various potential cognitive location aware applications are listed and some representative location-assisted network optimization applications with preliminary results are presented. Note that development of each of these systems can be considered as future work.

After providing the specific contributions of this dissertation, we summarize some of the directions of our future work in the sequel.

Each functionality of the proposed cognitive radio architecture with location and environment awareness engines is an open research area. Especially, the functionalities of location awareness engine, which are given as follows, are active research areas:

- Sensing interface (radiosensing, radiovision, radiohearing),
- Location sensing and adaptation (focus of this dissertation, still there are many open issues, which will be presented later in this section),
- statistical learning and tracking,
- Seamless positioning and interoperability,
- Mobility management,
- Secure positioning systems and privacy protection methods,
- Location aware systems.

During the development of this dissertation, we discovered several fundamental problems for the realization cognitive radio, which are presented as follows.

Since the available spectrum in cognitive radios is dynamic, statistical modeling of dynamic spectrum utilization for a given geographical region is a must in order to evaluate the performance of cognitive radio algorithms. This is a crucial and open issue in cognitive radio literature.

The propagation channel is the bottleneck of wireless systems. The observed channel at the wireless receiver mainly depends on the transmission parameters and the surrounding environment. Hence, the first task for developing a wireless system (i.e., transceiver) for a given environment and transmission parameters is to statistically model the propagation characteristics of the environment. A wireless channel is generally described by two main sets of statistics: large statistics and small statistics. The large and small statistics of the given channel environment are conventionally obtained by conducting channel measurement campaigns. However, in cognitive wireless systems, transmission parameters are dynamic due to the dynamic available spectrum and the goal driven autonomous operation feature of cognitive radios. Since the transmission parameters such as bandwidth, carrier frequency, transmit power are dynamic in cognitive systems, the observed channel and corresponding statistics are also dynamic. It is a challenging task to realize and design cognitive wireless systems for such dynamic channel environments. As a result, there is a need to develop rapid and low complexity channel statistics acquisition methods.

Two potential approaches for channel statistics acquisition in cognitive wireless networks are off-line and on-line channel statistics acquisition. In the first approach, the channel statistics are obtained from the cognitive base station for the given geographical area [24]. In this approach, it is assumed that cognitive radios have their position information. A cognitive radio provides its transmission parameters and position information to the cognitive base station in order to obtain the channel statistics information for its position. Then, the cognitive base station retrieves the channel statistics for the given position from a pre-built database by mapping the position to the corresponding channel statistics information [24]. The second approach, which is the on-line method, is based on the idea of acquiring channel statistics information between two cognitive radios in real-time (i.e., a cognitive base station and a cognitive radio node). It is obvious that this is a challenging task to achieve. As a result, development of rapid and low complexity channel statistics acquisition methods is a current research topic.

Since the utilized spectrum, transmission parameter, cognitive radio channel are dynamic, the cognitive radio receiver is dynamic as well. Therefore, development of dynamic, low complexity, and rapid cognitive radio receivers that can cope with dynamic spectrum utilization, transmission and channel conditions is an active research area.

The proposed CPS, range accuracy adaptation, whole and dispersed utilization methods are mainly studied for theoretical cases for proofing the concepts. In this dissertation, the CPS and range accuracy adaptation method are developed using time of arrival statistics. However, the analysis can be extended for the case of RSSI and AOA statistics. Furthermore, range estimation between two cognitive radios (i.e. 1-D location information) is considered. The current study can be extended to the estimation of 2-D and 3-D location information. In addition, CRLB, which is the optimal bound, is utilized for the parameter optimization in the range accuracy adaptation. More practical (or suboptimal) bounds such as ZZLB and Barankin bound can be considered for the parameter optimization and this can be investigated further.

In addition, a large number of research challenges and problems are identified by introducing the method of dispersed spectrum utilization. For instance, development of signaling, transmitter architectures and algorithms, channel behaviors, receiver structures and algorithms, and signal processing techniques for the dispersed spectrum utilization systems are open research areas. More specifically, we studied performance of dispersed spectrum utilization systems considering AWGN channel in order to proof the concept and explore the fundamental challenges. Therefore, the present study can be extended to the multipath channel case. In addition, we study the effects of carrier frequency offset (CFO) on the performance of the dispersed spectrum utilization systems in this study. However, additional practical impairments such as out-of-band radiation for each band can be included to the analysis. Furthermore, performance and complexity of the dispersed spectrum utilization systems for different waveforms such as OFDM, UWB [99], and CDMA can be investigated and compared. Finally, different combining technique can be developed for dispersed spectrum utilization systems.

REFERENCES

[1] "Human Consciousness," 2007. [Online]. Available: www.iddl.vt.edu/

[2] H. Celebi and H. Arslan, "Utilization of Location Information in Cognitive Wireless Networks," *IEEE Wireless Communications Magazine-Special issue on Cognitive Wireless Networks*, vol. 14, no. 4, pp. 6–13, Aug. 2007.

[3] Y. Xing, R. Chandramouli, and S. Mangold, "Dynamic Spectrum Access in Open Spectrum Wireless Networks," *IEEE J. Selec. Commun.*, vol. 24, no. 3, pp. 626–637, March 2006.

[4] N. Sai Shankar, C. Cordeiro, and K. Challapali, "Spectrum Agile Radios: Utilization and Sensing Architectures," in *First IEEE International Symposium on New Frontiers in Dynamic Spectrum Access Networks*, Baltimore, MD, USA, Nov. 2005, pp. 160–169.

[5] H. Arslan and M. E. Sahin, "Cognitive UWB-OFDM: Pushing Ultrawideband Beyond Its Limit via Opportunistic Spectrum Usage," *Journal of Communications and Networks-Special Issue on Spectrum Resource Optimization*, vol. 8, no. 2, pp. 151–157, June 2006.

[6] R. A. Altes, "A Theory for Animal Echolocation and Its Application to Ultrasonics," in *IEEE Ultrasonics Symposium*, Moneterey, California, USA, Nov. 1973, pp. 67–72.

[7] T. K. Horiuchi, "Seeing in the dark: neuromorphic vlsi modeling of bat echolocation," *IEEE Signal Processing Mag.*, vol. 22, no. 5, pp. 134–139, August 2005.

[8] D. Bank and T. Kampke, "High-Resolution Ultrasonic Environment Imaging," vol. 23, no. 2, pp. 370–381, April 2007.

[9] H. Arslan, *Cognitive Radio, Software Defined Radio, and Adaptive Wireless Systems*. Springer, June 2007.

[10] J. Mitola and G. Q. Maguire, "Cognitive radio: Making software radios more personal," *IEEE Personal Commun. Mag.*, vol. 6, no. 4, pp. 13–18, August 1999.

[11] "IEEE 1900 Standards Committee on Next Generation Radio and Spectrum Management," 2006. [Online]. Available: http://www.ieeep1900.org/

[12] H. Celebi and H. Arslan, "Cognitive Positioning Systems," *IEEE Trans. Wireless Commun.*, vol. 6, no. 12, pp. 4475–4483, Dec. 2007.

[13] J. O. Neel, "Analysis and design of cognitive radio networks and distributed radio resource management algorithms," Ph.D. dissertation, Virginia Polytechnic Institute and State University, VA, Sept. 2006.

[14] S. Haykin, "Cognitive Radio: Brain-empowered Wireless Communications," *IEEE J. Select. Areas Commun.*, vol. 23, no. 2, pp. 201–220, Feb. 2005.

[15] H. Celebi and H. Arslan, "Enabling location and environment awareness in cognitive radios," *Elsevier Computer Communications-Special Issue on Advanced Location-Based Services*, vol. 31, no. 6, pp. 1114–1125, April 2008.

[16] H. Celebi, H. Arslan, "Adaptive Positioning Systems for Cognitive Radios," in *IEEE Symposium on New Frontiers in Dynamic Spectrum Access Networks (DySpan)*, Dublin, Ireland, Apr. 2007, pp. 78–84.

[17] H. Celebi and H. Arslan, "Ranging Accuracy in Dynamic Spectrum Access Networks," *IEEE Commun. Lett.*, vol. 11, no. 5, pp. 405–407, May 2007.

[18] H. Celebi, I. Guvenc, and H. Arslan, "On the statistics of channel models for uwb ranging," in *Proc. IEEE Sarnoff Symposium*, Princeton, NJ, March 2006, to appear.

[19] S. Gezici, H. Celebi, H. V. Poor, and H. Arslan, "Fundamental limits on time delay estimation in dispersed spectrum cognitive radio systems," *IEEE Trans. on Wireless Communications*, June 2008, under revision.

[20] S. Haykin, "Cognitive radio: Brain-empowered wireless communications," *IEEE J. Select Areas Commun.*, vol. 23, no. 2, pp. 201–220, Feb. 2005.

[21] ——, "Cognitive radar: a way of the future," *IEEE Signal Processing Mag.*, vol. 23, no. 1, pp. 30–40, Jan. 2006.

[22] Y. Zhao, J. H. Reed, S. Mao, and K. K. Bae, "Overhead analysis for radio environment mapenabled cognitive radio networks," in *Proc. IEEE Workshop on Networking Technologies for Software Defined Radio Networks*, Reston, VA, Sep. 2006, pp. 18–25.

[23] I. Akyildiz, W. Lee, M. Vuran, and S. Mohanty, "Next generation/dynamic spectrum access/cognitive radio wireless networks: A survey," *Elsevier Computer Networks*, vol. 50, no. 13, pp. 2127–2159, 2006.

[24] H. Arslan and S. Yarkan, "Exploiting Location Awareness Towards Improved Wireless System Design in Cognitive Radio," *IEEE Communications Magazine*, 2007, to appear.

[25] D. Cabric, S. M. Mishra, and R. W. Brodersen, "Implementation issues in spectrum sensing for cognitive radios," in *IEEE Thirty-Eighth Asilomar Conference on Signals, Systems and Computers*, Pacific Grove, California, USA, Nov. 2004, pp. 772–776.

[26] H.-H. Nagel, "Steps Towards a Cognitive Vision System," *Artificial Intelligence Magazine*, vol. 25, no. 2, pp. 31–50, 2004.

[27] R. Koch, "Dynamic 3-D scene analysis through synthesis feedback control," *IEEE Trans. on Pattern Analysis and Machine Intelligence*, vol. 15, no. 6, pp. 556–568, June 1993.

[28] Y.-H. Lu and E. J. Delp, "Image-based location awareness and navigation: who cares?" in *IEEE Southwest Symposium on Image Analysis and Interpretation*, Lake Tahoe, Nevada, USA, March 2004, pp. 26–30.

[29] P. Luley, A. Almer, C. Seifert, G. Fritz, and L. Paletta, "A Multi-Sensor System for Mobile Services with Vision Enhanced Object and Location Awareness," in *IEEE International Mobile Commerce and Services*, Munich, Germany, July 2005, pp. 52–59.

[30] T. Starner, B. Schiele, and A. Pentland, "Visual context awareness via wearable computing," in *IEEE International Symposium on Wearable Computers*, Pittsburgh, PA, USA, Oct. 1998, pp. 50–57.

[31] A. Quazi, "An overview on the time delay estimate in active and passive systems for target localization," *IEEE Trans. Acoust., Speech, Signal Processing*, vol. 29, no. 3, pp. 527–533, 1981.

[32] A. Smith, H. Balakrishnan, M. Goraczko, and N. B. Priyantha, "Tracking Moving Devices with the Cricket Location System," in *2nd International Conference on Mobile Systems, Applications and Services*, Boston, MA , USA, June 2004.

[33] J. Agre, A. Akinyemi, L. Ji, R. Masuoka, and P. Thakkar, "A layered architecture for location-based services in wireless ad hoc networks," in *Proc. IEEE Aerospace Conference*, vol. 3, Big Sky, MT, USA, March 2002, pp. 1085–1097.

[34] N. Patwari, A. Hero, M. Perkins, N. Correal, and R. O'Dea, "Relative location estimation in wireless sensor networks," *IEEE Trans. on Signal Processing*, vol. 51, no. 8, pp. 2137–2148, Aug. 2003.

[35] "Standard Molodensky Datum Conversion," 2006. [Online]. Available: http://www.colorado.edu/geography/

[36] G. Sun, J. Chen, W. Guo, and K. Liu, "Signal processing techniques in network-aided positioning: a survey of state-of-the-art positioning designs," *IEEE Signal Processing Mag.*, vol. 22, no. 4, pp. 12–23, july 2005.

[37] S. Feng and W. Y. Ochieng, "User Level Autonomous Integrity Monitoring for Seamless Positioning in All Conditions and Environments," in *Proceedings of The European Navigation Conference*, Manchester, UK, May 2006.

[38] X. Li, "RSS-Based Location Estimation with Unknown Pathloss Model," *IEEE Trans. Wireless Commun.*, vol. 5, no. 12, pp. 3626–3633, Dec. 2006.

[39] "IEEE Standard Computer Dictionary: A Compilation of IEEE Standard Computer Glossaries," New York, NY, 1990. [Online]. Available: http://www.ieeexplore.ieee.org

[40] S. Capkun and J. Hubaux, "Secure positioning in wireless networks," *IEEE J. Select. Areas Commun.*, vol. 24, no. 2, pp. 221–232, Feb. 2006.

[41] "Geographic Location/Privacy (geopriv)," 2006. [Online]. Available: http://www.ietf.org/

[42] M. Brunato and R. Battiti, "Statistical learning theory for location fingerprinting in wireless LANs," *Elsevier Computer Networks*, vol. 47, no. 6, pp. 825–845, 2005.

[43] A. F. Molisch, "Ultrawideband Propagation Channels-Theory, Measurement, and Modeling," *IEEE Trans. Veh. Technol.*, vol. 54, no. 5, pp. 1528–1545, Sept. 2005.

[44] C. Sinka and J. Bito, "Rain attenuation countermeasure technique for broadband fixed wireless access networks," in *Twelfth International Conference on Antennas and Propagation*, vol. 1, UK, March 2003, pp. 441–444.

[45] M. Vossiek, L. Wiebking, P. Gulden, J. Wieghardt, C. Hoffmann, P. Heide, S. Technol, and G. Munich, "Wireless Local Positioning," *IEEE Microwave Magazine*, vol. 4, no. 4, pp. 77–86, 2003.

[46] "Federal Communications Commission (FCC) 911 Services," 2006. [Online]. Available: http://www.fcc.gov/911/enhanced/

[47] "StarFire: A Global High Accuracy Differential GPS System," 2006. [Online]. Available: http://www.navcomtech.com

[48] "A Taxonomy of Indoor and Outdoor Positioning Techniques for Mobile Location Services," 2003. [Online]. Available: www.acm.org

[49] F. van Diggelen, "Indoor GPS theory & implementation," in *IEEE Position, Location and Navigation Symposium*, Palm Springs, CA, USA, April 2002, pp. 240–247.

[50] "Geolocation Development Document," 2006. [Online]. Available: http://www.ieee802.org/22/

[51] C. Fretzagias and M. Papadopouli, "Cooperative Location-Sensing for Wireless Networks," in *Proc. IEEE Pervasive Computing and Communications*, Orlando, FL, March 2004, pp. 121–131.

[52] Y. Qi and H. Kobayashi, "On Relation among Time Delay and Signal Strength based Geolocation Methods," in *Proc. IEEE Globecom Conf.*, vol. 7, San Francisco, CA, Dec 2003, pp. 4079–4083.

[53] B. Fette, *Cognitive Radio Technology.* Newnes, 2006.

[54] S. Gezici, Z. Tian, G. B. Giannakis, H. Kobayashi, A. F. Molisch, H. V. Poor, and Z. Sahinoglu, "Localization via UWB Radios," *IEEE Signal Processing Mag.*, vol. 22, no. 4, pp. 70–84, July 2005.

[55] J. Hightower and G. Borriello, "A Survey and Taxonomy of Location Systems for Ubiquitous Computing," University of Washington, Tech. Rep., 2001.

[56] H. V. Poor, *An Introduction to Signal Detection and Estimation.* New York: Springer-Verlag, 1994.

[57] Y. Qi, "Analysis of wireless geolocation in a non-line-of-sight environment," Ph.D. dissertation, Princeton University, New Jersey, Nov. 2003.

[58] Y. Qi, H. Kobayashi, and H. Suda, "Analysis of wireless geolocation in a non-line-of-sight environment," *IEEE Trans. Wireless Commun.*, vol. 5, no. 3, pp. 672–681, march 2006.

[59] B. H. Fleury and P. E. Leuthold, "Radiowave propagation in mobile communications: an overview of European research," *IEEE Communications Magazine*, vol. 34, no. 2, pp. 70–81, 1996.

[60] B. Kim, N. K. Shankaranarayanan, P. S. Henry, K. Schlosser, and T. K. Fong, "The AT&T Labs broadband fixed wireless field experiment," *IEEE Communications Magazine*, vol. 37, no. 10, pp. 56–62, 1999.

[61] K. Sheikh, D. Gesbert, D. Gore, and A. Paulraj, "Smart antennas for broadband wireless access networks," *IEEE Communications Magazine*, vol. 37, no. 11, pp. 100–105, 1999.

[62] P. Grover, R. Agarwal, and A. K. Chaturvedi, "Geolocation Using Transmit and Receive Diversity," in *Proc. IEEE Globecom Conf.*, vol. 6, Dallas, TX, Dec 2004, pp. 3681–3684.

[63] S. Venkatraman, J. Caffery Jr., H-R, You , "A novel ToA location algorithm using LoS range estimation for NLoS environments," *IEEE Trans. Veh. Technol.*, vol. 53, no. 5, pp. 1515–1524, Sept. 2004.

[64] Z. Sahinoglu and I. Guvenc, "Multiuser interference mitigation in noncoherent uwb ranging via nonlinear filtering," *EURASIP Journal on Wireless Communications and Networking*, vol. 2006.

[65] W. Lehr and J. Crowcroft, "Managing Shared Access to a Spectrum Commons," in *Proc. of the first IEEE Symposium on New Frontiers in Dynamic Spectrum Access Networks*, Baltimore, MD, USA, Nov. 2005, pp. 420–444.

[66] "Dynamic Spectrum Sharing," 2006. [Online]. Available: http://www.sharedspectrum.com/?section=presentations

[67] D. Willkomm, J. Gross, and A. Wolisz, "Reliable Link Maintenance in Cognitive Radio Systems," in *First IEEE International Symposium on Dynamic Spectrum Access Networks (DySPAN)*, Baltimore, MD, USA, Nov. 2005, pp. 371–378.

[68] D. Landi and C. Fischer, "The effects of UWB interference on GSM systems," in *International Zurich Seminar on Communications*, Zurich, Switzerland, Feb. 2004, pp. 86–89.

[69] R. Giuliano and F. Mazzenga, "Performance Evaluation of UWB Sensor Network with Aloha Multiple Access Scheme," in *International Workshop on Wireless Ad Hoc Networks*, London, UK, May. 2005.

[70] X. Li, K. Pahlavan, and J. Beneat, "Performance of TOA Estimation Techniques in Indoor Multipath Channels," in *Proc. IEEE Int. Symp. on Personal, Indoor and Mobile Radio Commun.*, vol. 2, Lisbon, Portugal, 15-18 Sept. 2002, pp. 911–915.

[71] Y. Xing and R. Chandramouli and S. Mangold and S. Shankar N, "Dynamic Spectrum Access in Open Spectrum Wireless Networks," *IEEE J. Select. Areas Commun.*, vol. 24, no. 3, pp. 626–637, March 2006.

[72] Holloway, CL and Cotton, MG and McKenna, P., "A Model for Predicting the Power Delay Profile Characteristics Inside a Room," *IEEE Trans. on Vehicular Technology*, vol. 48, no. 4, pp. 1110–1120, July 1999.

[73] R.C. Qiu, I-T. Lu, "Multipath Resolving with Frequency Dependence for Wide-band Wireless Channel Modeling," *IEEE Trans. on Vehicular Technology*, vol. 48, no. 1, pp. 273–285, Jan 1999.

[74] R. Cardinali, Luca De Nardis, M.-G. Di Benedetto, P. Lombardo, "UWB Ranging Accuracy in High- and Low-Data-Rate Applications," *IEEE Trans. on Microwave Theory and Techniques*, vol. 54, no. 4, pp. 1865–1875, Apr 2006.

[75] P. Whittle, "The Analysis of Multiple Stationary Time Series," *Journal of the Royal Statistical Society, Series B (Methodological)*, vol. 15, no. 1, pp. 125–139, 1953.

[76] M.J.D. Rendas, J.M.F. Moura, "Cramer-Rao Bound for Location Systems in Multipath Environments," *IEEE Trans. on Signal Processing*, vol. 39, no. 12, pp. 2593–2610, Dec 1991.

[77] J.-Y. Lee and R. A. Scholtz, "Ranging in a Dense Multipath Environment Using an UWB Radio Link," *IEEE J. Select. Areas Commun.*, vol. 20, no. 9, pp. 1677–1683, December 2002.

[78] E. D. Zand, K. Pahlavan, and J. Beneat, "Measurement of TOA Using Frequency Domain Characteristics for Indoor Geolocation," in *Proc. IEEE Personal, Indoor and Mobile Radio Communications (PIMRC)*, vol. 3, Beijing, China, Sept. 2003, pp. 2213–2217.

[79] A. F. Molisch, "UWB Wireless Channels - Propagation Aspects and Interplay with System Design," Mitsubishi Electric Research Laboratories, Tech. Rep., December 2004. [Online]. Available: www.merl.com

[80] I. Guvenc and Z. Sahinoglu, "Threshold-Based TOA Estimation for Impulse Radio UWB Systems," in *in Proc. IEEE Int. Conf. UWB (ICU)*, Zurich, Switzerland, Sept. 2005, pp. 420–425.

[81] ——, "TOA Estimation with Different IR-UWB Transceiver Types," in *Proc. IEEE Int. Conf. UWB (ICU)*, Zurich, Switzerland, Sept. 2005, pp. 426–431.

[82] A. F. Molisch, K. Balakrishnan, D. Cassioli, C. C. Chong, S. Emami, A. Fort, J. Karedal, J. Kunisch, H. Schantz, U. Schuster, and K. Siwiak, "IEEE 802.15.4a Channel Model - Final Report," 2005, tech. rep. doc: IEEE 802.15-04-0662-02-004a. [Online]. Available: http://www.ieee802.org/15/pub/TG4a.html

[83] J. Foerster, "IEEE P802.15 Working Group for Wireless Personal Area Networks (WPANs), Channel Modeling Sub-committee Report - Final," Mar. 2003. [Online]. Available: http://www.ieee802.org/15/pub/2003/Mar03/

[84] A. F. Molisch, K. Balakrishnan, D. Cassioli, C. C. Chong, S. Emami, A. Fort, J. Karedal, J. Kunisch, H. Schantz, U. Schuster, and K. Siwiak, "A comprehensive model for ultrawideband propagation channels," to appear in Proc. IEEE Global Telecommun. Conf. (GLOBECOM), St. Louis, MO, Dec. 2005.

[85] I. Guvenc, Z. Sahinoglu, A. F. Molisch, and P. Orlik, "Non-coherent TOA estimation in IR-UWB Systems with Different Signal Waveforms," to appear in Proc. IEEE Int. Workshop on Ultrawideband Networks (UWBNETS), Boston, MA, July 2005, (invited paper).

[86] R. I. C. Chiang, G. B. Rowe, and K. W. Sowerby, "A quantitative analysis of spectral occupancy measurements for cognitive radio," in *Proc. IEEE IEEE Vehicular Technology Conference*, Dublin, Ireland, Apr. 2007.

[87] T. A. Weiss and F. K. Jondral, "Spectrum pooling: An innovative strategy for the enhancement of spectrum efficiency," *IEEE Commun. Mag.*, vol. 42, no. 3, pp. 8–14, March 2004.

[88] S. Brandes, I. Cosovic, and M. Schnell, "Reduction of out-of-band radiation in OFDM based overlay systems," *IEEE Commun. Lett.*, vol. 10, no. 6, pp. 420–422, June 2006.

[89] H. Mahmoud and H. Arslan, "Sidelobe suppression in OFDM-based spectrum sharing systems using adaptive symbol transition," *IEEE Commun. Lett.*, vol. 12, no. 2, pp. 133–135, Feb. 2008.

[90] J. G. Proakis, *Digital Communication*, 4th ed. New York: McGraw-Hill, 2001.

[91] S. Brandes, I. Cosovic, and M. Schnell, "Sidelobe suppression in ofdm systems by insertion of cancellation carriers," in *Proc. IEEE Veh. Technol. Conf.*, vol. 1, Dallas, TX, USA, Sep. 2005, pp. 152–156.

[92] H. Mahmoud and H. Arslan, "Spectrum shaping of ofdm-based cognitive radio signals," in *Proc. IEEE Radio and Wireless Symposium*, Orlando, FL, USA, Jan. 2008.

[93] A. Zeira and P. Schultheiss, "Realizable lower bounds for time delay estimation," *IEEE Trans. on Signal Processing*, vol. 41, no. 11, pp. 3102–3113, Nov. 1993.

[94] T. Fujii and Y. Suzuki, "Ad-hoc Cognitive Radio-Development to Frequency Sharing System by Using Multi-hop Network," in *Proc. IEEE International Symposium on New Frontiers in Dynamic Spectrum Access Networks*, Baltimore, MD, USA, Nov. 2005, pp. 589–592.

[95] H. Zheng and C. Peng, "Collaboration and Fairness in Opportunistic Spectrum Access," in *Proc. IEEE International Conference on Communications*, vol. 5, Seoul, South Korea, May 2005, pp. 3132–3136.

[96] Z. Sahinoglu and S. Gezici, "Ranging in the IEEE 802.15. 4a Standard," in *IEEE Wireless and Microwave Technology Conference*, Clearwater, FL, USA, Dec. 2006, pp. 1–5.

[97] M. J. Marcus, P. Kolodzy, and A. Lippman, "Reclaiming the Vast Wasteland: Why Unlicensed Use of the White Space in the TV Bands will not Cause Interference to DTV Viewers," New America Foundation: Wireless Future Program, Tech. Rep., 2005.

[98] H. Lin, R. Juang, and D. Lin, "Validation of an Improved Location-based Handover Algorithm Using GSM Measurement Data," *IEEE Trans. on Mobile Computing*, vol. 4, no. 5, pp. 530–536, 2005.

[99] S. Gezici, H. Celebi, H. Arslan, and H. V. Poor, "Theoretical limits on time delay estimation for ultra-wideband cognitive radios," in *Proc. IEEE International Conference on UWB (ICUWB)*, Hannover, Germany, Sept. 2008, invited Paper.

APPENDICES

Appendix A FIM Elements

$$
\begin{aligned}
[J_{\tau\tau}]_{mn} &= \frac{-2N\pi^2}{3}\Big(\frac{P_S}{P_R}\Big)^2[C_{\tau\tau}]_{mn} \ , \\
[J_{\beta\beta}]_{mn} &= \frac{N}{2}\Big(\frac{P_S}{P_R}\Big)^2[C_{\beta\beta}]_{mn} \ , \\
[J_{\alpha\alpha}]_{mn} &= \frac{N}{2}\Big(\frac{P_S}{P_R}\Big)^2\frac{[C_{\alpha\alpha}]_{mn}}{\alpha_m\alpha_n} \ , \\
[J_{\phi\phi}]_{mn} &= \frac{N}{2}\Big(\frac{P_S}{P_R}\Big)^2[C_{\phi\phi}]_{mn} \ ,
\end{aligned}
$$

$$
\begin{aligned}
[J_{\tau\beta}]_{mn} = [J_{\beta\tau}]_{mn} &= \frac{jN\pi}{2}\Big(\frac{P_S}{P_R}\Big)^2[C_{\tau\beta}]_{mn} \ , \\
[J_{\tau\alpha}]_{mn} = [J_{\alpha\tau}]_{mn} &= \frac{N}{2}\Big(\frac{P_S}{P_R}\Big)^2\frac{[C_{\tau\alpha}]_{mn}}{\alpha_n} \ , \\
[J_{\tau\phi}]_{mn} = [J_{\phi\tau}]_{mn} &= \frac{N\pi}{2}\Big(\frac{P_S}{P_R}\Big)^2[C_{\tau\phi}]_{mn} \ , \\
[J_{\alpha\beta}]_{mn} = [J_{\beta\alpha}]_{mn} &= \frac{-N}{2}\Big(\frac{P_S}{P_R}\Big)^2\frac{[C_{\alpha\beta}]_{mn}}{\alpha_m} \ , \\
[J_{\phi\beta}]_{mn} = [J_{\beta\phi}]_{mn} &= -j2N\Big(\frac{P_S}{P_R}\Big)^2[C_{\phi\beta}]_{mn} \ , \\
[J_{\phi\alpha}]_{mn} = [J_{\alpha\phi}]_{mn} &= \frac{jN}{4\pi}\Big(\frac{P_S}{P_R}\Big)^2\frac{[C_{\phi\alpha}]_{mn}}{\alpha_n} \ , \\
[C_{\tau\tau}]_{mn} = [C_{\phi\phi}]_{mn} &= (U_mH^* - HU_m^*)(U_nH^* - HU_n^*) \ , \\
[C_{\beta\beta}]_{mn} = [C_{\alpha\alpha}]_{mn} &= (U_mH^* + HU_m^*)(U_nH^* + HU_n^*) \ , \\
[C_{\tau\beta}]_{mn} = [C_{\tau\alpha}]_{mn} &= (U_mH^* - HU_m^*)(U_nH^* + HU_n^*) \ , \\
[C_{\tau\phi}]_{mn} &= [C_{\tau\tau}]_{mn} \ , \\
[C_{\alpha\beta}]_{mn} = [C_{\phi\beta}]_{mn} &= [C_{\phi\alpha}]_{mn} = [C_{\tau\beta}]_{mn} \ ,
\end{aligned}
$$

$$
\begin{aligned}
\gamma = J_{\beta\beta}[J_{\alpha\alpha}J_{\phi\phi} - J_{\alpha\phi}J_{\phi\alpha}] + J_{\beta\alpha}[J_{\alpha\phi}J_{\phi\beta} - J_{\alpha\beta}J_{\phi\phi}] \\
+ J_{\beta\phi}[J_{\alpha\beta}J_{\phi\alpha} - J_{\alpha\alpha}J_{\phi\beta}] \ .
\end{aligned}
$$

Appendix B Derivation of CRLB for Dispersed Spectrum Utilization

Let $\mathbf{A} = \begin{bmatrix} \mathrm{I}_{\tau\tau} & \mathbf{I}_{\tau a} \\ \mathbf{I}_{\tau a}^T & \mathbf{I}_{aa} \end{bmatrix}$, $\mathbf{B} = \begin{bmatrix} \mathbf{I}_{\tau\phi} & \mathbf{I}_{\tau\omega} \\ \mathbf{0} & \mathbf{0} \end{bmatrix}$ and $\mathbf{D} = \begin{bmatrix} \mathbf{I}_{\phi\phi} & \mathbf{I}_{\phi\omega} \\ \mathbf{I}_{\phi\omega}^T & \mathbf{I}_{\omega\omega} \end{bmatrix}$. Then, $\mathbf{I}$ can be expressed as $\mathbf{I} = \begin{bmatrix} \mathbf{A} & \mathbf{B} \\ \mathbf{B}^T & \mathbf{D} \end{bmatrix}$, and the first $(K+1) \times (K+1)$ block of $\mathbf{I}^{-1}$ is given by $\left(\mathbf{A} - \mathbf{B}\mathbf{D}^{-1}\mathbf{B}^T\right)^{-1}$ by the block matrix inversion formula.

From (5.7), (5.8) and (5.10)-(5.12), $\mathbf{B}\mathbf{D}^{-1}\mathbf{B}^T$ can be shown to be an all-zeros matrix except for the element in the first row and first column, which is given by ξ in (5.19). Then, the block matrix inversion formula can be applied to $\mathbf{A} - \mathbf{B}\mathbf{D}^{-1}\mathbf{B}^T$ in order to obtain the CRLB as follows

$$\left[\mathbf{I}^{-1}\right]_{11} = \left[\left(\mathbf{A} - \mathbf{B}\mathbf{D}^{-1}\mathbf{B}^T\right)^{-1}\right]_{11} = \frac{1}{(\mathrm{I}_{\tau\tau} - \xi) - \mathbf{I}_{\tau a}\mathbf{I}_{aa}^{-1}\mathbf{I}_{\tau a}^T} \ . \tag{B.1}$$

From (5.5), (5.6) and (5.9), (B.1) can be shown to be equal to the CRLB expression in (5.18) and (5.19). □

ABOUT THE AUTHOR

Hasari Celebi received his BS degree in Electronics and Communications Engineering in 2000 from Yildiz Technical University, Istanbul, Turkey and his MS degree in Electrical Engineering in 2004 from San Jose State University, San Jose, California, USA. He received his Ph.D. degree in Electrical Engineering in June 2008 from University of South Florida, Tampa, FL, USA. His research interests are location and environment awareness in cognitive radio systems, cognitive wireless networks, cognitive positioning systems, UWB communications and positioning, and software defined radio structures. He received distinguished graduate achievement award from University of South Florida in 2008. He is a member of IEEE.